2000

Analysis of stream offset along the San Gregorio Fault zone, San Mateo County, CA

Cynthia L. Hayek
San Jose State University

INFORMATION TO USERS

This manuscript has been reproduced from the microfilm master. UMI films the text directly from the original or copy submitted. Thus, some thesis and dissertation copies are in typewriter face, while others may be from any type of computer printer.

The quality of this reproduction is dependent upon the quality of the copy submitted. Broken or indistinct print, colored or poor quality illustrations and photographs, print bleedthrough, substandard margins, and improper alignment can adversely affect reproduction.

In the unlikely event that the author did not send UMI a complete manuscript and there are missing pages, these will be noted. Also, if unauthorized copyright material had to be removed, a note will indicate the deletion.

Oversize materials (e.g., maps, drawings, charts) are reproduced by sectioning the original, beginning at the upper left-hand corner and continuing from left to right in equal sections with small overlaps.

Photographs included in the original manuscript have been reproduced xerographically in this copy. Higher quality 6" x 9" black and white photographic prints are available for any photographs or illustrations appearing in this copy for an additional charge. Contact UMI directly to order.

Bell & Howell Information and Learning
300 North Zeeb Road, Ann Arbor, MI 48106-1346 USA
800-521-0600

ANALYSIS OF STREAM OFFSET ALONG THE SAN GREGORIO FAULT ZONE, SAN MATEO COUNTY, CA

A Thesis

Presented to

The Faculty of the Department of Geology

San José State University

In Partial Fulfillment

of the Requirements for the Degree

Master of Science

by

Cynthia L. Hayek

December 2000

UMI Number: 1402512

Bell & Howell Information and Learning Company
300 North Zeeb Road
P.O. Box 1346
Ann Arbor, MI 48106-1346

APPROVED FOR THE DEPARTMENT OF GEOLOGY

Dr. Richard Sedlock Thesis Advisor

Deborah R. Harden

Dr. Deborah Harden

David W Andersen

Dr. David Andersen

APPROVED FOR THE UNIVERSITY

ANALYSIS OF STREAM OFFSET ALONG THE SAN GREGORIO FAULT ZONE, SAN MATEO COUNTY, CA

by
Cynthia L. Hayek

The onshore San Gregorio fault near Año Nuevo displays several stream deflections, possibly indicating recent fault movement. The objective of this study is to determine if calculating the correlation coefficient of several drainage basin volumes across the fault zone can identify dextrally offset streams. If dextral slip has separated the lower drainages from their original headwaters, low correlation coefficients are expected. Restoration of lower drainages to their original position is expected to produce higher correlation coefficients.

A weak, positive correlation of streams in their present spatial configuration, a slow (1-5 mm/yr) rate of modern stream offset, and the small (< 1km) offset calculated for successfully restored streams, seem to negate the possibility of rapid Holocene fault movement. Streams north of Whitehouse Creek appear to be older than those to the south. However, stream development does not appear to progress uniformly from north to south, possibly due to the strike slip.

ACKNOWLEDGEMENTS

My thanks, empathy and sympathy go out to many who supported me during my graduate work. From Lawrence Livermore National Laboratory, I would like to thank my close friend and mentor Dr. Larry Hutchings for encouraging me towards pursuing a Master's degree, and Bill Glassley for helping me learn EarthVision. I would also like to thank the students, staff and faculty from San Jose State University, Geology Department. Specifically, I want to pay special tribute to my committee Dr. Richard Sedlock (advisor), Dr. Deborah Harden, and Dr. David Andersen for their patient editing for an impatient writer. I also want to express my appreciation to the Department personnel (Bob, Ellen, and Jade) who helped me graduate via long distance, and to Ginney for her friendship and help. I would also like to thank the U.S. Geological Survey, both in Salt Lake City and Phoenix, for their technical support. Finally, I would like to thank my shaman warrior princess – for everything.

Sometimes a scream is better than a thesis.
-- Ralph Waldo Emerson

TABLE OF CONTENTS

LIST OF ILLUSTRATIONS

LIST OF TABLES

INTRODUCTION

The San Gregorio fault zone (SGfz), part of the larger San Andreas fault (SAF) system, remains one of the most enigmatic fault zones in northern California. Very little is known about the SGfz, primarily because it is located mostly offshore with very limited onshore exposure (Figs. 1a and 1b). Most of the movement on the SGfz appears to be lateral, but a small component of vertical movement has also been documented (Weber, 1990).

The area chosen for this study is a 254-km^2-onland portion of the SGfz that extends from Pescadero State Beach to Año Nuevo Point (Fig. 2). Many streams within the study area exhibit an apparent right-lateral deflection, possibly indicating strike-slip movement within the fault zone. Past qualitative or semiquantitative studies of deflected streams in the thesis study area yield dextral slip rate estimates of either 4-10 mm/yr (Weber, 1990) or 0.5-1 mm/yr (Hamilton, 1984).

The objective of this study is to determine if calculating the correlation coefficient of several drainage basin volumes across the SGfz can indicate the presence of captured streams caused by dextral offset. If dextral slip detached the lower drainage basins from the original headwaters, correlation coefficients are expected to be low (near zero) or negative. Restored drainage basins are then expected to show higher correlation coefficients.

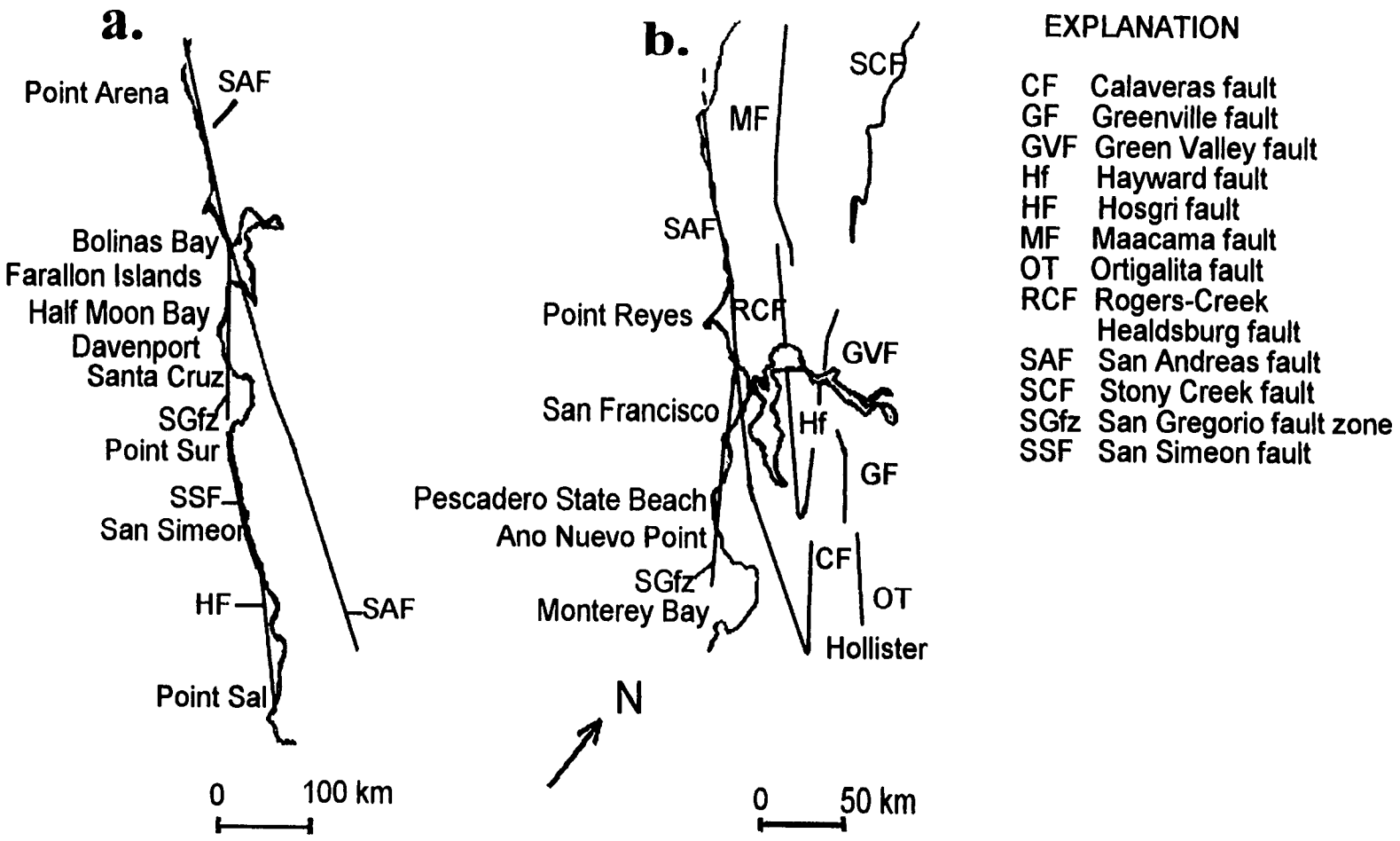

Figure 1. Location maps of the SGfz showing (a.) the San Simeon and Hosgri fault zones and (b.) the SGfz proper in relation to other Bay Area faults (modified from Brown, 1990).

EXPLANATION FOR FIGURE 2

Quaternary

Q Marine terraces, dunes, and alluvium

Tertiary

Purisima Formation

Tehana Member

Santa Cruz Mudstone

Cretaceous

Pigeon Point Formation

STREAMS

Ano Nuevo Creek (AN)
Arroyo de los Frijoles Creek (ADF)
Stream A (A)
Stream B (B)
Butano Creek (Bu)
Cascade Creek (C)
Cold Dip Creek (CD)
Elliot Creek (E)
Finney Creek (F)
Gazos Creek (G)
Green Oaks Creek (GO)
Little Butano Creek (LBu)
Old Womans Creek (OW)
Whitehouse Creek (W)

FAULTS

Ano Nuevo fault (ANF)
Coastways fault (CF)
Frijoles fault (FF)
Green Oaks fault (GOF)
Cascade thrust fault (CAF)

SYMBOLS

fault trace

thrust fault

dip slip movement +/-

strike-slip movement

strike and dip 30

plunging fold

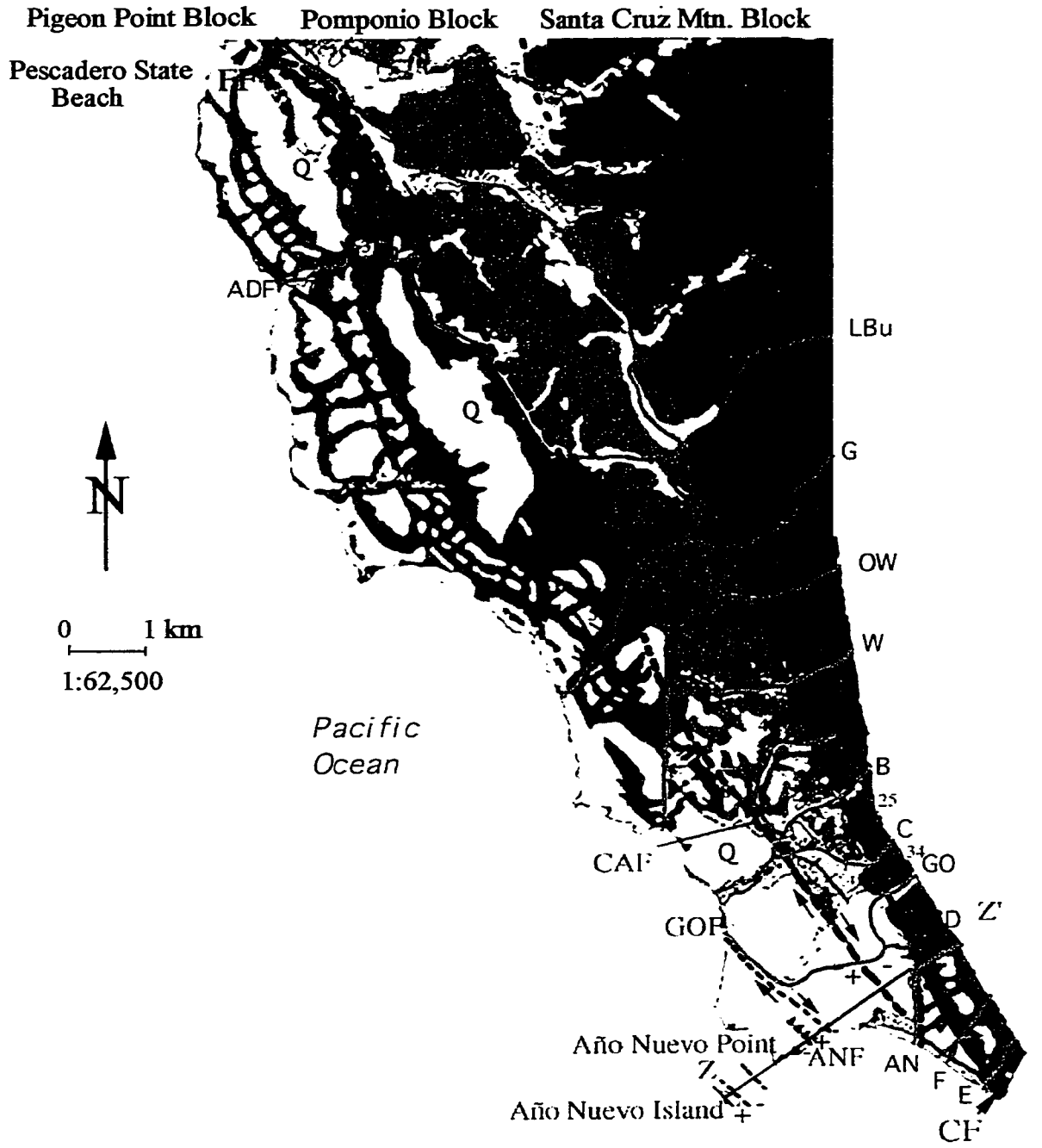

Figure 2. Geologic map of the study area (Brabb and Pampeyan, 1983). Symbol explanation is shown on p. 3. Cross section is shown on Figure 3.

In an attempt obtain the highest possible correlation coefficients for drainage basins in the study area, streams were restored by two different methods. The first method restored movement along the fault zone in one-kilometer increments, totaling three kilometers of restoration. The second method did not assume that all the basins should be restored the same amount, as in the first method, and instead restored all plausible basin configurations. Slip rates were then calculated for each of the successful restorations by evaluating (1) which marine terrace, of known age, was incised by the offset stream, and (2) the amount of offset required to restore the drainage basin configuration.

GEOGRAPHIC SETTING

The SGfz proper is about 200 km long and trends roughly parallel to the coastline from an inferred submarine juncture with the SAF west of San Francisco near Bolinas Bay (Greene et al., 1973) to the vicinity of Monterey Bay (Fig. 1b). The chiefly offshore SGfz runs onshore near Half Moon Bay and between Pescadero State Beach and Año Nuevo Point (Figs. 1b and 2). The SGfz may continue to the southeast as the San Simeon - Hosgri fault zone (SS-Hfz), crossing Point Sur and then paralleling the coast within the offshore continental shelf, until it terminates near Point Sal (Fig. 1a) (Weber and Cotton, 1980; Weber, 1990). If the SG-SS-Hfz is continuous, the total length is approximately 420 km (Weber, 1990). On the other hand, the SGfz may turn inland near Monterey Bay and connect to the Palo Colorado fault in the northern Santa Lucia Range (Rosenburg and Clark, 1999), transferring slip from the San Andreas fault.

The study area, a 254-km^2 section including the fault zone and several drainage basins near Año Nuevo, is approximately 45 km south of Half Moon Bay and 30 km north of Santa Cruz. Here the fault zone is predominantly controlled by two fault strands, the Frijoles and Coastways faults. Several smaller shear zones and thrust faults accompany these two major fault segments near Año Nuevo; however, the fault movement is thought to occur mostly on the Frijoles and Coastways fault segments.

REGIONAL SETTING

The SAF system in the Bay Area is a 100- to 300-km-wide zone of deformation (Ellsworth, 1990) containing numerous active fault strands including the San Gregorio, San Andreas, Hayward (which includes the Rodgers Creek-Healdsburg and Maacama fault extensions), Calaveras (including the Concord and Green Valley extensions), and possibly the Stony Creek, Greenville, and Ortigalita faults (Brown, 1990) (Fig. 1b). The SGfz is thought to form the western limit of the Pacific-North American plate boundary (J.C. Clark et al., 1984).

Seismicity and Earthquake Potential

Two magnitude (M) 6.1 earthquakes occurred within one hour of each other on October 22, 1926 in Monterey Bay, followed by two aftershocks located 20 km northwest of Santa Cruz (Weber and Cotton, 1980). Based on the size of the earthquakes and the location of the aftershocks, a 40-km rupture along the SGfz is inferred to have caused the earthquakes (Gawthrop, 1978). A half-length rupture (65-100 km) of the SGfz proper would generate a M 7.2-7.9 earthquake (Greene et al., 1973). If the SGfz is connected to the Hosgri fault to the south, and if considerable vertical movement occurs during an earthquake, magnitudes of up to 8.0-8.5 could occur along SG-SS-Hfz (Weber and Cotton, 1980). Recently, the fault zone has been reclassified as a Class A fault with a potential magnitude of 7.3 (McNally et al., 1999).

Modern Plate Boundary

The slip on the SAF system accommodates much of the relative motion between the Pacific (PAC) and North American (NA) plates. The PAC-NA zone of deformation extends from the Farallon Islands (Fig. 1a) east to central Utah and includes the Sierra Nevada microplate (Argus and Gordon, 1991) and the Basin and Range province (Kelson et al., 1992). Tectonic models, geodetic data, and geologic evidence are used to estimate the slip rate along the PAC-NA boundary.

The NUVEL-1A plate motion model predicts the PAC-NA slip rate near the southern tip of San Francisco Bay to be 46 mm/yr directed N34W, almost parallel to the SAF (DeMets et al., 1994). Finite rotations indicate a more northerly PAC-NA azimuth and 10 mm/yr of compression since the change in plate motions 3.9 to 3.4 Ma (Harbert, 1991). The complex faulting near Año Nuevo records this change in plate motion, showing a change from Miocene transtension, transrotation, rifting, and translation to Pliocene and Quaternary transpression and translation (Hall et al., 1995). Transpression likely formed many of the small thrust faults and high-angle strike-slip faults found near the study area (Figs. 2 and 3).

Geodetic studies near the latitude of the Bay Area yield a 39 mm/yr slip rate between the Pacific Plate and Sierra Nevada microplate (Argus et al., 1998), indicating that a large percentage of PAC-NA motion occurs within California alone. According to geologic and paleoseismic observations in central California, the SAF itself accommodates about 34 mm/yr of this slip (Sieh and Jahns, 1984). To the north, the slip rate on the SAF decreases as the SAF zone becomes wider (Fig. 1b) and slip is

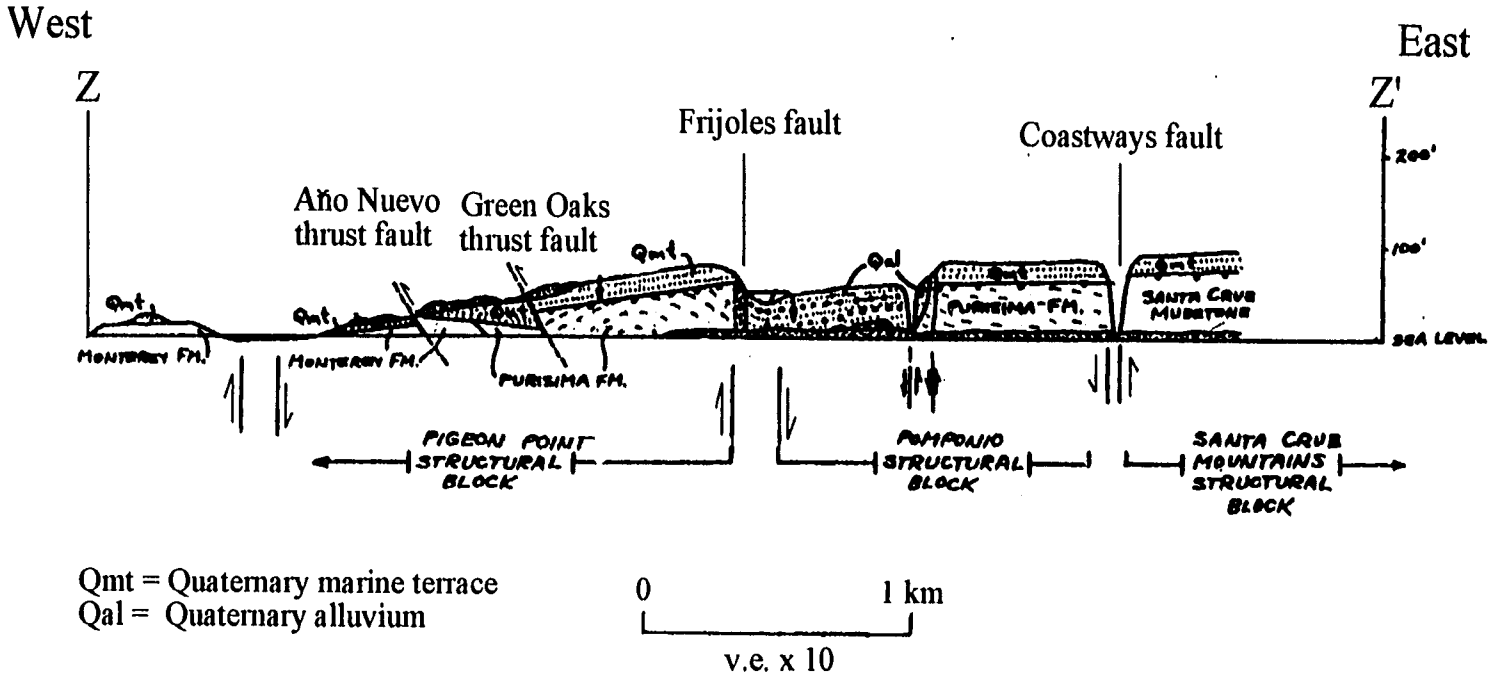

Figure 3. Cross section of southern portion of study area of Figure 2 (Weber and Cotton, 1980). Cross-section line is shown on Figure 2.

distributed among the other Bay Area faults (Table 1; Kelson et al., 1992). The rate of modern strike-slip motion along the northern section of the SAF decreases from 22 ± 6 mm/yr near Hollister (Fig. 1b; Sims, 1991) to 19 ± 4 mm/yr near the mouth of San Francisco Bay (Addicott, 1969; Cummings, 1983; Hall, 1984; WGCEP, 1990). The slip rate then increases to 24 ± 4 mm/yr north of San Francisco near Point Reyes (Fig. 1b; Prentice, 1989; Neimi and Hall, 1992). These calculations yield a slip deficit of 5-7 mm/yr of slip along the Peninsula section west of San Francisco between Hollister and Point Reyes.

This slip deficit may be explained by slip on undiscovered fault(s), deformation occurring as folds, or transfer of slip from the SGfz to the SAF at its junction near Bolinas Bay. Weber and Cotton (1980) proposed a slip rate of 7 ± 1 mm/yr for the SGfz, which agrees closely with the slip deficit estimate for the SAF (Table 1). Assuming this SGfz slip rate, Kelson et al. (1992) determined that recognized faults in the Bay Area account for all of the predicted plate motion, and that significant unrecognized faults do not exist in this region.

Dextral Slip within the San Gregorio Fault Zone

It is not yet known if strike-slip motion is transferred between the SAF and the SG-SS-Hfz near Monterey Bay or at the SAF/SGfz juncture near Bolinas Bay. The SGfz fault geometry, kinematics, and continuity in the central California coastal region are complex and undefined. However, north of San Francisco the total offset along the SAF is greater than along the central California segment, presumably due to the additive effect

of the offset assumed for the SGfz (J.C. Clark et al., 1984). The maximum total offset of the southern SAF in central California is 305 to 315 km (Turner, 1969; Huffman, 1972; Matthews, 1973; Nilsen and Clark, 1975), and the estimated offset of the SAF north of San Francisco is approximately 512 to 560 km (Hill and Dibblee, 1953), a difference of 197 to 255 km.

Table 1. Slip rates of faults related to the San Andreas system (Kelson et al., 1992). SAF - San Andreas fault; SGfz - San Gregorio fault zone.

Fault	Slip Rate mm/yr	Reference
	Point Reyes latitude	
SAF	24 ± 4	Prentice (1989), Niemi and Hall (1992)
Rogers Creek	8 ± 2	Schwartz et al. (1992)
Green Valley	6 ± 2	Kelson et al. (1992)
Vacaville	2 ± 2	Knuepfer (1977), M.M. Clark et al. (1984)
	Farallon Islands latitude	
SGfz	7 ± 1	Weber and Cotton (1980)
SAF	19 ± 4	Addicott (1969), Cummings (1983), Hall (1984) WGCEP (1990)
Hayward	9 ± 1	Lienkaemper et al. (1989) and (1991)
Concord	6 ± 2	Kelson et al. (1992)
	San José latitude	
SGfz	7 ± 1	Weber and Cotton (1980)
SAF	19 ± 4	Addicott (1969), Cummings (1983), Hall (1984), WGCEP (1990)
Monte Vista	1.5 ± 1.0	Sieh (1975), Hay et al. (1980)
Hayward	9 ± 1	Lienkaemper et al. (1989) and (1991)
Calaveras	8 ± 2	Kelson et al. (1992)
Greenville	0.6 ± 0.1	Kelson et al. (1992)
Midway	0.1 ± 0.1	Sowers et al. (1992)
	Hollister latitude	
SGfz	7 ± 1	Weber and Cotton (1980)
SAF	22 ± 6	Sims (1991)
Calaveras	12 ± 3	M.M. Clark (1988), Sims (1991), Lienkaemper et al. (1991)
Ortigalita	0.4 ± 0.4	Anderson et al. (1982), M.M. Clark. et al. (1984)
San Joaquin	1 ± 1	Lettis (1982), M.M. Clark et al. (1984)

Several proposed offsets along the SG-SS-Hfz (Table 2) may account for the missing displacement required in northern California. The most recent data from Clark (1998) and Hall et al. (1995) in Table 2 indicate that the SG-SS-Hfz has accommodated as much as 150-160 km of strike slip since middle Miocene (10 to 12 Ma) to late Miocene time. Late Cretaceous basement and overlying Tertiary rocks show roughly similar offsets, which supports the initiation of strike slip in the Miocene.

Sedlock and Hamilton (1991) suggested that most displacement on the SGfz occurred prior to the Miocene, and that apparently offset Neogene sedimentary sequences could be explained by *in situ* deposition. They suggested that pre-Eocene rocks were transported up to 150 km during pre-Miocene time, followed by accumulation of the Neogene sections in the offshore basins. They noted that Neogene basins of central California are continuous across the fault zone and suggest little or no late Cenozoic lateral slip (Hamilton, 1984). They also disputed Hall's (1975) correlation of similar late Miocene rocks near San Simeon and Point Sal because the strata are not nearly so similar in the younger parts of the stratigraphic sections.

Assuming 150 km of offset and a mid- to late Miocene origin for the SGfz, a constant slip rate of 13-15 mm/yr is required, which is higher than most faults in the Bay Area except the SAF (Table 1). Clark (1998) suggested that the slip rate for the SGfz has not been constant in the past, and that slip rates averaged 25-30 mm/yr during the late Miocene (10-8 Ma), 16 mm/yr during the late Miocene to late Pliocene (8-3 Ma), and 6 mm/yr during the late Pliocene to Holocene (3-0 Ma).

Table 2. Displaced features along the San Gregorio fault zone and the San Simeon-Hosgri fault zone.

Displacement (km)	Displaced feature	Reference
	San Gregorio fault zone	
≤ 30	Miocene rocks	Sedlock and Hamilton (1991)
80-90	Gravity anomalies	Silver (1974)
90-115	Franciscan and Salinian contact	Wentworth (1972)
110-130	Paleogene - Pliocene sedimentary rocks/basement rocks	Clark (1966); Ross (1972)
105-130	Gravity ridge	Silver et al. (1971)
70-150	Bedrock units	Silver and Normark (1978); Nagel and Mullins (1983)
150-160	Basement and overlying Tertiary sedimentary rocks	J.C. Clark et al. (1984); Clark (1998)
160	Miocene rocks	Hall et al. (1995)
180	Conglomerate	Burnham (1999)
	San Simeon - Hosgri fault zone	
≤ 30	Miocene rocks	Sedlock and Hamilton (1991)
60-105	Sliver of Miocene sandstone with Franciscan source	Hall (1995)
85-105	Similar K-bearing graywacke-shale	Gilbert (1973); Hsu (1969)
85-130	Mesozoic ophiolites and Tertiary rocks	Hall (1975)
160	Miocene rocks	Hall et al. (1995)

Those who emphasize the progressive eastward shift of transform motion since the transform boundary first originated 29 Ma hypothesize that the SGfz zone is an early member of the SAF system, although its trend is more northerly than that of the SAF and nearly matches the trends of more recent faults in northern California (Page, 1990). If the SGfz originated with the transform system during Oligocene time, a 5 mm/yr slip rate is required to produce 150 km of total slip.

CHARACTERIZATION OF STUDY AREA

East of Año Nuevo Point, the SGfz is about 3 km wide and includes at least five northwest-striking faults (Weber and Cotton, 1980; J.C. Clark et al., 1984). Although movement along the SGfz generally is considered to be chiefly right-lateral, ten degrees of convergence along the fault zone (Weber, 1990) created the thrust faults between Año Nuevo Point and San Gregorio Beach, including the Cascade and Año Nuevo thrust faults (Fig. 2). Fault-plane solutions indicate that most of these thrust faults dip about 65 degrees eastward (Weber and Cotton, 1980).

The total onland length of the SGfz between Año Nuevo Point and Pescadero State Beach is 18 km. Most of the right-lateral slip within the fault zone is concentrated on the Frijoles and Coastways fault segments (Fig. 2; Weber and Cotton, 1980). These two primary fault strands separate three distinct structural blocks: the Pigeon Point, the Pomponio (a graben), and the Santa Cruz Mountain (Figs. 2 and 3). The Frijoles and the Coastways fault segments bound the Pomponio block, which is 4.5 km wide at the northwest end of the onland exposure and narrows to 1 km wide near Año Nuevo Point (Weber and Cotton, 1980).

Lithology

Right-lateral and dip-slip motion on the Frijoles and Coastways fault segments has juxtaposed four distinct rock types, as shown in Plate 1 and Figures 2 and 3. From east to west, these units include the Santa Cruz Mudstone (upper Miocene), the Purisima

Formation (upper Miocene to Pliocene), the Pigeon Point Formation (Upper Cretaceous), and the Monterey Formation (middle Miocene). East of the fault zone, the Santa Margarita Sandstone (upper Miocene) depositionally underlies the Santa Cruz Mudstone and unconformably overlies the Butano Sandstone (middle to lower Eocene).

The Santa Cruz Mudstone, Santa Margarita Sandstone, and Butano Sandstone crop out within the Santa Cruz Mountain block (Plate 1). The Purisima Formation is located both within the fault-bounded Pomponio block and in the Pigeon Point block (Plate 1). The Pigeon Point Formation is the predominant unit of the Pigeon Point block, and unconformably underlies the Purisima Formation in both the Pigeon Point and Pomponio blocks. The Monterey Formation is located in the Pigeon Point block, where it is faulted against the Pigeon Point and Purisima formations (Fig. 3). Unconformably overlying the bedrock units are Quaternary alluvial, eolian, and marine deposits (Figs. 2 and 3; Plate 1).

Pigeon Point Formation (Upper Cretaceous)

The Pigeon Point Formation contains successions of turbidity current deposits, submarine canyon or slope fill, and shallow-shelf deposits (Weber et al., 1979). It consists of more than 2,600 m (Brabb et al., 1983) of thick beds of folded and faulted brownish-gray, interbedded sandstone and siltstone that grade upward into sandy pebble to cobble conglomerate, pebbly mudstone, and coarse-grained sandstone (Weber et al., 1979). The conglomerate contains well-rounded pebbles, cobbles, and boulders of red and gray, fine-grained or porphyritic felsic volcanic rocks.

Butano Sandstone (middle to lower Eocene)

The Butano Sandstone represents a deep-sea fan deposit (Weber et al., 1979). It consists of 900 m of light-gray to buff feldspathic sandstone, buff silty claystone, glauconitic sandstone, and tuffaceous siltstone (Brabb et al., 1983). In some areas, the bedding is chaotic (Brabb et al., 1983). The base of the section is marked by a thin conglomerate atop underlying serpentinite (Brabb et al., 1983)

Monterey Formation (middle Miocene)

The Monterey Formation ranges from 120 to 450 m thick in the field area (Brabb et al., 1983). It consists of grayish- to blackish-brown porcelaneous shale with chert, porcelaneous mudstone, impure diatomite, calcareous claystone, and small amounts of siltstone and sandstone near the base (Brabb et al., 1983).

Santa Margarita Sandstone (upper Miocene)

The Santa Margarita Sandstone is a shallow-water transgressive unit (Weber et al., 1979) and grades upward from a quartz- and feldspar-pebble conglomerate to a fine- to very coarse-grained, light-colored, friable arkosic sandstone (Brabb et al., 1983). In some areas it is bituminous (Weber et al., 1979). The thickness ranges from 60 m (Brabb et al., 1983) to a maximum of 130 m (Weber et al., 1979).

Santa Cruz Mudstone (upper Miocene)

The Santa Cruz Mudstone is composed of more than 1,000 m (Brabb et al., 1983) of yellowish-brown mudstone. The mudstone ranges from siliceous (Clark, 1966) to nonsiliceous (Brabb et al., 1983), with scattered concretions of dolomite (Weber et al., 1979). This unit generally is less siliceous than the Monterey Formation (Brabb et al., 1983). Bedding thicknesses range from several centimeters to a meter. The exposed sections grade from mudstone into a sandy siltstone near the top of the unit (Weber et al., 1979).

Purisima Formation (upper Miocene to Pliocene)

The Purisima Formation, which is divided into five members, is at least 360 m thick west of and 1,725 m thick east of the SGfz (Weber et al., 1979). The five members of the Purisima Formation include (from oldest to youngest): (1) the Tahana, (2) the Pomponio Mudstone, (3) the San Gregorio Sandstone, (4) the Lobitos Mudstone, and (5) the Tunitas Sandstone (Brabb et al., 1983). The Purisima Formation is very heterogeneous and consists of thickly bedded mudstone and porcelaneous shale, chert, and silty mudstone; poorly to moderately indurated olive-gray siltstone; sandstone and rhyolitic tuff with rare lenses composed of mollusk shells; and rare carbonate concretions (Weber et al., 1979; Brabb et al., 1983). The Pomponio Mudstone Member closely resembles the Monterey Formation. The Purisima Formation lies conformably on the Santa Cruz Mudstone east of the SGfz (north of the study area) and is in angular

discordance with the underlying, steeply dipping beds of the Pigeon Point Formation west of the SGfz (Weber et al., 1979).

Quaternary Deposits

Pleistocene marine terrace deposits (< 30 m thick) on all three structural blocks consist of poorly consolidated and well- to poorly sorted sand and gravel (Brabb et al., 1983). Holocene alluvial deposits consisting of unconsolidated fine- to coarse-grained sand, silt, and gravel of variable thickness are found mostly within the graben structure of the Pomponio block (Brabb et al., 1983). Holocene dune and beach deposits on the Pigeon Point block range in thickness from less than 6 m to more than 30 m and consist of well-sorted sand and some pebbles, cobbles, and silt (Brabb et al., 1983).

Geomorphology

Surficial expression of the SGfz is evident in several areas between Año Nuevo and Pescadero State Beach. The most evident geomorphic feature is a large trough parallel to the Coastways fault that extends from Gazos Creek to north of the study area (Fig. 4; Hamilton, 1984). Hamilton attributed this trough to the susceptibility of the main trace of the SGfz (Coastways) to erosion.

Several smaller features also indicate the presence of faulting, including linear channels, scarps, offset colluvial deposits, offset shoreline angles, sag ponds, and shear zones (Weber and Lajoie, 1980). Several streams show apparent dextral or sinistral deflection or stream capture.

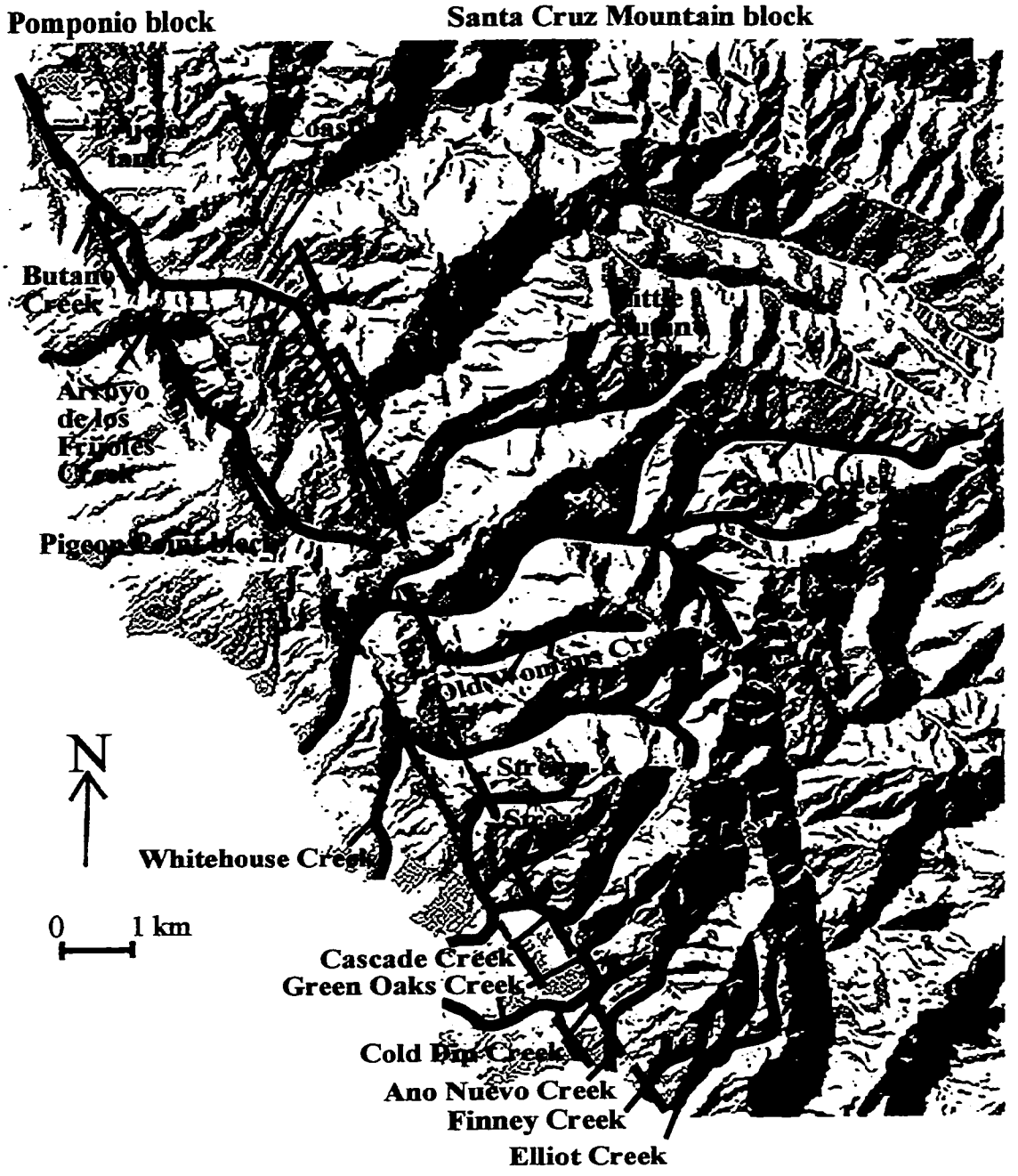

Figure 4. Digital USGS topographic image showing the stream drainage pattern and trough (hachured area) along the fault zone.

Thornburg (1999) observed that "there is no trace of active faulting where the Coastways fault crosses the floodplains and low terraces" and that "the extreme youth of the sedimentary fill explains why there is no geomorphic expression of the active San Gregorio fault across these coastal valleys."

Topography

The Santa Cruz Mountain block contains the highest elevations (520 m) and steepest terrain of the study area. This block presents a sharp topographical contrast with the elevations ($\leq$ 180 m) of the Pomponio and Pigeon Point blocks to the west. Headwaters of all large streams included in this study are located on the Santa Cruz Mountain block (Fig. 4). Most streams flow westward from the Santa Cruz Mountain block across the Pomponio block and the Pigeon Point block to the Pacific Ocean (Figs. 2 and 4). Streams at the south end of the study area that cross the Pomponio but not the Pigeon Point block include Finney Creek and Año Nuevo Creek. Elliot Creek reaches the Pacific Ocean east of the Coastways fault and does not enter the Pomponio block.

Marine Terraces

On the tectonically uplifted coast between Santa Cruz and Año Nuevo, high sea level and erosional processes associated with storm-wave surf zones cut into the bedrock to form marine platforms (Bradley and Griggs, 1976). Marine and terrestrial (marine terrace) sediment is deposited on the wavecut platforms. Sequential uplift of these platforms and their overlying terrace deposits formed the stair-step morphology of the

Ben Lomond terraces a few kilometers south of the study area near Davenport and Santa Cruz, California. The six Pleistocene marine terraces exposed near Santa Cruz and Davenport, California (from youngest to oldest) include: (1) Santa Cruz, (2) Cement, (3) Western, (4) Wilder, (5) Blackrock, and (6) Quarry.

Four terraces were mapped by Weber and Cotton north of Año Nuevo. Correlation of these marine terraces with those near Davenport is difficult because of surficial disruption from shear zones, concealment by landslides and alluvium, erosion caused by uplift, and a possible discontinuity with terraces near Año Nuevo. Weber (Weber and Cotton, 1980) mapped the youngest and most identifiable terraces south of Whitehouse Creek (Fig. 5). Marine terraces north of Whitehouse Creek are difficult to identify, and no maps have yet been published. Only terraces younger than Blackrock have been identified in the study area (Fig. 5).

Most of these marine terraces are cut into the soft Santa Cruz Mudstone, which expedited their formation (Bradley and Griggs, 1976). The more siliceous portions of the mudstone slowed further erosion once platforms were stranded on interfluves, which explains the development and preservation of the terraces in the study area near Año Nuevo Point and Santa Cruz (Bradley and Griggs, 1976).

According to Bradley and Griggs (1976), the Santa Cruz terrace, which also is commonly referred to as the first emergent terrace, contains three separate terraces: Davenport, Highway 1, and Greyhound. Weber (1999) recognized only one lower

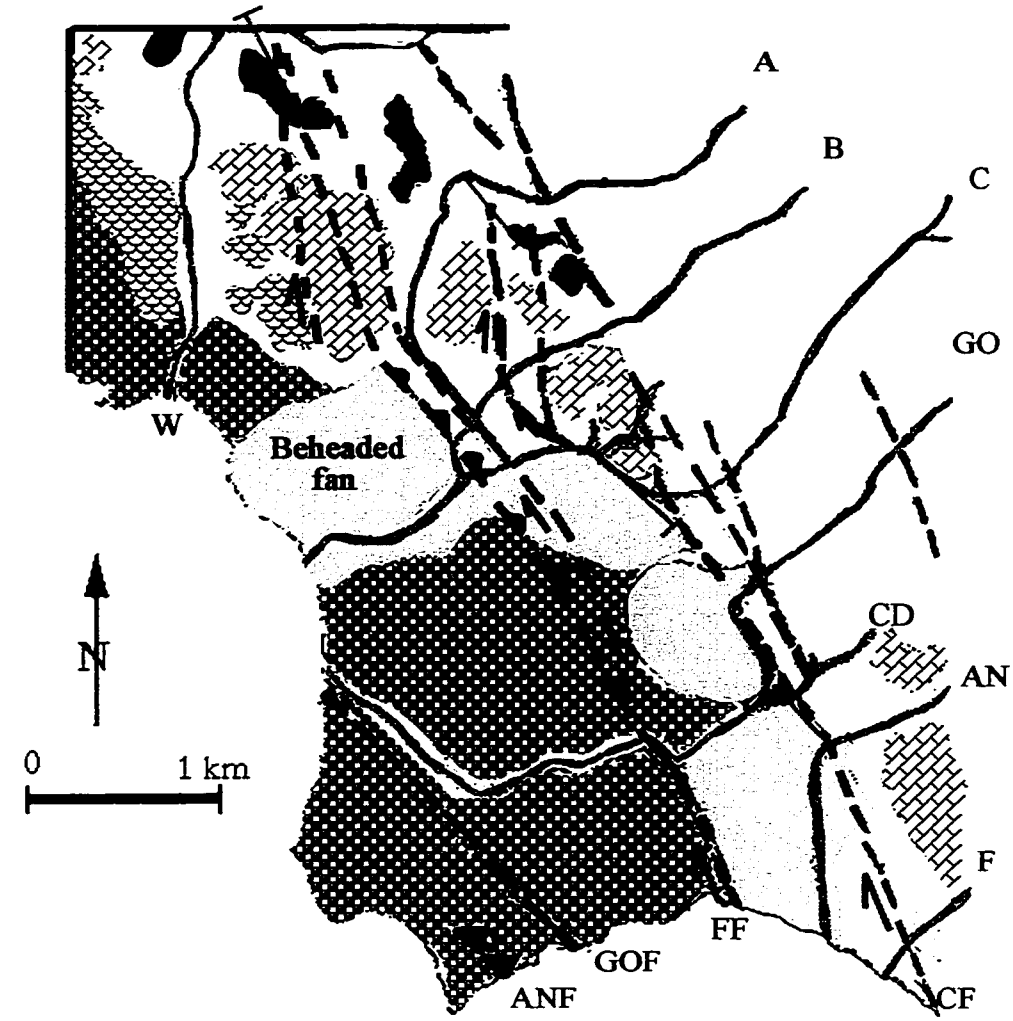

EXPLANATION

Santa Cruz terrace
Cement terrace
Western terrace
Wilder terrace
Alluvial fan
Fault trace
Modern stream offset

STREAMS

W	Whitehouse Creek
A	Stream A
B	Stream B
C	Cascade Creek
GO	Green Oaks Creek
CD	Cold Dip
AN	Ano Nuevo Creek
F	Finney Creek

FAULTS

ANF	Ano Nuevo thrust fault
CF	Coastways fault
FF	Frijoles fault
GOF	Green Oaks fault

Figure 5. Marine terraces in the study area as mapped by Weber and Cotton (1980), and studied streams.

terrace, the Highway 1. Multiple terraces may also exist in the Wilder and are suspected in the Blackrock (Bradley and Griggs, 1976).

Figures 6a-g are schematic diagrams showing the possible sequential development and offset of the marine terraces and streams near Año Nuevo. In my work, I assumed that stream development and incision of marine terraces were initiated by base-level lowering and subaerial exposure of the marine terraces, and that dextral slip was continuous during stream and terrace development. If these assumptions are valid, then the established ages of the marine terraces can be used to provide maximum ages for subsequently offset streams and minimum rates of dextral slip on the SGfz.

Streams

Several drainages west of the SGfz near Año Nuevo display apparent dextral offset, including: Butano Creek, Arroyo de los Frijoles Creek, Gazos Creek, Old Womans Creek, Whitehouse Creek, Stream A, and Cascade Creek (Fig. 4; Plate 1). Streams that do not show apparent right-lateral displacement include Elliot Creek, Finney Creek, Año Nuevo Creek, and Stream B.

The lower drainage of Año Nuevo Creek appears to follow a splay of the Coastways fault (Weber and Cotton, 1980), indicating a preferential flow along the fault zone. This splay is known as the Año Nuevo Creek fault, which captured the flow of Año Nuevo Creek about 12,000 years ago (Weber, 1990). The abandoned Año Nuevo Creek drainage is now occupied by Green Oaks Creek (Weber, 1990).

6a.) Formation of Quarry (Q), Blackrock (Bl), and Wilder (Wi) terraces, with dextral slip along Coastways fault (CF). Stream segment Xwi of headwaters X formed on the Wilder terrace and was then offset.

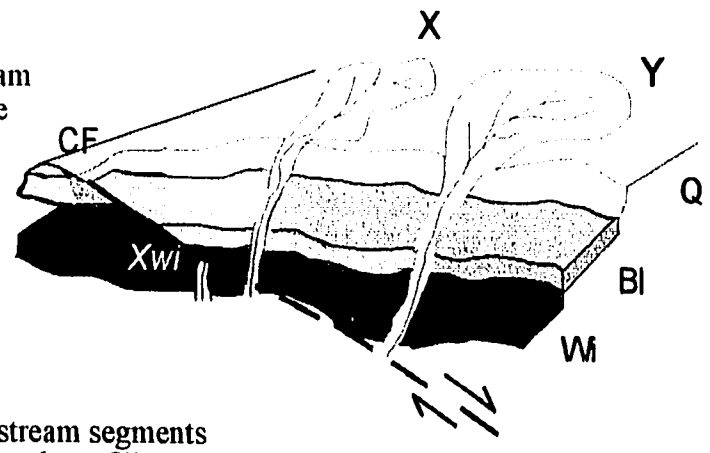

6b.) Formation of Western terrace (We), new headwaters V and stream segments Vwe, Xwe, Ywe1, and Ywe2 on Western terrace. Dextral slip along CF. Segment Ywe2 formed on We after Ywe1 was offset.

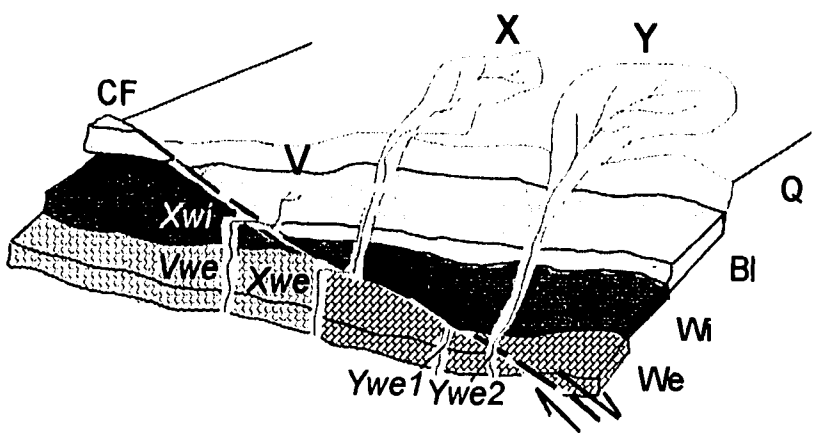

Figure 6. Schematic diagram showing the hypothetical development and offset of marine terraces and streams within the SGfz. Q, Quarry; Bl, Blackrock; Wi, Wilder; We, Western; Ce, Cement; SC, Santa Cruz; CF, Coastways fault; and FF, Frijoles fault. Views are to the northeast.

Figure 6. - Continued

6c.) Formation of Cement terrace (Ce) and new headwaters Z. Formation of Vce, Xce, Zce, and Yce1 stream segments. No new offset along fault zone.

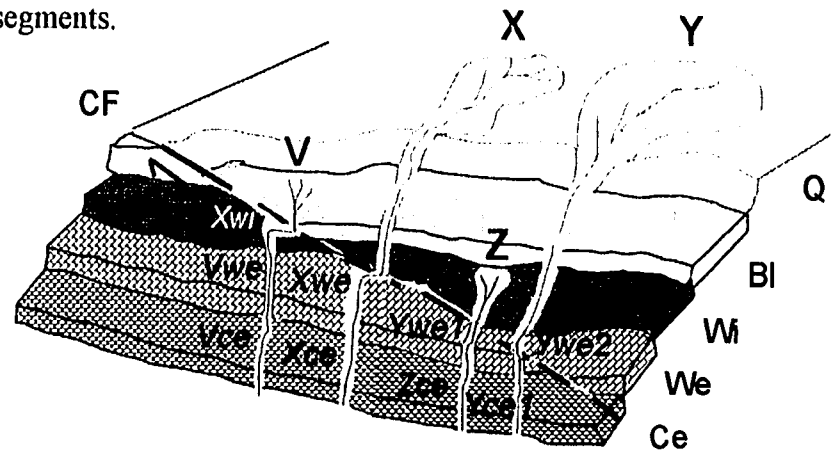

6d.) Dextral slip along CF, formation of Yce2, a beheaded drainage, and apparent left-lateral displacement of a stream. No new terrace formation. Streams V and Y display no apparent displacement, yet their lower reaches were offset substantially.

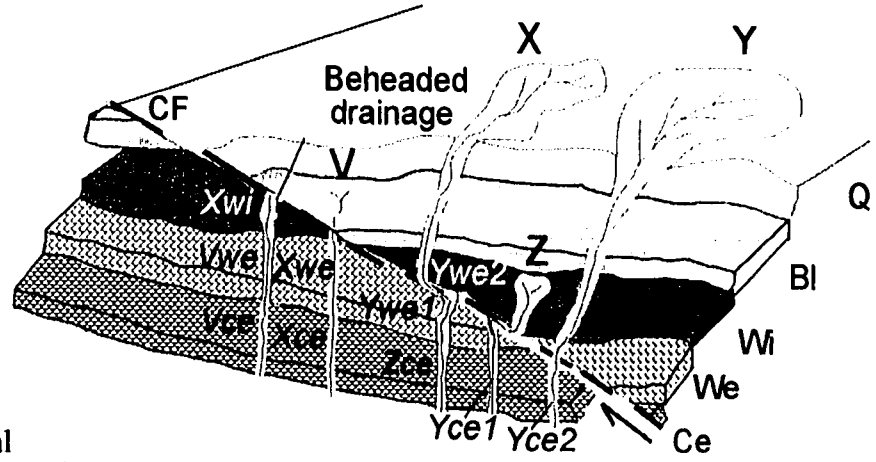

Figure 6. - Continued

6e.) Development of new headwaters U. Streams are dissecting terraces east of fault zone. No new offset along fault zone.

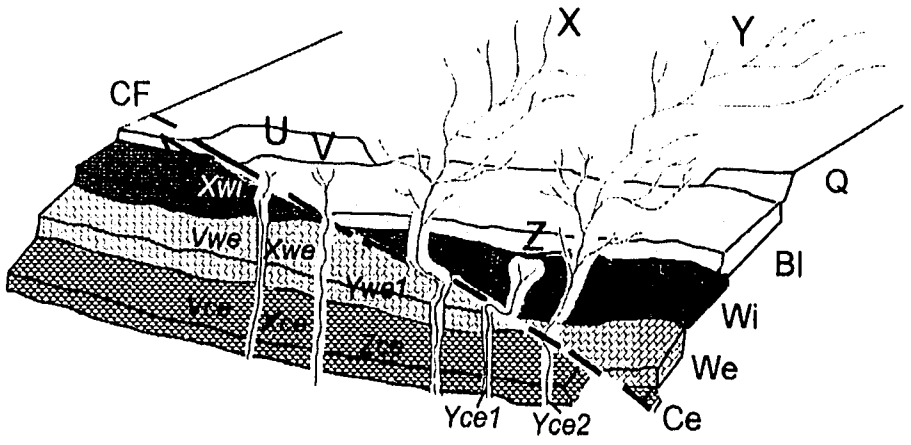

6f.) Formation of Santa Cruz terrace (SC), then dextral slip on CF. Creation of two beheaded drainages, and a shared lower reach (UVsc). Streams X, Y, and Z display no offset.

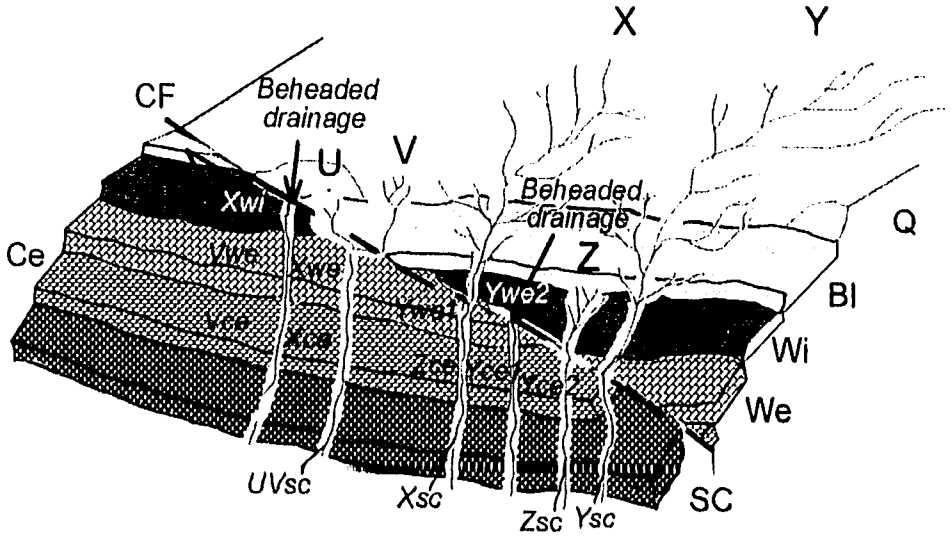

Figure 6. - Continued

6g.) Modern configuration of terraces and streams. Dextral slip along Frijoles segment. Creation of two new headwaters, one underfit lower reach, and one beheaded drainage. Alluvial fans may cover Cement terrace between fault traces. Constant uplift on the Santa Cruz Mountain block and increasing stream dissection may have caused erosion of marine terraces east of SGFZ.

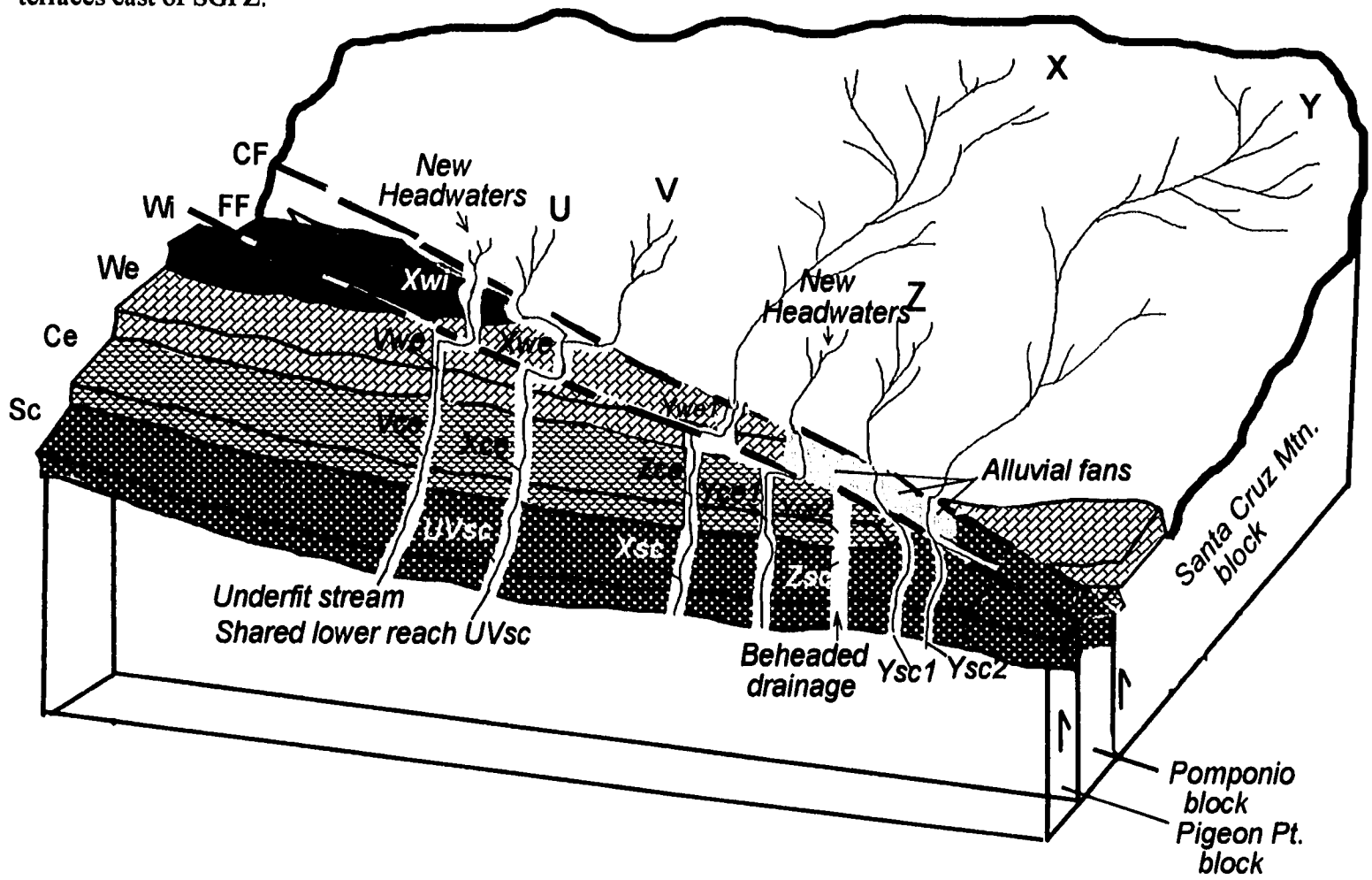

PREVIOUS WORK

Previous workers have estimated the slip rate of the SGfz by analyzing the apparent dextral offset of Neogene stratigraphic packages (Table 2), Pleistocene shoreline angles and fluvial deposits, Holocene archeological artifacts, and modern streams. Most Quaternary slip-rate estimates for the SGfz range from 4 to 11 mm/yr, although Hamilton (1984) and Hamilton and Sedlock (1991) interpreted the evidence to indicate only 1 to 3 mm/yr. The most recent work indicates that the Frijoles segment appears to be the most active within the fault zone (Stevenson and Ettreim, 1999; Weber et al., 1999b).

Offset Pleistocene Shoreline Angles and Faulted Strata

Recently, Weber et al. (1999a) modified an earlier slip-rate estimate of 6-11 mm/yr (Weber et al., 1979) for offset Pleistocene shoreline angles of marine terraces near Año Nuevo to 4-11 mm/yr. Hamilton (1984) argued that the mapped offset shoreline angles may not be offset at all (Fig. 7), and inferred a more irregular shoreline with little to no lateral movement.

Dating of Marine Terraces

The marine terraces can be used as approximate time datums to estimate the slip rate of the SGfz by analyzing which marine terrace contains the deflected portion of a stream. Therefore, it is essential to evaluate the accuracy of the terrace ages in order to bracket slip rates. Several investigators have attempted to date the marine terraces near

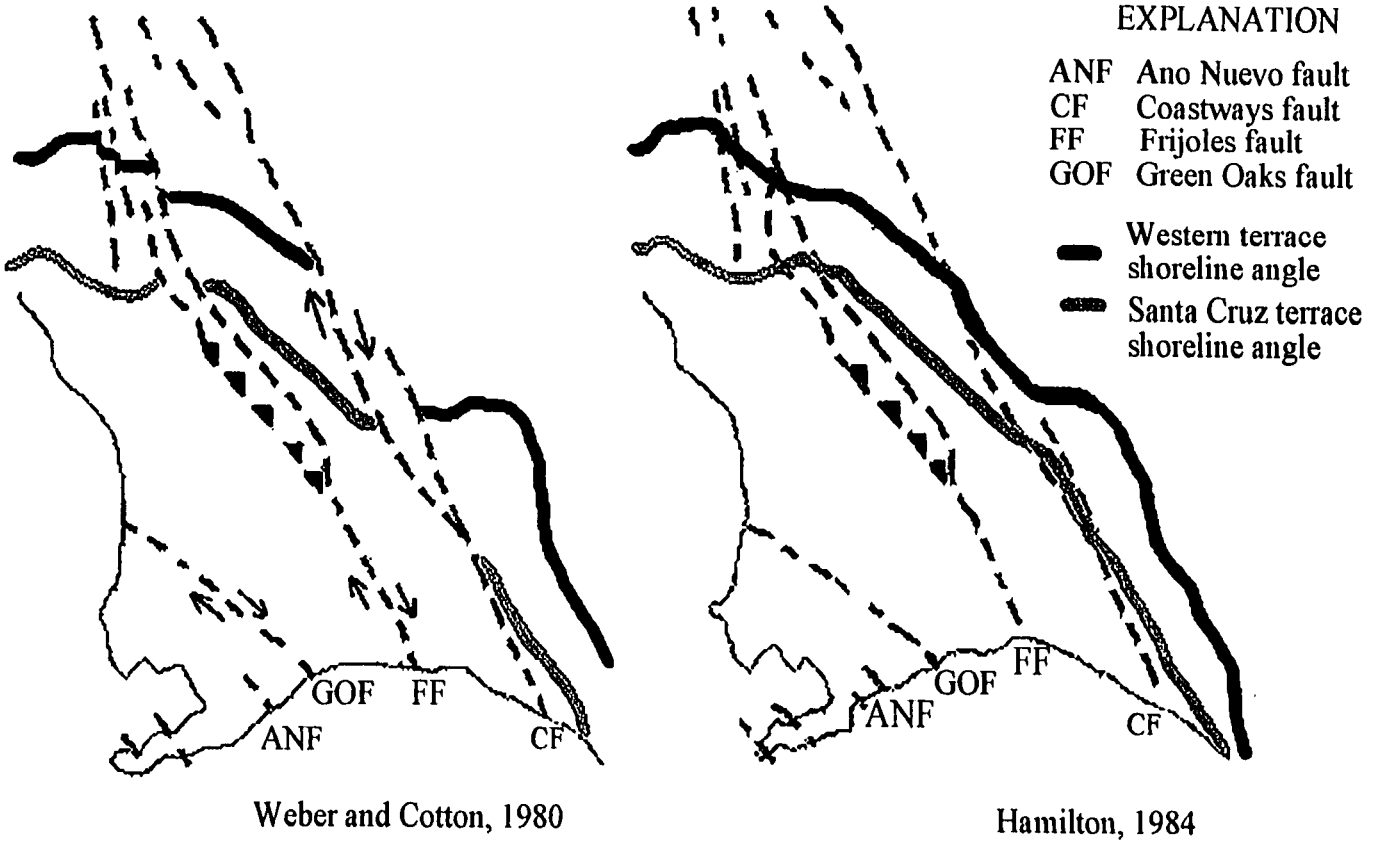

Figure 7. Interpretations of shoreline angles of marine terraces and fault offsets as mapped by Weber and Cotton (1980) and Hamilton (1984).

Año Nuevo and Davenport using various geochronologic techniques. Because the Santa Cruz terrace is the only fossil-bearing terrace near Año Nuevo and Davenport, it is the only terrace that can be dated directly; the older terrace ages are estimated assuming constant uplift rates and tilt rates, or correlation with eustatic highstands of known ages (Table 3).

Santa Cruz Terrace

According to Bradley and Griggs (1976), the Santa Cruz terrace includes three different platforms: Greyhound, Davenport, and Highway 1. The Highway 1 terrace is located within the study area, but the Greyhound and Davenport terraces are located farther south (Bradley and Griggs, 1976). According to Bradley and Griggs' (1976) interpretation of the eustatic sea level curve of Bloom et al. (1974), the Highway 1 terrace is 125 ka, which corresponds to isotope state 5e (slightly higher than modern sea level). Similarly, Lajoie (personal communication, 1996) determined that the Highway 1 terrace is 124 ka (isotope stage 5e).

Weber et al. (1999a) suggested that the Highway 1 terrace is 103 ka (isotope stage 5c). However, Bradley and Griggs (1976) inferred that a transgressive unit at 105 ka produced deposits that partly covered the Highway 1 and Davenport terraces. These young deposits may be those identified by Weber; if so, the Highway 1 terrace probably formed 125 ka and was partly covered with sediment about 103-105 ka.

Table 3. Estimated ages of marine terraces in the Santa Cruz region. Dashes represent platforms that were not dated. Ages are in thousands of years. The 5e and 5c refer to oxygen isotope stages used to identify global sea levels.

Marine Terrace	Assumed Uplift Rate[1] (0.16-0.26 mm/yr)	Tilt Rates[1] (1-9 m/km)	Assumed Uplift Rate[2] (0.1-0.3 mm/yr)	Global Sea Level Highstands[3]
6th - Quarry	1200	1000	----	19-780
5th - Blackrock	900	1050	430	15-610
4th - Wilder	700	750	320	13-515
3rd - Western	450	450	213	11-440
2nd - Cement	260	-----	125	9-320
1st - Santa Cruz Highway 1	5e-125	-----	5c-103	5e-124

[1]Bradley and Griggs, 1976.
[2]Weber et al., 1999a.
[3]Lajoie, personal communication, 1996.

Older Marine Terraces

Three sets of ages (Table 3) are estimated for the older terraces at Ben Lomond, which have been uplifted and tilted toward the Pacific Ocean since the late Tertiary (Bradley and Griggs, 1976; Lajoie, personal communication, 1996; Weber et al., 1999a). Bradley and Griggs dated the older terraces by using the age of the Santa Cruz terrace (125 ka) and calculating the ages of the older terraces, assuming constant uplift rates of 0.16-0.26 mm/yr and tilt rates of 1-9 m/km. Weber et al. (1999a) used the difference between rates of uplift on the Santa Cruz Mountain block (0.4 and 0.55 m/ka) and Pigeon Point block (0.15 and 0.30 m/ka) to determine that the late Quaternary uplift rate across the SGfz is 0.1 to 0.3 m/ka, with 0.15 the best estimate. They then used this uplift rate to estimate the ages of the terraces.

Lajoie (personal communication, 1996) counted sea level high stands of known ages back from the youngest Santa Cruz terrace to date the older terraces. He also noted that there is a large uncertainty when correlating any of the Santa Cruz terraces with terraces mapped west of the SGfz, and that independent age estimates for terraces calculated from direct dating techniques have not been convincing.

Apparent Offset of Streams and an Alluvial Fan

Two researchers, G. Weber and D. Hamilton, previously studied stream deflections near Año Nuevo and determined slip rates of 4-10 mm/yr (Weber, 1990) and 0.5-1.0 mm/yr (Hamilton, 1984), respectively. Weber studied streams south of Whitehouse Creek, and Hamilton studied streams north of Whitehouse Creek.

Streams South of Whitehouse Creek

According to Weber (1990), both the Cascade Creek and Año Nuevo Creek displacements (Fig. 5) occurred after the formation of the Highway 1 marine terrace and indicate Pleistocene fault movement since about 104 ka. Weber noted that Cascade Creek flows 426-823 m northwest of its projected path as it leaves the Santa Cruz Mountain block and shows no evidence of stream capture (Fig. 5). Therefore, he suggested that the creek has been deflected from its headwaters at a rate of 4-8 mm/yr. Weber (1990) also inferred that the abandoned drainage now occupied by the underfit Green Oaks Creek was previously occupied by a larger stream, Año Nuevo Creek (Fig. 5). The offset required for this association is 457 to 1,005 m (since about 100 ka), which indicates a slip rate of 5-10 mm/yr.

Weber (1990) also suggested that a beheaded fan that lies north of Cascade Creek was formed by the drainage lying immediately north of Cascade Creek (Stream B in Figs. 4 and 5; Plate 1). Weber did not publish a slip rate for this feature, but according to Figure 5, the fan was transported about 500-600 m along the Frijoles fault on the Highway 1 terrace, yielding a slip rate of 5-6 mm/yr.

Streams North of Whitehouse Creek

Hamilton (1984) determined a slip rate of 0.5-1.0 mm/yr for the SGfz based on the deflection of five streams (Table 4) north of the streams measured by Weber (1990). Hamilton initially assumed that Gazos Creek was once connected to Arroyo de los Frijoles Creek. He suggested that the current lower reach of Gazos Creek was originally

the lower reach of Old Womans Creek prior to capture by the Gazos Creek headwaters. He also assumed that stream deflection began 1 Ma, his arbitrarily chosen age for the Quarry terrace.

Table 4. Modern slip rates of the SGfz based on Hamilton's (1984) measurements of deflected streams north of and including Whitehouse Creek. Ages of marine terraces are from Table 3.

		Hamilton (1984)	Recalculated in this paper
Deflected Stream	Offset (km)	Slip Rate (mm/yr) Quarry = 1 Ma	Slip Rate (mm/yr) Quarry = 780 ka
Pomponio Creek	0.4	0.4	0.5
Pescadero Creek	0.9	0.9	1.2
Arroyo de los Frijoles Creek + Upper Gazos Creek	1.35	1.35	1.7
Old Womans Creek + Lower Gazos Creek	0.85	0.85	1.1
Whitehouse Creek	0.60	0.60	0.8

Hamilton's calculated slip rates of streams north of Gazos Creek were smaller than the slip rate calculated for the Arroyo de los Frijoles and Gazos Creeks restoration, so he inferred that the latter association probably was not valid. Hamilton did not explain the faster slip rate calculated for the beheaded Arroyo de los Frijoles and Gazos association, nor did he offer an alternate headwaters for Arroyo de los Frijoles Creek.

I recalculated Hamilton's slip rates using the same amount of displacement but the younger 780 ka age for Quarry terrace calculated by Lajoie (Table 3). The slip rates I calculated, 0.5-1.7 mm/yr (Table 4, column 4), are not significantly different from those calculated by Hamilton, 0.4-1.35 mm/yr (Table 4, column 3).

Offset During the Holocene

The SGfz near Half Moon Bay (Fig. la), sometimes referred to as the Seal Cove fault, has five active strands (Simpson et al., 1997). Two of these strands offset dated Holocene archeological sites near Half Moon Bay. Displacements of up to 3 m for the last event on the SGfz, 220 to 730 years ago, indicate a 4-13 mm/yr Holocene slip rate and the possibility of M = 7 earthquakes for the SGfz (Simpson et al., 1997). Trench studies across the fault zone indicate that two earthquakes have occurred since 670 AD (Simpson and Lettis, 1999). Offset paleochannels (80 to 85 ka) suggest cumulative post-late Pleistocene displacement of 300 to 360 m and a slip rate of 3.5 to 4.5 mm/yr (Simpson and Lettis, 1999).

Near Año Nuevo Point, trench work by Thornburg (1998) indicates recent ground surface rupture events during the last 6-8 ka, with a dextral slip rate of 0.2 to 0.5 mm/yr and a vertical uplift rate of 0.1 mm/yr. Recent trenching by Weber and Thornburg (1999) indicates that the Frijoles fault segment accommodates a majority of the Holocene displacement; the Coastways fault receives only a small portion of the late Holocene slip. Seismic profiles across the SGfz by Stevenson and Eittreim (1999) indicate that the onshore Frijoles fault is the primary and most recently active trace of the SGfz.

OBJECTIVES

The primary objective of this study was to determine if calculating the correlation coefficient of several drainage basin volumes across the SGfz could indicate the presence of captured streams caused by dextral offset. If dextral slip detached the lower drainage basins from the original headwaters, correlation coefficients were expected to be low (near zero) or negative. Restored drainage basins were then expected to show higher correlation coefficients.

Several stream reconstructions were created to obtain the highest possible correlation coefficients for drainage basins. Slip rates were then calculated for each of the successful restorations by evaluating which marine terrace, of known age, was incised by the offset stream and the amount of offset required to restore the drainage basin configuration.

A secondary objective of this study was to determine relative ages of streams in the study area by characterizing drainage basins through geomorphologic parameters, such as drainage basin volume. I also attempted to asses the relative amounts of uplift and erosion along the fault zone by comparing the degree of stream incision across all three structural blocks.

METHODS

Task #1: Stream Characterization

In order to compare drainage evolution within the study area, the stream order, magnitude, total length, basin area, drainage density, and basin volume were measured for each upstream segment east of the fault zone (Plate 1). Upper reaches include Little Butano Creek (LBu), Gazos Creek (G), Old Womans Creek (OW), Whitehouse Creek (W), Stream A (A), Stream B (B), Cascade Creek (C), Green Oaks Creek (GO), Cold Dip Creek (CD), Año Nuevo Creek (AN), Finney Creek (F), and Elliot Creek (E).

Stream incision was calculated for the five largest drainages that cross all three structural blocks: Arroyo de los Frijoles Creek, Little Butano Creek, Gazos Creek, Old Womans Creek, and Whitehouse Creek. Both the upper and lower basins were used for this calculation.

Several methods were used to calculate stream variables, including traditional procedures for calculating stream order, magnitude, length, drainage basin area and density. A computer software program was used to calculate drainage basin volume with digitized maps.

The stream characterization data were evaluated by determining the degree of correlation between the measured stream variables using correlation coefficients. A high correlation indicates that the variables evolved at approximately the same rate within the basin; a low correlation indicates independent evolution of such variables.

Stream Order, Magnitude, and Length

Stream order refers to the stream position in the hierarchy of tributaries (Leopold, 1992), whereas stream magnitude refers to sum of the orders and describes the cumulative hydrodynamics of the drainage basin (Mayer, 1990). Stream magnitude, order, and total length were measured from traced projections of drainage basins east of the Coastways fault. These projections were traced from 1:24,000 USGS topographic maps. The methods used to determine stream order and magnitude are shown in Figure 8.

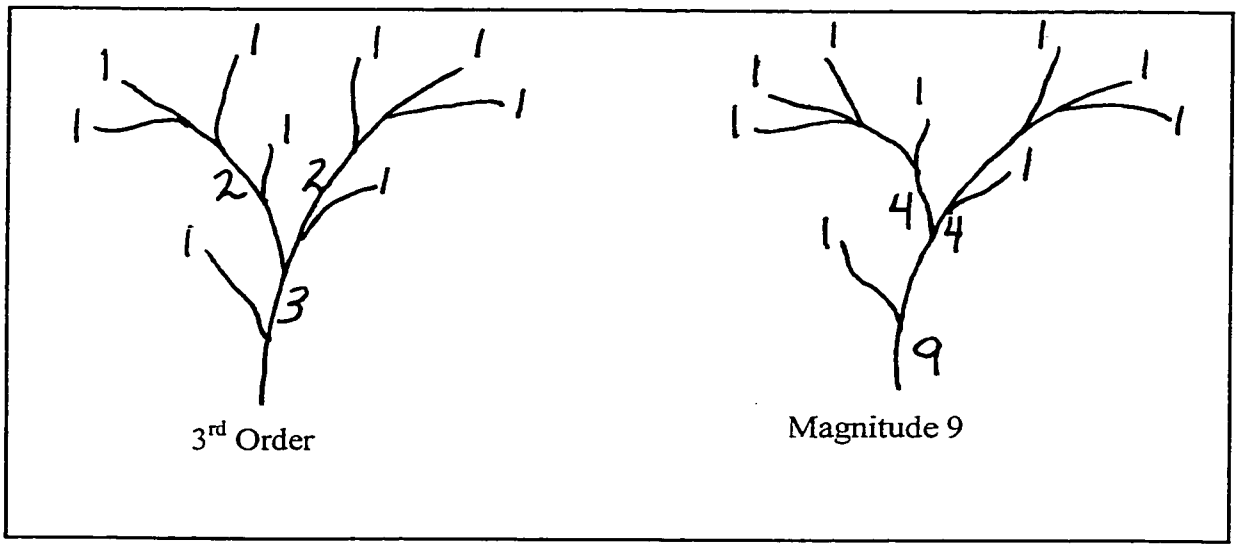

Figure 8. Sample stream order and stream magnitude calculations.

Drainage Basin Area and Density

Each drainage basin was outlined on a 1:24,000 USGS topographic map, and its area (A_d) was measured with an electronic planimeter. The sum of the lengths of stream

segments (ΣL) and the drainage basin area (A_d) were used to calculate the drainage density (D_d), which is a measure of the degree of dissection (Mayer, 1990):

$$\text{Drainage Density } (D_d) = \frac{\Sigma L \text{ (km)}}{A_d \text{ (km}^2\text{)}}$$

Drainage Basin Volume

The volume of each drainage basin (i.e., the volume of material that was eroded during stream development) was calculated using Dynamic Graphics Incorporated's EarthVision software application, which enables the analysis of geospatial relationships. EarthVision was used to convert digital elevation models (DEMs) into three dimensional (3-D) surface grids and to calculate the volumes of drainage basins east and west of the Coastways fault.

Five 10-meter USGS DEMs (Franklin Point, Pigeon Point, Año Nuevo, Big Basin, and San Gregorio) were imported into EarthVision. The DEMs (1:24,000 with a 40-foot contour interval) were imported as scattered data points and converted into 2-D grids. Two parallel grids were generated for each drainage basin (Fig. 9). Grid G1 represented the original DEM topography, and grid G2 represented the inferred paleosurface prior to stream erosion. Grid G2 was generated by EarthVision using same X and Y points as G1; however, the Z value was interpolated using the height of the drainage basin divides (G1) on either side of the channel.

Each grid contained data points that were arranged 10 m apart horizontally (Fig. 9). Four data points defined a grid cell (g) that was 10 x 10 m (Fig. 9). Each grid cell

was divided into twenty-five subcells (2 x 2 m) with the point in the center called a subgrid point. The height of each subgrid point was interpolated from the surrounding grid node values. The average height of the 25 subgrid points was determined to be the height of one grid cell (g_z). This method of averaging the height of the grid cell is called the "subgridding approach."

The volume of one grid cell is calculated as the difference between the Z values of the parallel grid cells multiplied by its area $[(g2_z - g1_z)(g1_x \times g1_y)]$. The sum of all the grid cell volumes within the basin boundary (Plate 1) represents the drainage basin volume.

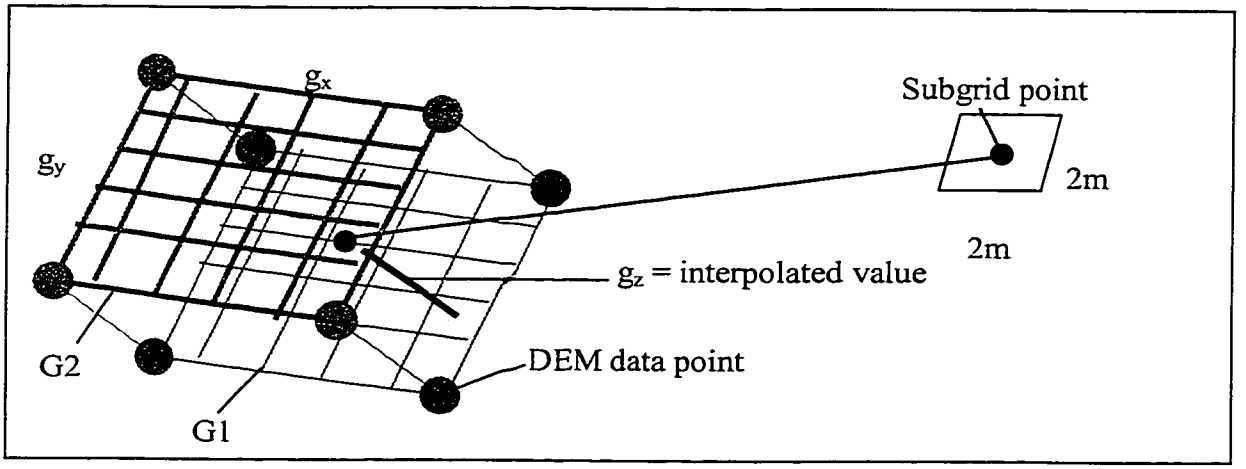

Figure 9. Schematic diagram of two parallel grid cells.

Correlation of Stream Variables

The correlation coefficient (r), a measure of the interdependence between two groups of variables, was used to determine whether stream order, magnitude, total stream

length, drainage basin area and volume, and drainage density are correlative. The correlation coefficient is defined as:

$$r_{xy} = \frac{1/n\ \Sigma(x_i - \mu_x)(y_i - \mu_y)}{\sigma_x \sigma_y}$$

where $-1 \leq r \leq 1$,
n = sample number,
x_i = value from x,
μ_x = mean of x,
y_i = value from y,
μ_y = mean of y,
σ_x = standard deviation of x, and
σ_y = standard deviation of y.

If large values of group x are associated with large values of group y, then r = 1. If small values of group x are associated with large values of group y, then r = -1. If values from the two groups are unrelated, then r = 0. Spearman's nonparametric correlation coefficient (r') is analogous to the parametric correlation coefficient r (Davis, 1986). For the nonparametric analysis of ranked ordinals, the data are calculated as follows:

$$r'_{xy} = 1 - \frac{6\Sigma\,[R(x_i) - R(y_i)]^2}{n(n^2-1)}$$

where R = the ranked values,
x_i = values of group x,
y_i = values of group y, and
n = the number of samples.

Stream Incision

Stream incision, or incision ratio, is measured as the width of a drainage divided by the mean height from the stream bottom to the drainage divide. The drainages chosen for incision analysis were: (1) Arroyo de los Frijoles Creek + Little Butano Creek, (2) Gazos Creek, (3) Old Woman Creek + Gazos Creek, and (4) Whitehouse Creek (Plate 1). These streams were chosen because each crosses all the structural blocks and because they are longer than other streams within the study area.

Stream incision was calculated from several cross-sections using 1:24,000 USGS topographic maps with a 40-foot contour interval. Cross-sections were constructed across streams where opposing drainage divides have roughly similar elevations (Plate 1). Some cross-section endpoints were located at benchmarks to improve the accuracy of the calculated incision ratio. However, to account for the intrinsic error associated with estimating elevations on topographic maps and the lack of benchmarks at every cross-section, an estimated 40-foot uncertainty, one contour interval, was assumed for each basin-height measurement.

Task #2: Apparent Deflection of Modern Streams

Apparent stream deflections were measured on 1:24,000 USGS topographic maps. These measurements were made parallel to the Coastways and Frijoles faults. Stream deflection measurements north of and including Whitehouse Creek were compared to Hamilton's (1984) measurements. The measured offset of lower Green

Oaks Creek from Año Nuevo Creek, and the deflection of Cascade Creek were compared to Weber's 1990 measurements.

It was assumed that stream origin and offset occurred shortly after subaerial exposure of the marine terraces. Therefore, the minimum and maximum ages of the marine terraces (Table 3) bracket the onset of stream formation and offset, and are used to estimate minimum and maximum slip rates.

Task #3: Paleodrainage Reconstructions

In order to reconstruct the original drainage basins, I made three major assumptions regarding basin development in the study area. First, I assumed that factors affecting stream erosion rates, such as lithology, structure, climate, and vegetation, are homogenous within each structural block and, thus, that streams erode or deposit at the same rate. Second, I assumed that stream flow was directed perpendicular, not parallel, to the fault zone. Third, I assumed that the majority of dextral slip occurred mainly along the Coastways segment of the SGFz.

Drainage basin volumes east and west of the SGfz were calculated in Task #1. A correlation coefficient (r) was calculated to determine the relationship between the upper and lower basin volumes in their present configuration. In an attempt obtain the highest possible correlation coefficients for drainage basins in the study area, streams were restored by two different methods.

The first set of reconstructions (A1-A3) involved restoring slip along the SGfz by moving streams west of the Coastways fault southeast along the fault zone in one-

kilometer increments, totaling 3 km of restoration. For example, A1 is offset 1 km, A2 is offset 2 km, and A3 is offset 3 km. Large, modern lower reaches west of the SGfz that receive water from more than one upper reach were omitted from the final paleodrainage reconstructions A1-A3, with the assumption that these lower reaches were altered.

The second set of paleodrainage reconstructions (B1-B12) was created by sorting and matching all the upper and lower basins in order of descending volume in an attempt to detect stream configurations with high correlation coefficients. Unlike A1-A3, this second set of reconstructions was not based on the assumption that all lower reaches have the same incremental offset along the Coastways fault zone. Instead, reconstructions B1-B12 assumed that older streams would likely show greater dextral offset.

For both sets of reconstructions, a stream restoration was rejected if: (1) the amount of dextral slip created an unreasonable southern boundary of the marine terrace shoreline angle, (2) it required sinistral rather than dextral slip, or (3) it created lower reaches that were underfit for their headwaters. Slip rates for the successful reconstructions were calculated using the minimum and the maximum ages of marine terraces from Table 3. Stream offset on terraces north of Whitehouse Creek (not mapped) is assumed to have occurred on Blackrock or Quarry terraces.

RESULTS

Task #1: Stream Characterization

Stream magnitude, order, and drainage basin area were measured from the traced map projections in Appendix A. Drainage basin volume, basin area, stream length, and stream magnitude generally increase northward (Table 5). Assuming that drainages with larger volumes are older than those with smaller volumes, then streams in the study area must have originated at different times. If this assumption is true, then basins north of Whitehouse Creek are generally older than those to the south (Table 5a). However, the location of drainage basins from north to south does not match the list of descending drainage basin volumes listed in Table 5a, indicating a complex stream development history like that shown in Figure 6.

Parametric statistical analyses (Table 5b) of stream magnitude, total length, drainage basin area, volume, and drainage density show a strong positive correlation, indicating that these parameters probably evolve at the same rate within the drainage basins. Nonparametric analysis shows that stream magnitude and order (Table 5c) are weakly correlated.

Stream incision ratios were calculated along profiles shown on Plate 1, which are the same cross-sections shown in Appendix B. Stream incision is greatest on the uplifted blocks (Santa Cruz Mountain and Pigeon Point blocks) and near the fault zones (Table 6 and Fig. 10); it is lower and/or deposition is greater within the Pomponio block, which is the graben between the Santa Cruz Mountain and Pigeon Point blocks. Because the

Table 5. Quantitative analyses of stream characteristics and statistical analyses of upper drainage basins east of the SGfz.

Upper Drainage Basins (North to South)	Upper Drainage Basins (Sorted by Volume)	Volume (km^3)	A_d (km^2)	ΣL (km)	D_d = (ΣL/ A_d)	Magnitude	Order
a) Little Butano Creek	Gazos Creek	2.391	33.03	104.3	3.8	237	5th
Gazos Creek	Whitehouse Creek	0.680	10.82	42.8	3.9	116	4th
Old Womans Creek	Little Butano Creek	0.572	12.38	36.0	3.5	68	4th
Whitehouse Creek	Año Nuevo Creek	0.362	8.03	26.5	3.3	55	3rd
Stream A	Old Womans Creek	0.218	7.02	25.5	3.6	62	4th
Stream B	Elliot Creek	0.172	3.96	14.7	3.7	45	3rd
Cascade Creek	Cascade Creek	0.160	4.44	21.0	4.7	48	3rd
Green Oaks Creek	Green Oaks Creek	0.033	2.12	5.3	2.5	14	3rd
Cold Dip Creek	Finney Creek	0.020	1.30	4.0	3.1	12	3rd
Año Nuevo Creek	Stream B	0.012	1.71	8.0	4.7	33	4th
Finney Creek	Stream A	0.011	1.62	6.3	3.8	18	3rd
Elliot Creek	Cold Dip Creek	0.004	0.97	3.4	3.5	9	3rd

b) Parametric correlation coefficient (r)	
Area & Length	0.99
Volume & Area	0.99
Magnitude & Length	0.99
Magnitude & Area	0.99
Volume & Length	0.98
Magnitude & Volume	0.98
Magnitude & Density	0.84
Density & Length	0.81
Density & Area	0.78
Density & Volume	0.73

c.) Nonparametric (r') correlation coefficient	
Magnitude & Order	0.36

Table 6. Incision ratios for streams near Año Nuevo Point. Cross-section lines are shown in Plate 1. Data are graphically shown in Figure 10. Cross-sections F-F', G-G', and C-C' are listed twice because Gazos Creek and Old Womans Creek share the same lower reaches.

Stream	Cross Section	Width (W) (ft)	Height (H) (ft)	Incision I = W/H	Uncertainty (±) [I - W/(40 + H)]
Arroyo de los Frijoles and Little Butano Creeks	I-I'	4420	330	13	1.5
	J-J'	5980	370	16	1.6
	E-E'	6760	340	20	2.1
	D-D'	5500	600	9.2	0.57
	U-U'	6760	860	7.9	0.35
Gazos Creek	F-F'	1430	390	3.7	0.34
	G-G'	3900	500	7.8	0.58
	C-C'	4160	500	8	0.6
	B-B'	4000	690	5.8	0.32
	V-V'	7000	1200	5.8	0.19
	T-T'	10400	1100	9.5	0.33
Old Womans Creek	F-F'	1430	390	3.7	0.34
	G-G'	3900	500	7.8	0.58
	C-C'	4160	500	8	0.6
	N-N'	3900	670	5.8	0.33
	S-S'	3180	560	5.7	0.38
Whitehouse Creek	A-A'	1300	185	7.0	1.3
	O-O'	2900	270	11	1.4
	Y-Y'	6890	560	12	0.82
	R-R'	6730	1010	6.7	0.25
	W-W'	7540	960	7.9	0.31

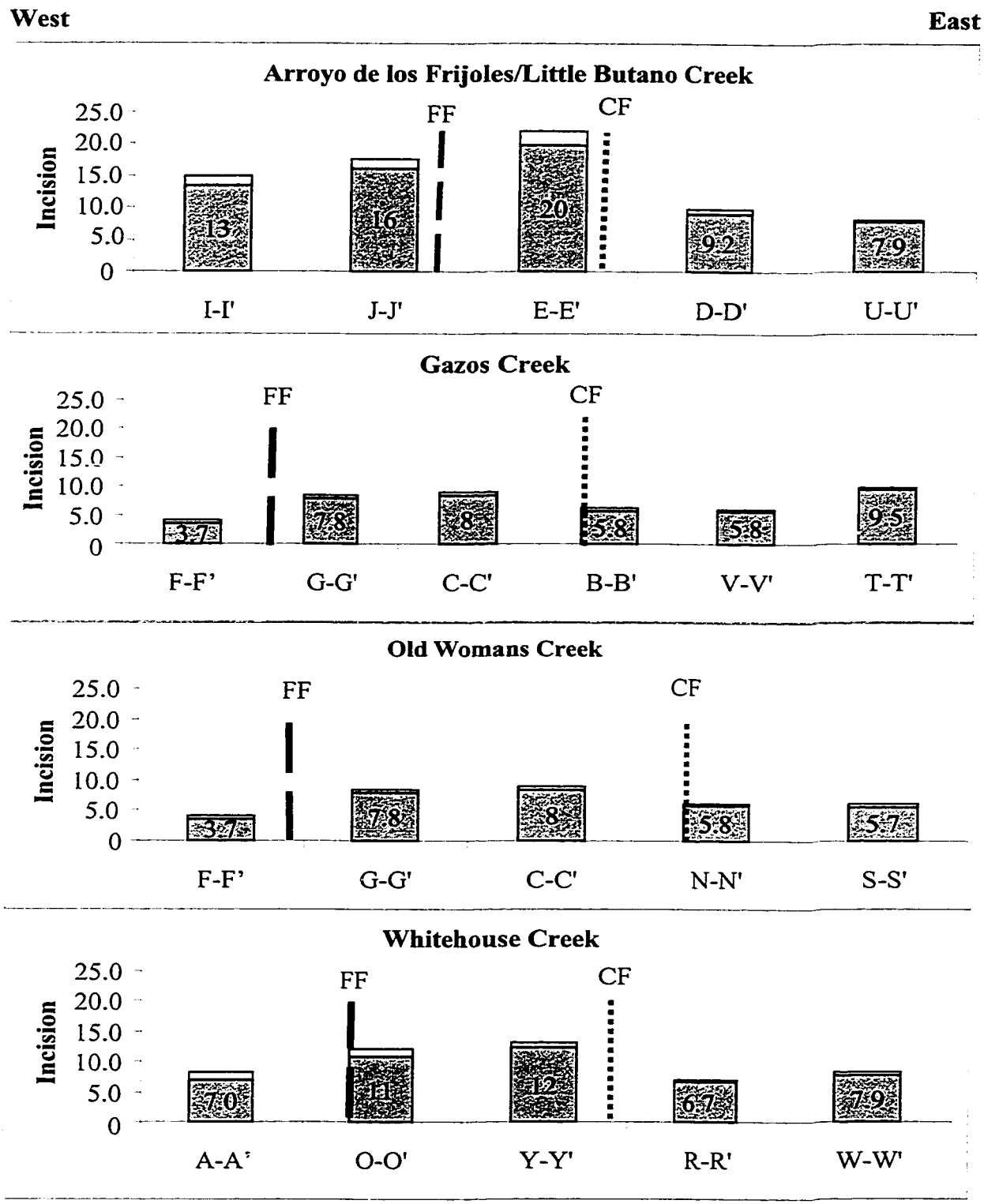

Figure 10. Incision ratios of streams. The incision is dark gray, the uncertainty is light gray, the Frijoles fault (FF) is dashed, and the Coastways fault (CF) is dotted.

Santa Cruz Mountain block is more incised than the Pigeon Point block, more dip-slip movement may have occurred along the Coastways fault segment than along the Frijoles fault segment. Cross-sections F-F', G-G', and C-C' are listed twice in Table 6 because Gazos Creek and Old Womans Creek share the same lower reaches (Plate 1).

Task #2: Apparent Deflection of Modern Streams

Streams south of Whitehouse Creek that may be offset by the Coastways fault include: (1) Stream A, offset on Wilder terrace, (2) Cascade Creek, offset on Highway 1, and (3) Año Nuevo Creek, offset on Highway 1 (Fig. 5). The deflected portion of Whitehouse Creek appears to lie along a shear zone of the Frijoles fault segment, which may have also displaced the Wilder terrace (Fig. 5). The beheaded fan was not included in this study because it is possible that the fan was at one time contiguous with Stream A, and recent active uplift along the Frijoles segment (Fig. 5) may have diverted its flow along the more easterly part of the Frijoles shear zone. Stream offset north of and including Whitehouse Creek was measured by Hamilton (1984) and stream offset south of and including Whitehouse Creek was measured by me.

The modern slip rates estimated by this technique are 1-3 mm/yr for the Frijoles fault and 1-5 mm/yr for the Coastways fault (Table 7). Slip rates south of Whitehouse Creek appear to be 1-2 mm/yr faster than those to the north. The Frijoles slip rate south of Whitehouse Creek was greater primarily because of the larger offset (0.90 km) and younger marine terrace (Wilder) I used in Table 7b.

Table 7. Slip rates of deflected streams (a.) north and (b.) south of Whitehouse Creek. Estimated ages of marine terraces are from Table 3. It is assumed that stream origin and offset occurred shortly after subaerial exposure of the marine terraces.

			Slip Rate (mm/yr)					
		Offset[1]	Quarry-Blackrock		Wilder		Highway 1	
Stream	Fault	(km)	1200	430	700	320	125	103
a.) Slip rates north of Whitehouse Creek								
Arroyo/ Gazos	C	1.35	1.12	3.11				
Gazos/Old Womans	C	.85	0.71	2.0				
Whitehouse	F	.60	.50	1.14				
b.) Slip rates south of Whitehouse Creek								
Whitehouse	F	0.90			1.3	2.8		
Stream A	C	0.4			0.6	1.3		
Cascade	C	0.6					4.8	5.8
Año Nuevo/ Green Oaks	C	0.5					4	4.8
		Mean Slip Rates (mm/yr) rounded to the nearest whole number						
Frijoles fault	a.)		1	1				
	b.)				1	3		
Coastways fault	a.)		1	3				
	b.)				1	1	4	5

[1]Slip along the Frijoles (F) and Coastways (C) fault segments are considered to be independent in this analysis because this analysis concerns modern *stream deflection*, not *total slip* across the fault zone.

Task #3: Paleodrainage Reconstructions

Many of the upper drainage basins east of the Coastways fault have a greater volume than the lower drainage basins west of the fault, except Stream B and possibly Stream A, which appear to have underfit lower reaches (Table 8 and Fig. 11). This observation is consistent with the higher incision ratios for the upper reaches, as discussed above.

Table 8. Volumes of lower and upper drainage basins. Graph of data shown in Figure 11. The upper basin of Butano and lower basin of Elliot lack a distinguishable reach, so no volumes were calculated. Both Gazos Creek headwaters and Old Womans Creek flow into the lower reaches of Gazos Creek.

r = 0.32

Lower Drainage Basins	Vol. km^3	Upper Drainage Basins	Vol. km^3
Butano Creek	0.8630	*No upper reach*	---------
Gazos Creek	0.1102	Gazos Creek + Old Womans	2.6093
Whitehouse Creek	0.0512	Whitehouse Creek	0.6800
Arroyo de frijoles Creek	0.3746	Little Butano Creek	0.5717
Año Nuevo Creek	0.0018	Año Nuevo Creek	0.3618
No lower reach	----------	Elliot Creek	0.1716
Cascade Creek	0.0003	Cascade Creek	0.1601
Green Oaks Creek	0.0007	Green Oaks Creek	0.0333
Finney Creek	0.0001	Finney Creek	0.0200
Stream B	0.0134	Stream B	0.0117
Stream A	0.0110	Stream A	0.0115

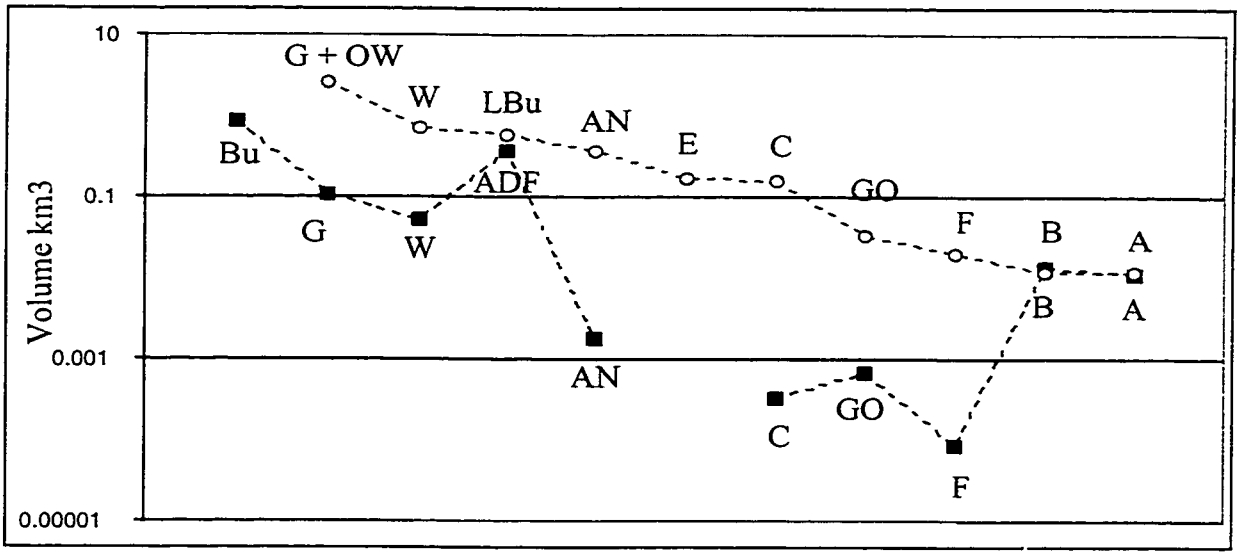

Figure 11. Comparison of the drainage basin volumes across the fault zone. Upper stream segments ○ and lower stream segments ■. The streams include: Stream A (A), Año Nuevo (AN), Arroyo de los Frijoles (ADF), Stream B (B), Butano (Bu), Cascade (C), Elliot (E), Finney (F), Gazos (G), Green Oaks (GO), Little Butano (LBu), Old Womans (OW), and Whitehouse (W). Upper basins are sorted in descending order and aligned with their respective lower basins. No horizontal scale is implied.

The present position of streams yields a weak, positive correlation ($r = 0.32$) between the upper and lower drainage basins. This weak association may have been caused by either strike slip or dip slip within the fault zone or a recent change in sea level. Any change in sea level or movement along the fault zone would create a disturbance in the drainages, requiring streams within each drainage basin to either erode or deposit sediment to re-attain equilibrium. Streams in the study area may be in the process of attaining equilibrium after the most recent change in sea level or movement along the fault zone, which may explain the weak, positive correlation.

Paleodrainage Reconstructions A1-A3

Paleodrainage reconstructions A1-A3 are listed in Table 9 and shown spatially in Figures 12-14. Each reconstruction shows progressively more displacement; the amount of restored slip is least in A1 (1 km) and greatest in A3 (3 km). The timing of slip was determined using the minimum and the maximum ages (Table 3) of the marine terrace that was incised by the offset lower reach (Table 10, column 4). The minimum and maximum slip rates were calculated using these terrace ages (Table 10, column 5). The alluvial cover (indicated in Fig. 12-14) makes it difficult to determine if offset occurred on the Cement or Santa Cruz terraces, so two slip rates are shown in Table 10. Slip rates were rounded to the nearest whole number (Table 10, column 6). The range in slip rate estimates using the Santa Cruz terrace are 1-10 mm/yr (A1), 2-19 mm/yr (A2), or 3-29 mm/yr (A3); slip rates using the Cement terrace are slightly lower.

Table 9. Paleodrainage reconstructions A1-A3. Whitehouse Creek, Stream A, Stream B, Cascade Creek, Green Oaks Creek, and Año Nuevo Creek were the only lower reaches used in reconstructions A1-A3.

Lower reach segment	Possible upper reach	Recon-struction	Figures
Whitehouse Creek	Stream A	A1	12
	Stream B	A2	13
	Cascade Creek (southern limit)	A3	14
Stream A	Stream B	A1	12
	Cascade Creek	A2	13
	Green Oaks Creek (southern limit)	A3	14
Stream B	Cascade Creek	A1	12
	Green Oaks Creek	A2	13
	Año Nuevo Creek (southern limit)	A3	14
Cascade Creek	Green Oaks Creek	A1	12
	Cold Dip Creek	A1	12
	Año Nuevo Creek	A2	13
	Finney Creek (southern limit)	A3	14
Green Oaks Creek	Finney Creek	A2	13
	Elliot Creek (southern limit)	A3	14
Año Nuevo Creek	Finney Creek	A1	12
	Elliot Creek	A2	13

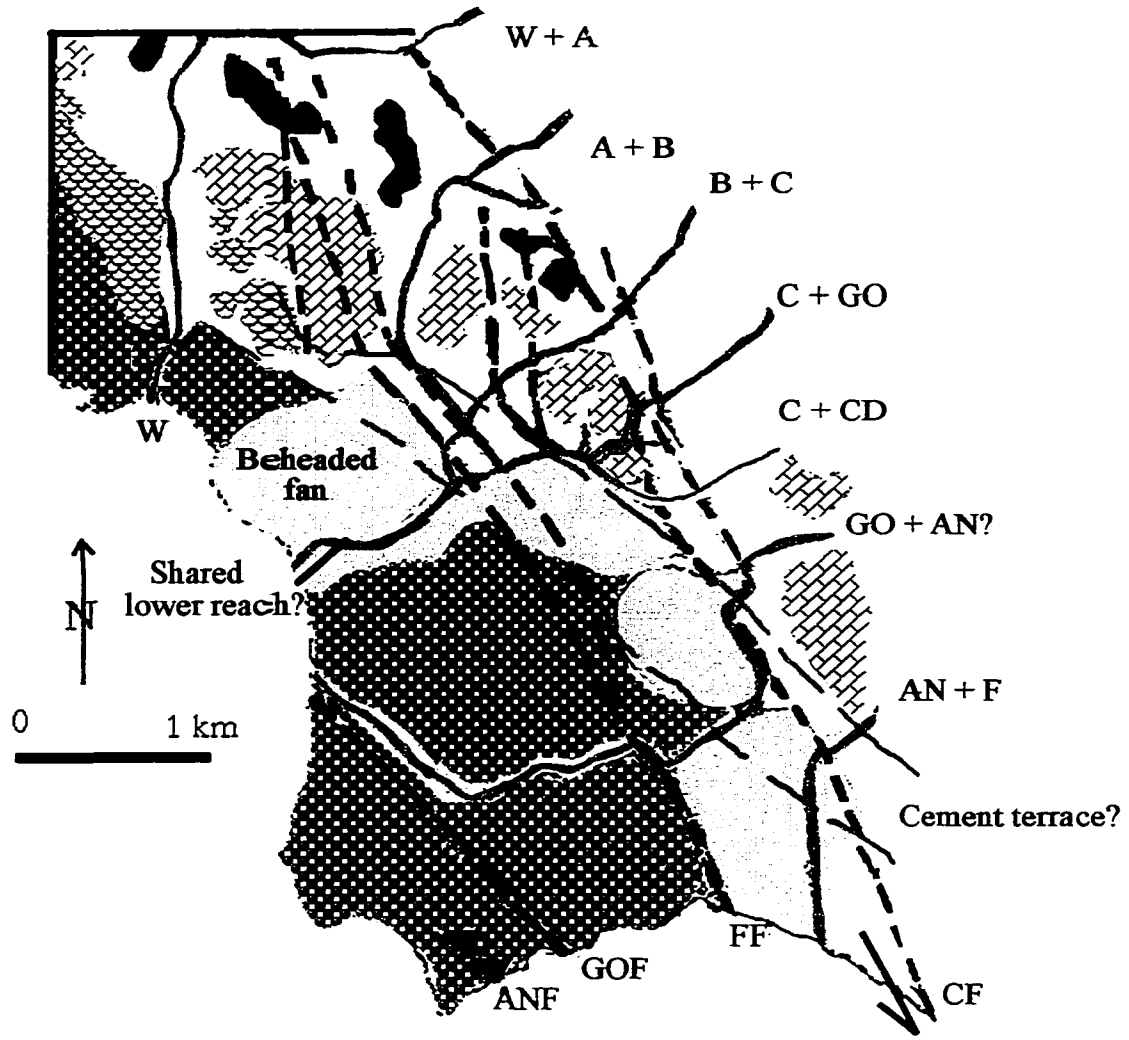

EXPLANATION

- Santa Cruz terrace
- Cement terrace (exposed)
- Western terrace
- Wilder terrace
- Alluvial fan
- Fault trace
- Inferred boundaries of Cement terrace

STREAMS

A	Stream A
AN	Ano Nuevo Creek
B	Stream B
C	Cascade Creek
CD	Cold Dip
F	Finney Creek
GO	Green Oaks Creek
W	Whitehouse Creek

FAULTS

ANF	Ano Nuevo thrust fault
CF	Coastways fault
FF	Frijoles fault
GOF	Green Oaks fault

Figure 12. Paleodrainage reconstruction A1 with 1 km of offset along the Coastways fault.

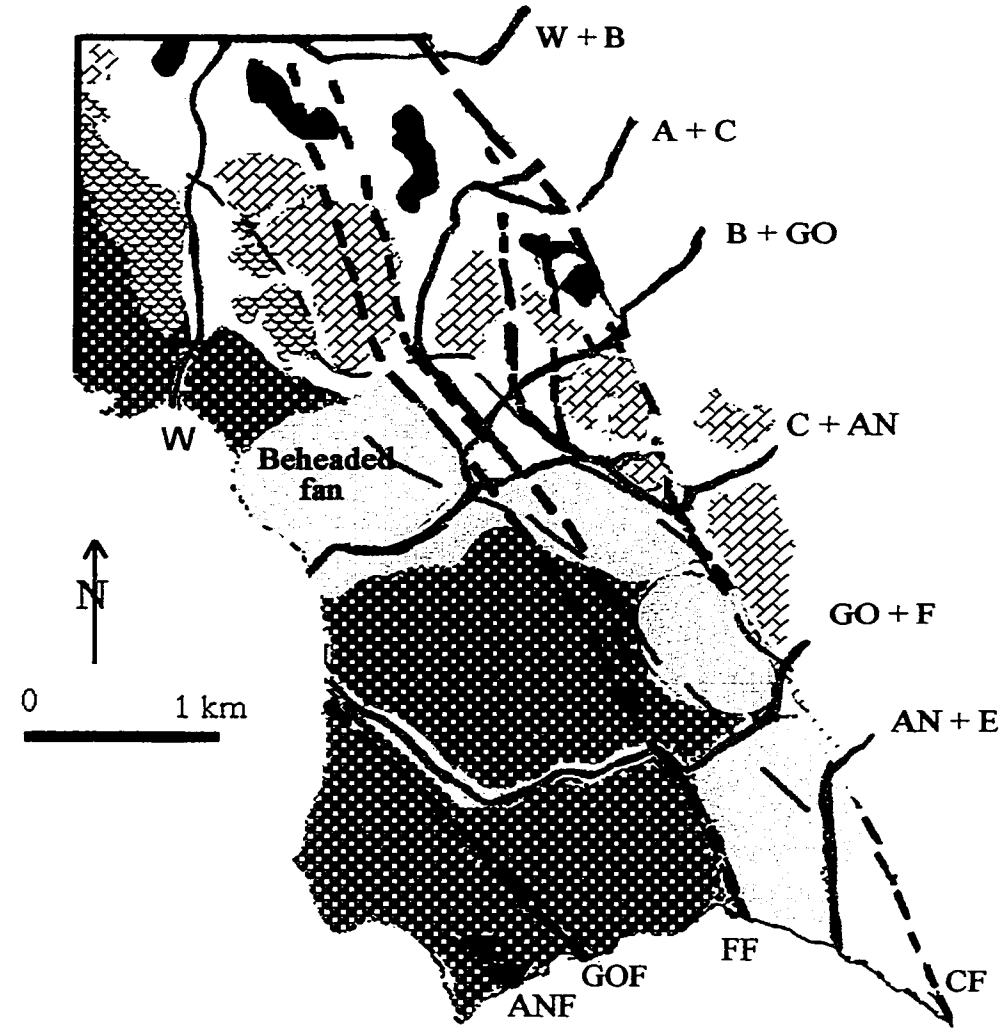

EXPLANATION

- Santa Cruz terrace
- Cement terrace (exposed)
- Western terrace
- Wilder terrace
- Alluvial fan
- Fault trace
- Inferred boundaries of Cement terrace

STREAMS

A	Stream A
AN	Ano Nuevo Creek
B	Stream B
C	Cascade Creek
GO	Green Oaks Creek
E	Elliot Creek
F	Finney Creek
W	Whitehouse Creek

FAULTS

ANF	Ano Nuevo thrust fault
CF	Coastways fault
FF	Frijoles fault
GOF	Green Oaks fault

Figure 13. Paleodrainage reconstruction A2 with 2 km of offset along the Coastways fault.

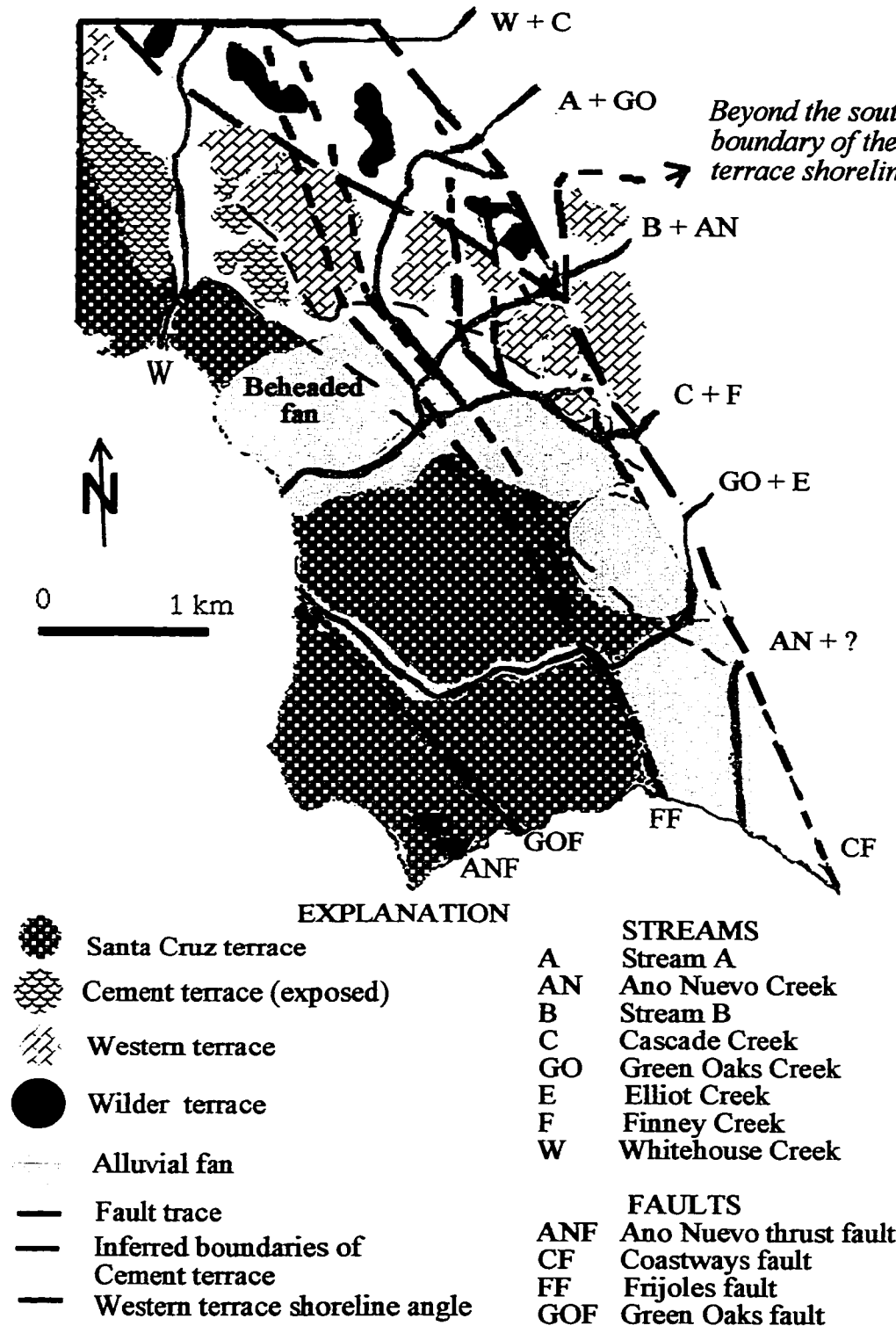

Figure 14. Paleodrainage reconstruction A3 with 3 km of offset along the Coastways fault.

Table 10. Paleodrainages reconstructed using one-kilometer incremental offsets (A1-A3). Stream offsets are approximate and rounded to the nearest whole number. Estimated ages of marine terraces are from Table 3. It is assumed that stream origin and offset occurred shortly after subaerial exposure of the marine terraces. The final slip rate is rounded to the nearest whole number.

Lower Stream	Upper Stream	[1]Marine Terrace	Age of offset (ka)	Min/max slip rates (mm/yr)	Range of slip rates (mm/yr)
1km Offset (A1; Fig. 12)					
Whitehouse Creek	Stream A	Bl – Wi	1050-320	.95-3.1	1-10
Stream A	Stream B	Wi	750-320	1.3-3.1	
Stream B	Cascade Creek	We	450-213	2.2-4.7	
Cascade Creek	Green Oaks Creek	We	450-213	2.2-4.7	
Año Nuevo Creek	Finney Creek	SC/Ce	125-103/320-125	8-9.7/3.1-8	(with Cement = 1-8)
2 km Offset (A2; Fig. 13)					
Whitehouse Creek	Stream B	Bl-Wi	1050-320	1.9-6.3	2-19
Stream A	Cascade Creek	Wi	750-320	2.7-6.3	
Stream B	Green Oaks Creek	We	450-213	4.4-9.4	
Cascade Creek	Año Nuevo Creek	We	450-213	4.4-9.4	
Green Oaks Creek	Finney Creek	SC/Ce	125-103/320-125	16-19.4/6.3-16	
Año Nuevo Creek	Elliot Creek	SC/Ce	125-103/320-125	16-19.4/6.3-16	(with Cement = 2-16)
3 km Offset (A3; Fig. 14) Southern limit of the marine terraces					
Whitehouse Creek	Cascade Creek	Bl-Wi	1050-320	2.9-9.4	3-29
Stream A	Green Oaks Creek	Wi	750-320	4.0-9.4	
Stream B	Año Nuevo Creek	We	450-213	6.7-14.1	
Cascade Creek	Finney Creek	SC/Ce	125-103/320-125	24-29/9.4-24	
Green Oaks Creek	Elliot Creek	SC/Ce	125-103/320-125	24-29/9.4-24	(with Cement = 3-24)

[1]Marine terraces include: Blackrock (Bl), Wilder (Wi), Western (We), Cement (Ce), and Santa Cruz (SC).

Reconstruction A1 has a reasonable geometric stream configuration (Fig. 12), but has a weak, inverse correlation (-0.15) between upper and lower basin volumes. Reconstruction A2 has a reasonable geometric stream and marine terrace configuration (Fig. 13), but it shows a strong, inverse correlation (-0.51) between upper and lower basin volumes. Reconstruction A3 creates an unreasonable shoreline configuration of the Western marine terrace boundary (Fig. 14), yet it is the only reconstruction of the three with a positive correlation (0.18) between upper and lower basin volumes. In comparison, the present stream configuration shows a higher correlation (0.72) between the same upper and lower basin volumes (Fig. 15).

Lower Finney Creek was omitted from reconstructions A1-A3 because it is located only on the Santa Cruz Mountain block. Lower reaches that receive or were suspected of having received flow from more than one headwater (Butano Creek, Arroyo de los Frijoles Creek, and Gazos Creek) were omitted because they may have an increased lower basin volume.

Figure 15. Modern stream configuration and paleodrainage reconstructions A1-A3 for the upper (O) and lower (■) drainage basins south of Whitehouse Creek. Upper basins are sorted by descending volume. Streams include: Stream A (A), Año Nuevo Creek (AN), Stream B (B), Cascade Creek (C), Elliot (E), Finney Creek (F), Green Oaks Creek (GO), and Whitehouse Creek (W). r = correlation coefficient; UF = underfit lower reaches.

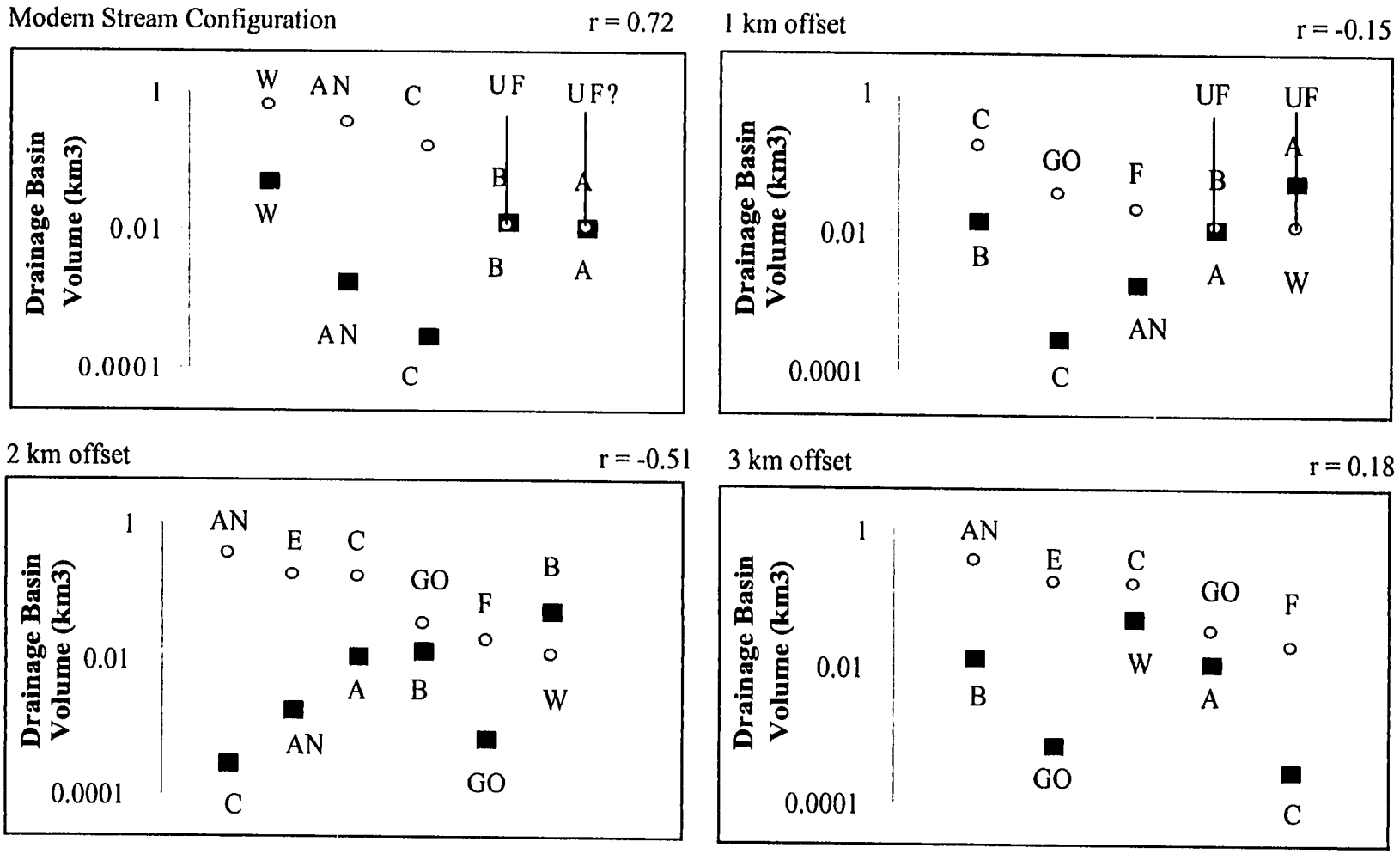

Paleodrainage Reconstructions B1-B12

Table 11 lists the feasible reconstructions from B1b-B12b, with their required offsets and respective slip rates. Reconstructions that are duplicates from Task #2 and the A1-A3 reconstructions are identified in the comments column of Table 11. Paleodrainage reconstructions B1-B12 (Fig. 16) show all the possible combinations of upper and lower basins within the study area, indicating that all the reconstructions yielded high correlation coefficients (0.79-1).

Most upper basins can be matched with two or more lower basins (Table 11); for example, upper Año Nuevo Creek is matched with lower Año Nuevo Creek (B3b), lower Cascade Creek (B1b), and lower Green Oaks Creek (B2b). Basins with such multiple possible correlatives cannot be used to determine unique matches and, thus, unique slip rates. In contrast, the upper basins of Stream B, Cold Dip Creek, Little Butano Creek, and Old Womans Creek are matched with a single lower basin (shaded rows in Table 11), and indicate 0-1.0 km of dextral offset and a 0-10 mm/yr slip rate.

All restorations that moved lower basins to the left of the upper basins shown in B1a required sinistral movement; restorations farther to the right than in B12a yielded only underfit lower reaches. The B1a-B12a paleodrainage reconstructions that (1) placed lower basins beyond the reasonable southern boundary of the Western marine terrace shoreline (see Fig. 14), (2) required sinistral fault slip, or (3) created underfit lower reaches are indicated in Figure 16.

Table 11. Paleodrainage reconstructions B1b-B12b. Data are sorted in alphabetical order by upper streams. Upper streams with only one matching lower reach are shaded. Marine terrace ages (not shown) are from Table 3. Offset is measured to the nearest whole number. Stream abbreviations are those used in Figure 2.

Recon-struction	Upper Stream	Lower Stream	Offset (km)	Marine terrace and slip rate (mm/yr)					Comments
				Quarry-Blackrock	Wilder	Western	Cement	Santa Cruz	
B3b	AN	AN	0						No slip
B1b	AN	C	2						A2 – Table 10, Fig. 13
B2b	AN	GO	1						Task #2 – Table 7, Fig. 5
B10b	B	A	1		1-3				A1 – Table 10, Fig. 12
B7b	C	A	2						A2 – Table 10, Fig. 13
B8b	C	B	1						A1 – Table 10, Fig. 12
B4b	C	C	1						Task #2 – Table 7, Fig. 5
B9b	CD	C	1				3-8	8-10	A1 – Table 10, Fig. 12
B5b	E	AN	2						A2 – Table 10, Fig. 13
B2b	E	F	1						No mapped marine terraces
B8b	F	AN	1						A1 – Table 10, Fig. 12
B5b	F	F	0						No slip
B7b	F	GO	2						A2 – Table 10, Fig. 13
B5b	G	ADF	2						No mapped marine terraces
B5b	G	ADF	5						No mapped marine terraces
B6b	G	Bu	1						No mapped marine terraces
B6b	G	Bu	6						No mapped marine terraces
B4b	G	G	0						No slip
B9b	GO	B	2						A2 – Table 10, Fig. 13
B5b	GO	C	1						A1 – Table 10, Fig. 12
B6b	GO	GO	0						No slip
B7b	Lbu	ADF	0	0					No slip
B8b	OW	G	1	1-2					No mapped marine terraces
B6b	W	ADF	4						No mapped marine terraces
B5b	W	G	3						No mapped marine terraces
B4b	W	W	0						Task #2 – Table 7, Fig. 5

Figure 16. Paleodrainage reconstructions B1-B12. Upper (O) and lower basin (■) volumes are sorted in descending order. Stream pairs were omitted if the reconstructions extended beyond the southern limit of the marine terrace shoreline angle (BSLMT), required sinistral movement (RSM), or created underfit lower drainages (UF). Reconstructions that were not omitted from (a.), shown in bold, are graphed again in (b.) with the required offset rounded to the nearest whole number. r_1= correlation coefficient of all paired streams (a.), including those omitted from the reconstructions; r_2 = correlation coefficient of remaining feasible reconstructions (b.). Stream abbreviations are those used in Figure 2.

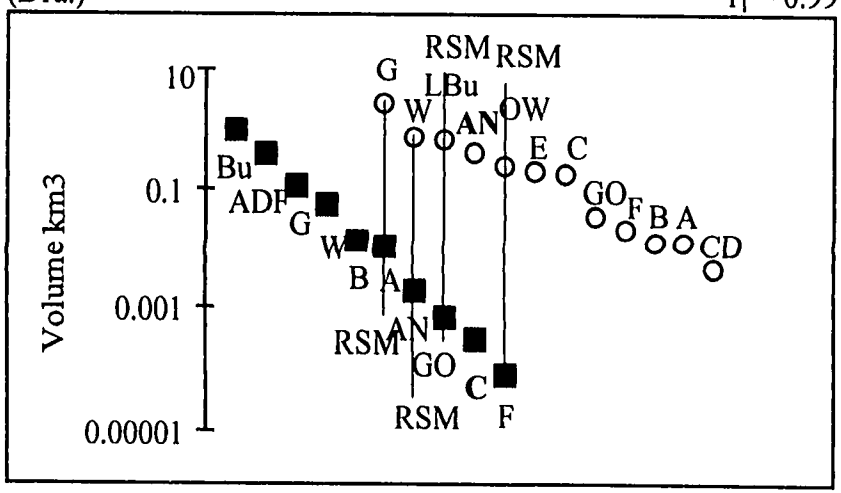

Same reconstruction A2 (Fig. 13)
Lower Cascade Creek + Upper Año Nuevo Creek

(2 km offset)

Figure 16 – Continued

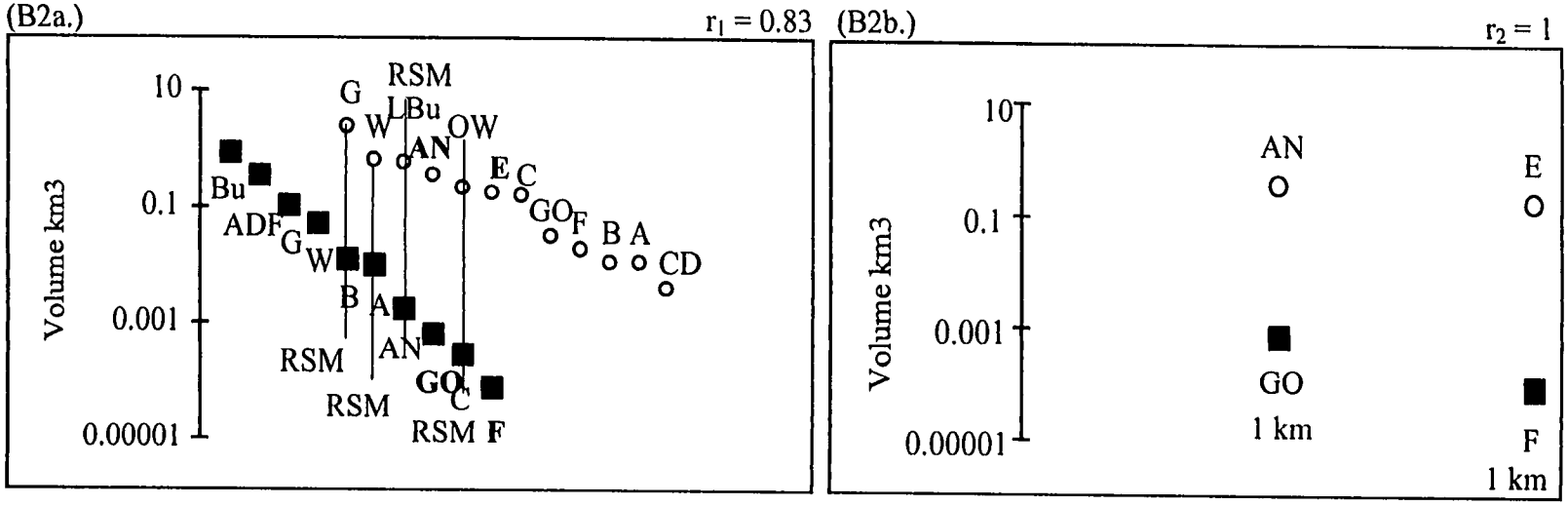

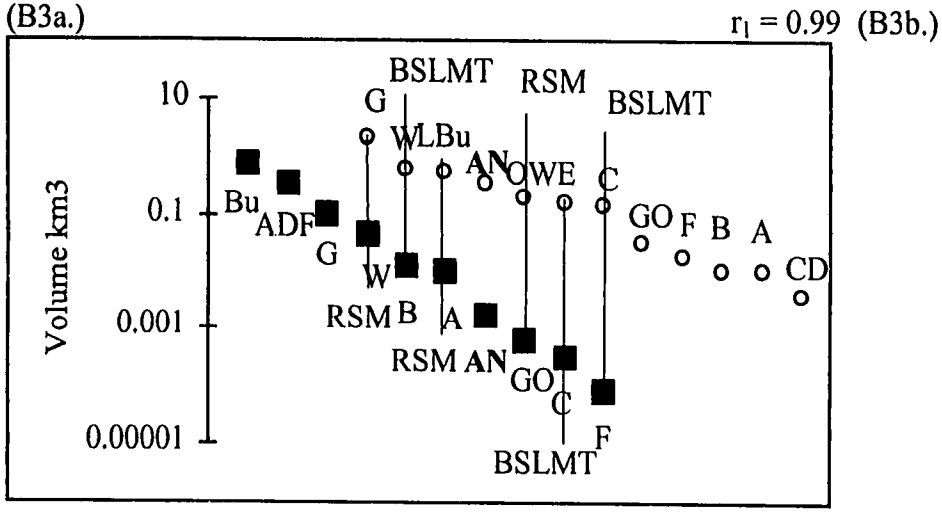

No slip on fault zone

Figure 16 – Continued

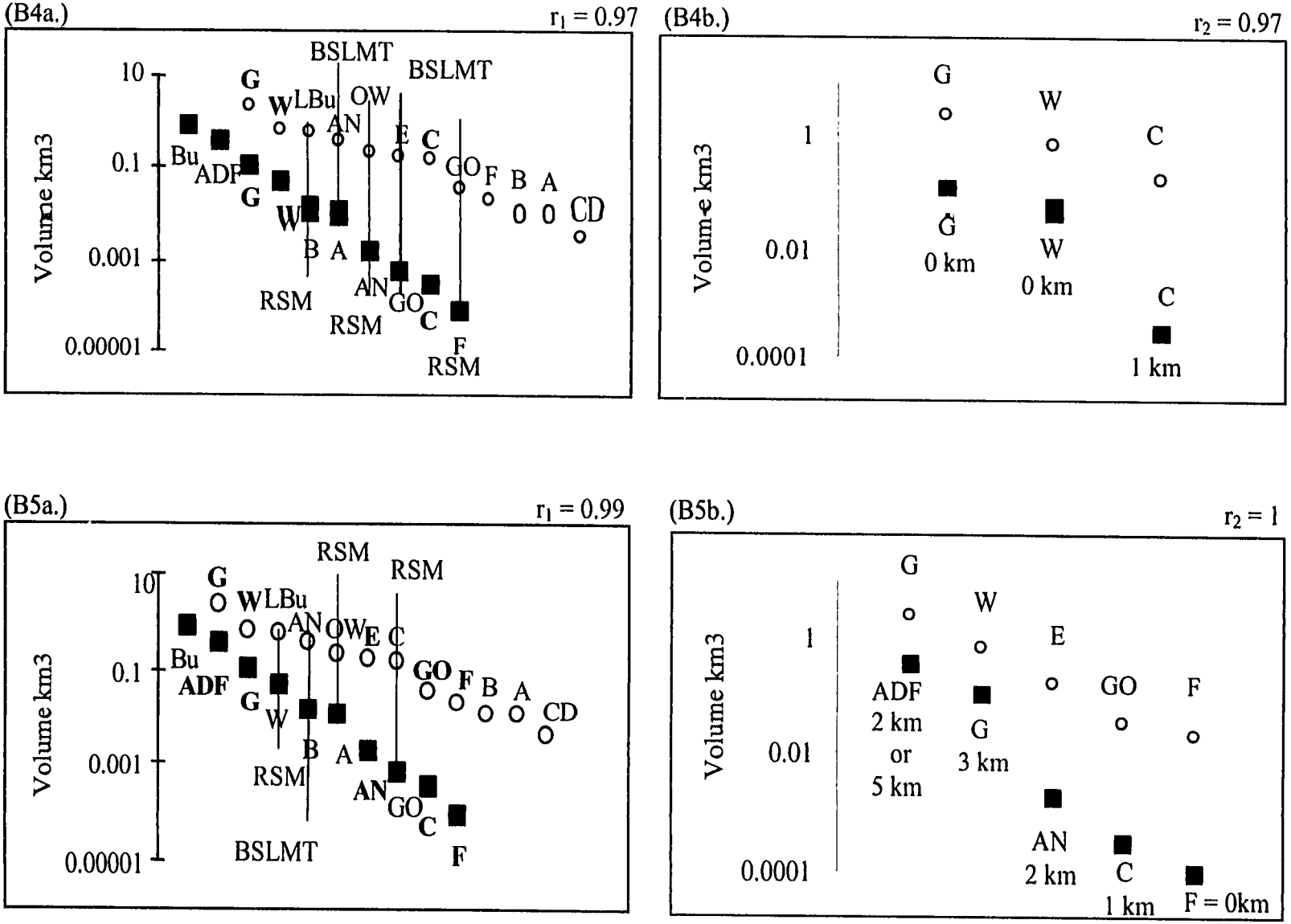

Figure 16 – Continued

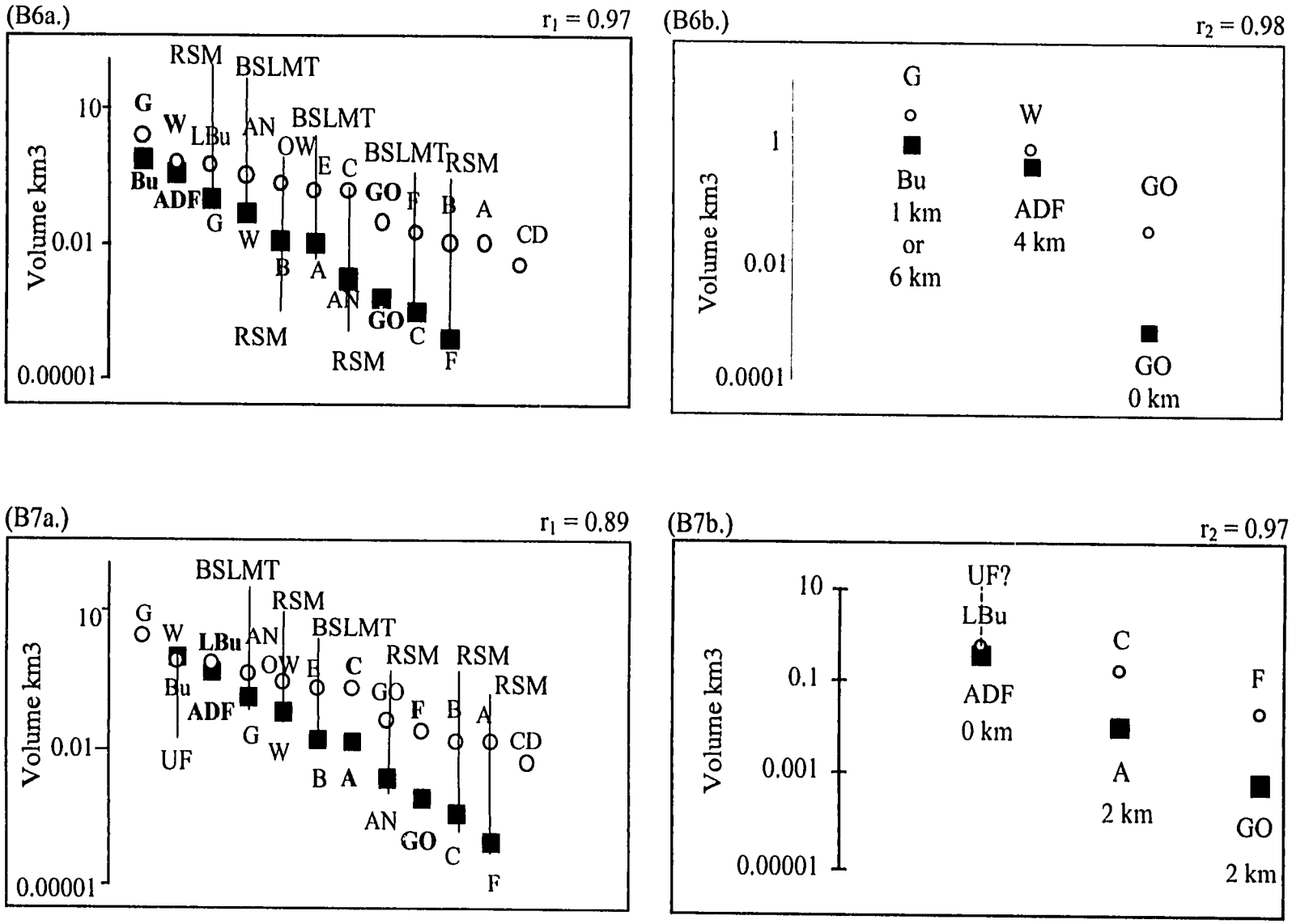

Figure 16 – Continued

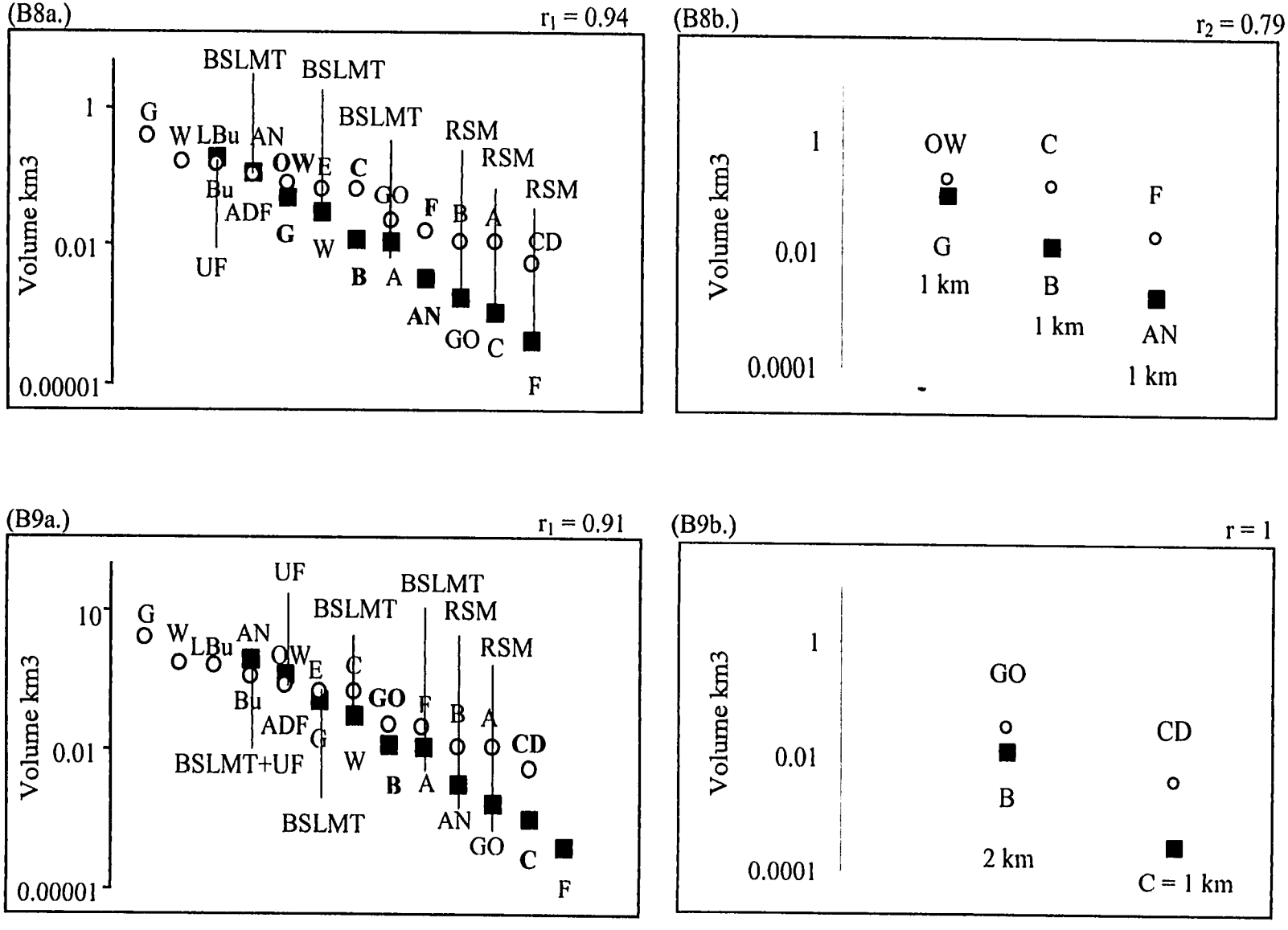

Figure 16 - Continued

(B10a.) $r_l = 0.85$ (B10b.)

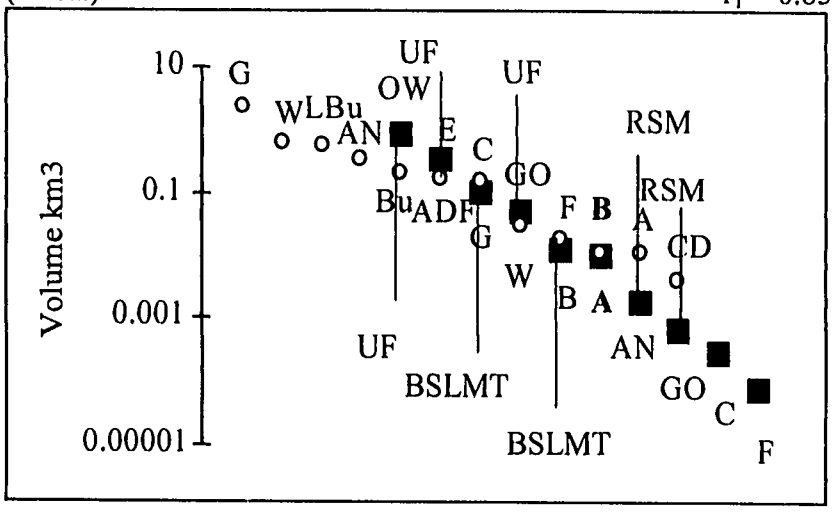

Same as reconstruction A1 (Fig. 12)
Lower Stream A + Upper Stream B
Lower Stream A may be underfit for
Upper Stream B

(1 km offset)

(B11a.) $r = 0.92$ (B11b.)

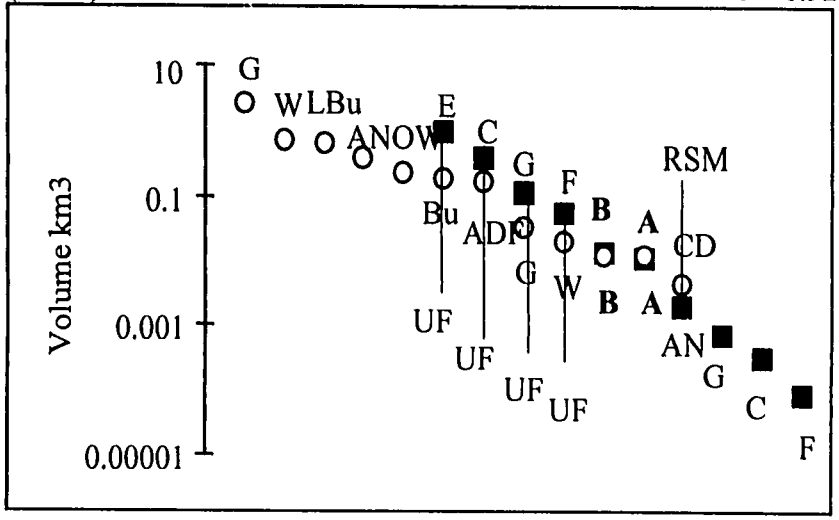

No slip along fault zone

(B12a.) (lower reaches are in italics) r = 0.96

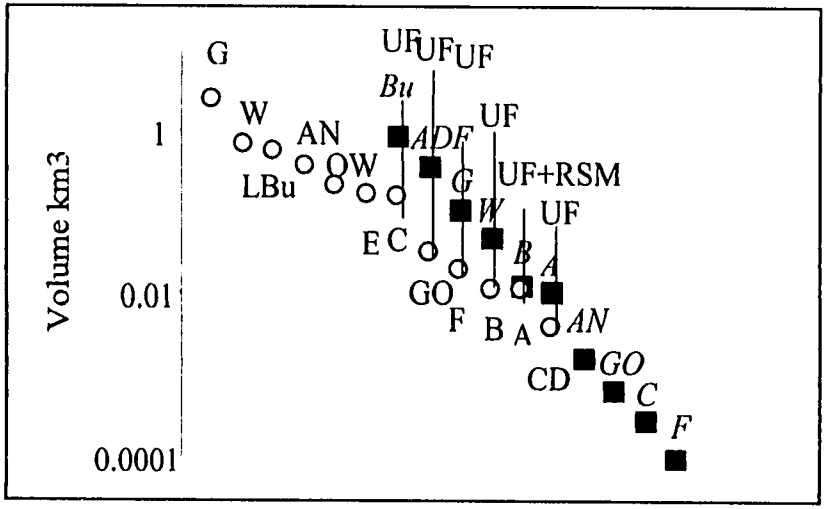

All reconstructions from this point create underfit lower reaches.

DISCUSSION

One of the major assumptions behind this research is that, within each structural block, streams erode at the same rate. It is assumed that the three structural blocks have similar soil resistance, infiltration capacity, vegetation, and microclimate. Because most streams cross all three structural blocks, the factors controlling the amount of erosion are similar, and streams probably developed at the same rate throughout this small study area.

If the rate of stream erosion is variable, then the stream characterization (Task #1) and volumetric analyses of streams (Task #3) may be invalid. This area is riddled with fault splays, fracture zones, and folds from the tectonic activity of the SGfz, which could provide structurally weakened zones. The geologic map (Fig. 2 and Plate 1) indicates that the bedrock in each structural block strikes parallel and dips perpendicular to the fault zone; this dipping bedrock may expose sections of variably resistant layers of the Pigeon Point Formation, Purisima Formation, and Santa Cruz Mudstone.

Another complication is the preferential stream flow along small fault segments of the SGfz and within the trough north of Whitehouse Creek (Figs. 2 and 4). Examples of possible preferential stream flow in the study area are the lower reaches of Año Nuevo Creek, Green Oaks Creek, Stream A, Arroyo de los Frijoles Creek, and Butano Creek. Año Nuevo Creek follows a small fault splay, lower Green Oaks Creek flows south along the Coastways fault then north along the Año Nuevo thrust, Stream A and Arroyo de los Frijoles Creek flow parallel to the Frijoles fault, and Butano Creek flows along the trough

north of Whitehouse Creek. Preferential stream flow is likely along Old Womans Creek, given the perfect alignment of this stream with the Coastways fault segment, so the "deflection" of this stream is questionable.

Task #1: Stream Characterization

Many of the correlation coefficients for the basin measurements indicate that stream magnitude, total length, drainage basin area and volume, and perhaps density appear to evolve at the same rate. Assuming that streams erode at the same rate, streams with larger basins, therefore, must be older. Gazos Creek, with the greatest basin volume, basin area, total length, and magnitude, is likely the oldest stream, and Cold Dip Creek is probably the youngest stream. Streams north of Whitehouse Creek generally appear to be older than those to the south. However, the spatial distribution of streams from north to south does not match the sorted descending magnitudes of Table 5a, possibly indicating that stream development evolved similarly to the schematic diagrams of Figure 6.

Task #2: Apparent Deflection of Modern Streams

Hamilton (1984) assumed that streams north of Whitehouse Creek are offset on Quarry terrace. Near Davenport, extensive drainage systems similar to those in the study area have cut into Quarry and Blackrock terraces. Therefore, it may be valid to assume that streams north of Whitehouse Creek incise the Quarry and Blackrock terraces.

Slip rates calculated south of Whitehouse Creek may be more reliable because marine terraces are not mapped north of Whitehouse Creek. Slip rates calculated for apparent offset of modern streams south of Whitehouse Creek (1-5 mm/yr) are higher than those calculated for streams north of Whitehouse Creek (1-2 mm/yr). The disparity between slip rates north and south of Whitehouse Creek is partly due to the additional 0.3 km that I measured for the offset of Whitehouse Creek, and the younger terrace age (Wilder rather than Quarry or Blackrock) that I used to calculate the slip rate. The slip rate increase also may be due to the questionable marine terrace ages rather than to an actual increase in slip rate since the initiation of Whitehouse Creek.

Slip rates calculated in Table 7b are lower than those calculated by Weber (1990) because of the larger stream deflections he measured and the younger Santa Cruz terrace age (100 ka) he used to calculate slip rates. Weber calculated 4-8 mm/yr and 5-10 mm/yr for the deflections of Cascade Creek and Año Nuevo Creek, respectively. Task #2 calculations indicate a 1-6 mm/yr slip rate along Cascade Creek and a 4-5 mm/yr slip rate along Año Nuevo Creek.

For Task #2, it is assumed that the marine terrace map (Fig. 5) and terrace ages (Table 3) are correct, and that the age of the terrace that is incised by the deflected portion of the stream should approximate the maximum age of the most recent fault slip, which gives the minimum slip rate along the fault segment. It is unknown if both the Frijoles and Coastways fault segments were active in the past (i.e., the Frijoles may be a new fault) or if one triggers movement on the other; therefore, the slip rates for the fault segments are considered independent of each other.

Task #3: Paleodrainage Reconstructions

The complex drainage pattern of streams and the uncertainty regarding the marine terraces make any stream restoration difficult if not impossible using the methods outlined in this paper. In addition, obtaining a strong positive correlation coefficient for a paloedrainage configuration is highly unlikely, given the changes that may occur to the lower basin development over time (e.g., lower basin beheaded from upper basin, capture of more than one upper basin watershed, or capture of an upper basin watershed of greater/lesser magnitude).

The paleodrainage reconstructions indicate that neither incremental restoration nor realignment to maximize correlation coefficients can satisfactorily produce reliable slip rates for this study area. However, the weak positive correlation ($r = 0.32$) of all upper and lower basins in their present configuration indicates that streams may be in the process of attaining equilibrium in their present spatial arrangement. The higher correlation ($r = 0.72$) of the lower reaches not omitted from reconstructions A1-A3 (Whitehouse Creek, Año Nuevo Creek, Cascade Creek, Green Oaks Creek, Stream B, and Stream A) may indicate that these lower reaches have already reached equilibrium. Lower reaches that have not yet fully attained equilibrium, may have lowered the overall correlation of all the streams to 0.32.

Reconstructions B1-B12 identified several upper basin–lower basin matches with high (> 0.79) correlation coefficients, but all such matches are rendered unlikely by one or more geometric or geologic difficulties. However, other matches seem to be unique

correlations of an upper basin with a single lower basin, and suggest $\leq$1 km of total dextral slip and a 0-10 mm/yr slip rate.

The slow rate of modern slip calculated in Task #2 (1-5 mm/yr), the positive correlation of streams in their present spatial configuration calculated in Task #3, and the unique lower basin solutions for reconstructions B1-B12 indicating only 0-1 km of offset make it unlikely that the SGfz has experienced rapid Holocene movement.

The uncertainty associated with both the age and areal extent of the marine terraces complicated the determination of the slip rates. The range of proposed ages of the marine terraces produced a correspondingly large range in slip rates. In addition, the lack of a map defining the boundaries of Cement terrace and of terraces north of Whitehouse Creek also complicated slip-rate calculations.

CONCLUSIONS

Stream reconstructions, either by incremental one-kilometer restoration of lower basins along the fault zone or by matching upper and lower basin volumes to create feasible paleodrainage configurations yielding high correlation coefficients, did not prove to be satisfactory methods to calculate slip rates along the San Gregorio fault zone. The complex drainage pattern of streams in the study area, in addition to the uncertainty regarding age and areal extent of the marine terraces, made stream restoration difficult.

The weak positive correlation ($r = 0.32$) of all upper and lower basins in their present configuration indicates that many streams may be in the process of attaining equilibrium in their present spatial arrangement. The possibility of rapid Holocene fault movement appears unlikely based on: (1) the positive correlation of streams in their present spatial configuration, (2) the slow slip rate (1-5 mm/yr) of modern stream offset since the emergence of the Highway 1 terrace (<105 ka), and (3) the small amount ($\leq$1 km) of offset calculated for volumetrically correlated paleodrainage configurations.

Streams north of Whitehouse Creek appear to be older than those to the south. However, streams do not appear to have developed uniformly from north to south, perhaps due to tectonism within the fault zone.

REFERENCES CITED

Addicott, W.A., 1969, Late Pliocene mollusks from San Francisco Peninsula, California, and their paleogeographic significance: Proceedings of the California Academy of Sciences, Fourth Series, v. 7, p. 57-93.

Anderson, L.W., Anders, M.H., and Ostena, D.A., 1982, Late Quaternary faulting and seismic hazard potential, Eastern Diablo Range, California, *in* Hart, E.W., Hirschfeld, S.E., and Schulz, S.S., eds., Proceedings of the Conference on Earthquake Hazards in Eastern San Francisco Bay Area, California Division of Mines and Geology Special Publication 62, p. 197-206.

Argus, D.F., and Gordon, R.G., 1991, Current Sierra Nevada-North America motion from very long baseline interferometry: Implications for the kinematics of the western United States: Geology, v. 19, p. 1085-1088.

Argus, D.F., Heflin, M.B., Donnellan, A., Webb, F.H., Dong, D., Hurst, K.J., Jefferson, D.C., Lyzenga, G.A., Watkins, M.M., Zumberge, J.F., 1998, Shortening and thickening of metropolitan Los Angeles measured and inferred by using geodesy: Geology, v. 27, p. 703-706.

Bloom, A.L., Broecker, W.A., Chappell, J.M.A., Matthews, R.K., and Mesolella, K.J., 1974, Quaternary sea level fluctuations on a tectonics coast: New $^{230}Th/^{234}U$ dates from the Huon Peninsula, New Guinea: Quaternary Research, v. 4, p. 185-205.

Brabb, E.E., 1970, Preliminary Geologic Map of the Central Santa Cruz Mountains, California: U.S. Geological Survey, Open-File Report 70-36, scale 1:62,500.

Brabb, E.E., and Pampeyan, E.H., 1983, Geologic Map of San Mateo County, CA: U.S. Geological Survey, Miscellaneous Field Studies Map I-1257-A, 1 sheet, scale 1:62,500.

Bradley, W.C., and Addicott, W.O., 1968, Age of first marine terrace near Santa Cruz, California: Geological Society of America Bulletin, v. 79, p. 1203-1210.

Bradley, W.C., and Griggs, G.B., 1976, Form, genesis and deformation of central California wave-cut platforms: Geological Society America Bulletin, v.87, p. 433-449.

Brown, R.D. Jr, 1990, Quaternary Deformation, *in* Wallace, R.E., ed., The San Andreas fault system, California: U.S. Geological Survey, Professional Paper 1515, p. 83-113.

Burnham, Kathleen, 1999, A multidisciplinary approach to conglomerate analysis suggests 180 (+ or – 5 km) post-Eocene dextral offset of the San Gregorio-northern San Andreas Fault: AAPG Bulletin, v. 83, p. 682-683.

Clark, J.C., 1966, Tertiary stratigraphy of the Felton-Santa Cruz area, Santa Cruz Mountains, California [abs]: Dissertation Abstracts, v. 27, p. 1184-B.

Clark, J.C., 1998, Neotectonics of the San Gregorio fault zone: Age dating controls on offset history and slip rates [abs]: Annual Convention of the Pacific Section of the American Association of Petroleum Geologists, v. 82, p. 844-845.

Clark, J.C., Brabb, E.E., Greene, H.G., Ross, D.C., 1984, Geology of Point Reyes and implications for San Gregorio fault history *in* Crouch, J.K., and Bachman, S.B., eds., Tectonics and Sedimentation Along the California Margin: Pacific Section SEPM, v. 38, p. 67-86.

Clark, M.M., 1988, Recently active traces of Calaveras fault at San Felipe Creek: U.S. Geological Survey Open-File Report 88-16, 141 p.

Clark, M.M., Harms, K.K., Lienkaemper, J.J., Harwood, D.S., Lajoie K.R., Matti, J.C., Perkins, J.A., Rymer, M.J., Sarna-Wojcicki, A.M., Sharp, R.V., Sims, J.D., Tinsley, J.C., Ziony, J.I., 1984, Preliminary slip-rate table and map of late-Quaternary faults of California: U.S. Geological Survey Open-File Report 84-106, p. 17.

Cummings, J.C., 1983, The Woodside facies, Santa Clara formation and late Quaternary slip on the San Andreas fault, San Mateo County, California [abs.]: Program and Abstracts for the 58th Annual Meeting, Pacific Section, American Association Petroleum Geologists, Society Exploration Geophysicists, SEPM, Sacramento, California, p. 82.

Davis, John C., 1986, Statistics and Data Analysis in Geology, 2nd edition: New York, Wiley & Sons, Inc., 646 p.

DeMets, E., Gordon, R.G., Argus, D.F., and Stein, S., 1994, Effect of recent revisions in the geomagnetic reversal time scale on estimates of current plate motions: Geophysical Research Letters, v. 21, p. 2191-2194.

Ellsworth, W., 1990, Earthquake History, 1769-1989, *in* Wallace, R.E., ed., The San Andreas fault system, California: U.S. Geological Survey Professional Paper 1515, p. 189-205.

Gawthrop, W.H., 1978, Seismicity and tectonics of the central California coast region, *in* E.A. Silver and W.R. Normark, eds., San Gregorio-Hosgri fault zone, California: California Division of Mines and Geology Special Report 137, p. 45-56.

Gilbert, Wyatt G. 1973, Franciscan Rocks near Sur Fault Zone, Northern Santa Lucia Range, California: Geological Society of America Bulletin, v. 84, p. 3317-3328.

Graham, S.A. and Dickinson, W.R., 1978, Apparent offsets of on-land geologic features across the San Gregorio-Hosgri fault trend, *in* E.A. Silver and W.R. Normark, eds., San Gregorio-Hosgri fault zone, California: California Division of Mines and Geology Special Report 137, p. 13-23.

Greene, H.G., Lee, W.H.K., McCullock, D.S., and Brabb, E.E., 1973, Faults and earthquakes in the Monterey Bay region, California: U.S. Geological Survey, Miscellaneous Field Studies Map MF-518, 4 sheets, scale 1:200,000.

Hall, C.A., Jr., 1975, San Simeon-Hosgri fault system, coastal California: economic and environmental implications: Science, v. 190, p. 1291-1294.

Hall, C.A, Sutherland, M.J., and Ingersoll, R.V., 1995, Miocene paleogeography of west-central California - offset along the San Gregorio-Hosgri fault zone, *in* Fritsche, A.E., ed., Cenozoic paleogeography of the western United States - II: Pacific Section, SEPM, book 75, p. 85-112.

Hall, N.T., 1984, Holocene history of the San Andreas fault between Crystal Springs Reservoir and San Andreas Dam, San Mateo County, California: Seismological Society of America Bulletin, v. 74, p. 281-299.

Hamilton, D.H., 1984, The tectonics boundary of coastal central California [Ph. D dissertation]: Stanford University, Palo Alto, CA, 290 p.

Harbert, W., 1991, Late Neogene relative motions of the Pacific and North American plates: Tectonics, v. 10, p. 1-15.

Hay, E.A., Cotton, W.R., and Hall, N.T., 1980, Shear couple tectonics and the Sargent-Berrocal fault system in northern California: California Division of Mines and Geology Special Report 140, p. 41-49.

Hill, M.L., and Dibblee, T.W., Jr., 1953, San Andreas, Garlock, and Big Pine faults, California - a study of the character, history, and tectonic significance of their displacements: Geological Society of America Bulletin, v. 64, p. 443-510.

Hsu, D.H., 1969, Role of cohesive strength in mechanics of overthrust faulting and of landsliding: Geological Society of America Bulletin, v. 80, p. 927-952.

Huffman, O.F., 1972, Lateral displacement of upper Miocene rocks and the Neogene history of offset along the San Andreas fault in central California: Geological Society of America Bulletin, v. 83, p. 2913-2946.

Kelson, K.I, Lettis, W.R., and Lisowski, M., 1992, Distribution of geologic slip and creep along faults in the San Francisco Bay region, *in* Borchardt, Glenn, and others, eds., Proceedings of the Second Conference on Earthquake Hazards in the Eastern San Francisco Bay Area: California Department of Conservation, Division of Mines and Geology Special Publication 113, p. 31-38.

Knuepfer, P.L., 1977, Geomorphic investigations of the Vaca and Antioch fault systems, Solano and Contra Costa counties, California [MS thesis]: Stanford University, Palo Alto, CA, 53 p.

Lajoie, K.R., Wehmiller, J.F., Kvenvolden, K.A., Peterson, Etta, and Wright, R.H., 1975, Correlation of California marine terraces by amino acid stereochemistry: Geological Society of America Abstracts with Programs, v. 7, no. 3, p. 338-339.

Leopold L., Gordon, M.G., Wolman, M., Miller, J.P., 1992, Fluvial processes in geomorphology: New York, Dover Publications Inc., 450 p.

Lienkaemper, J.J., Borchardt, Glenn, Wilmesher, J.F., and Meier, D., 1989, Holocene slip rate along the Hayward fault, northern California [abs]: EOS, Transactions of the American Geophysical Union, v. 70, p. 1349.

Lienkaemper, J.J., Borchardt, Glenn, and Lisowski, Michael, 1991, Historic creep rate and potential for seismic slip along the Hayward fault, California: Journal of Geophysical Research, v. 96, p. 18, 261-18, 283.

Mathews, V.M., III, 1973, Pinnacles-Neenach correlation: A restriction for models of the origin of the Transverse Ranges and the big bend in the San Andreas fault: Geological Society of America Bulletin, v. 84, p. 683-688.

Mayer, L., 1990, Introduction to quantitative geomorphology: Englewood Cliffs, New Jersey, Prentice Hall Inc., 380 p.

McNally, K.C. and Stakes, D.S., 1999, Implications of the San Gregorio fault zone seismicity for Monterey Bay coastal hazard assessment [abs]: 1999 AAPG Bulletin, v. 83, p. 696.

Nagel, David K. and Mullins, Henry T., 1983, Late Cenozoic offset and uplift along the San Gregorio fault zone, Central California continental margin: AAPG Bulletin, v. 67, p. 91-103.

Neimi, T.M., and Hall, N.T., 1992, Late Holocene slip rate and recurrence of great earthquakes on the San Andreas fault in northern California: Geology, v. 20, p. 195-198.

Nilsen, T.H., and Clarke, S.H., Jr., 1975, Sedimentation and tectonics in the early Tertiary continental borderland of central California: U.S. Geological Survey Professional Paper 925, 64 p.

Page, B.M, 1990, Evolution and complexities of the transform system in California, U.S.A: Annales Tectonicæ, v. IV, p. 53-69.

Prentice, C.S., 1989, Earthquake geology of the northern San Andreas fault near Point Arena, California [Ph.D. dissertation] California Institute of Technology, Pasadena, 186 p.

Rosenburg, L. and Clark, J.C., 1999, Southern San Gregorio fault: stepover segmentation vs. through-going tectonics [abs]: AAPG Bulletin, v. 83, p. 700.

Ross, D.C., 1972, Petrographic and chemical reconnaissance study of some granitic and gneissic rocks near the San Andreas Fault from Bodega Head to Cajon Pass, California: U.S. Geological Survey Professional Paper, Report: P 0698, 92 p.

Schwartz, D.P., Pantosti, D., Hecker, S., Okumura, K., Budding, K.E., and Powers, T., 1992, Late Holocene behavior and seismogenic potential of the Rodgers Creek fault zone, *in* Borchardt, Glenn, and others, eds., Proceedings of the Second Conference on Earthquake Hazards in the Eastern San Francisco Bay Area: California Department of Conservation, Division of Mines and Geology Special Publication 113, p. 393.

Sedlock, R. L., and D.H. Hamilton, 1991, Late Cenozoic tectonic evolution of southwestern California: Journal of Geophysical Research, v. 96, p. 2325-2352.

Sieh, K., 1975, An investigation of the potential for ground rupture along fault traces in the Los Altos Hills, California: Unpublished report for W.R. Cotton and Associates and Town of Los Altos Hills Planning Commission, 55 p.

Sieh, K.E. and Jahns, R., 1984, Holocene activity of the San Andreas fault at Wallace Creek, California: Geological Society of America Bulletin, v. 95, p. 883-896.

Silver, E.A, 1971, Tectonics of the Mendocino triple junction: Geological Society of America Bulletin, v. 82, 2965-2977.

Silver, E.A., 1974, Structural interpretation from free-air gravity of the California continental margin, 35° to 40°N [abs]: Geological Society of America Abstracts with Programs, v. 6, p. 253.

Silver, E.A., and Normark, W.R, eds., 1978, San Gregorio-Hosgri fault zone, California: California Division of Mines and Geology Special Report 137, 56 p.

Simpson, G.D, Thompson, S.C, Noller, J.S., and Lettis, W.R., 1997, The northern San Gregorio fault zone: Evidence for the timing of late Holocene earthquakes near Seal Cove, California: Bulletin of the Seismological Society of America, v. 87, p. 1158-1170.

Simpson, G.D., and Lettis, W.R., 1999, Slip Rate and earthquake history of the northern San Gregorio fault, Half Moon Bay to Moss Beach, CA [abs.]: Pacific Section Annual Convention, American Association of Petroleum Geologists, v. 83, p. 701.

Sims, J.D., 1991, Distribution and rate of slip across the San Andreas transform boundary, Hollister area, central California: Geological Society of America Abstracts with Programs, v. 23, p. 98.

Sowers, J.M., Noller, J.S., Unruh, Jr., 1992, Quaternary deformation and blind-thrust faulting on the east flank of the Diablo Range near Tracy, California, *in* Borchardt, Glenn, and others, eds., Proceedings of the Second Conference on Earthquake Hazards in the Eastern San Francisco Bay Area: California Department of Conservation, Division of Mines and Geology Special Publication 113, p. 377.

Stevenson, A. and Eittreim, S., 1999, Morphology and structure of the San Gregorio fault system across the continental shelf south of Point Año Nuevo [abs.]: Pacific Section Annual Convention, American Association of Petroleum Geologists, v. 83, p. 703.

Strahler, A.N., 1957, Quantitative analysis of watershed geomorphology: American Geophysical Union Transcript, v. 38, pp. 913-920.

Thornburg, Jennifer, 1998, A paleoseismic study on the San Gregorio fault zone, San Mateo County, California [MS thesis], University of California Santa Cruz, 52 p.

Thornburg, Jennifer, 1999, Historic sedimentation in San Gregorio Creek: Implications for absence of geomorphic expression of recent surface rupture along the San Gregorio fault zone, San Mateo County, California: AAPG Bulletin, v. 67, p. 703.

Turner, D.L., 1969, K-Ar ages of California Coast Range volcanics - implications for San Andreas fault displacement [abs.]: Geological Society America Abstracts with Programs, v. 1, p. 70.

Weber, G.E., 1990, Late Pleistocene slip rates on the San Gregorio fault zone at Point Año Nuevo, San Mateo County, California: Pacific Section AAPG Volume and Guidebook, Book GB67, p. 193-203.

Weber, G.E., Lajoie, K.R., and Griggs, G.B., 1979, Coastal Tectonics and Coastal Geologic Hazards in Santa Cruz and San Mateo Counties, CA Field Trip Guide: Cordilleran Section of the Geological Society of America 75th Annual Meeting, p. 1-187.

Weber, G.E., and Cotton, W.R., 1980, Geologic investigation of recurrence intervals and recency of faulting along the San Gregorio fault zone, San Mateo County, California, California: U.S. Geological Survey Open-File Report 81-263, 133 p.

Weber, G.E., Nolan, J.E., and Zinn, E., 1999a, Late Quaternary slip across the San Gregorio fault zone, San Mateo County, California; Estimates from marine terrace offsets: AAPG Bulletin, v. 67, p. 705.

Weber, G.E, Thornburg, J., and Nolan, J.E., 1999b, Recurrence intervals, recency of movement and Holocene slip rates across the San Gregorio fault zone at Point Año Nuevo, San Mateo County, California: AAPG Bulletin, v. 67, p. 705.

Wentworth, C.M., 1972, Geology, San Andreas offset, and seismic environment of the Gualala block; Sonoma and Mendocino counties, California: Journal of Research of the U.S. Geological Survey, v. 1, p. 95-108.

WGCEP (Working Group on California Earthquake Probabilities), 1990, Probabilities of large earthquakes in the San Francisco Bay region, California: U.S. Geological Survey Circular 1053, p. 51.

APPENDIX A

Stream magnitude, order, and basin area. All streams (except Gazos Creek) were measured from 1:24,000 USGS topographic maps. Gazos Creek was reduced to 1:30,000. All stream inflections (V's) were included for magnitude and order. Basin area was calculated with an electronic planimeter. Streams are arranged alphabetically. For basin boundary locations, see Plate 1.

Stream A (A)

Magnitude = 18
Order = 3rd
Basin Area = 1.62 km^2

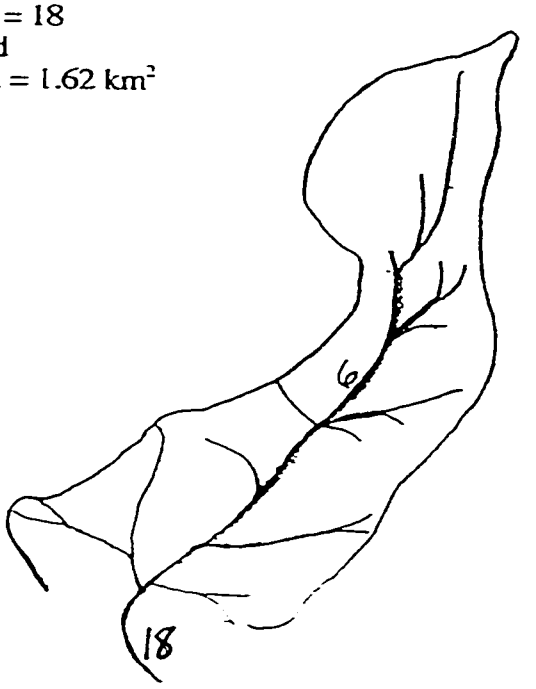

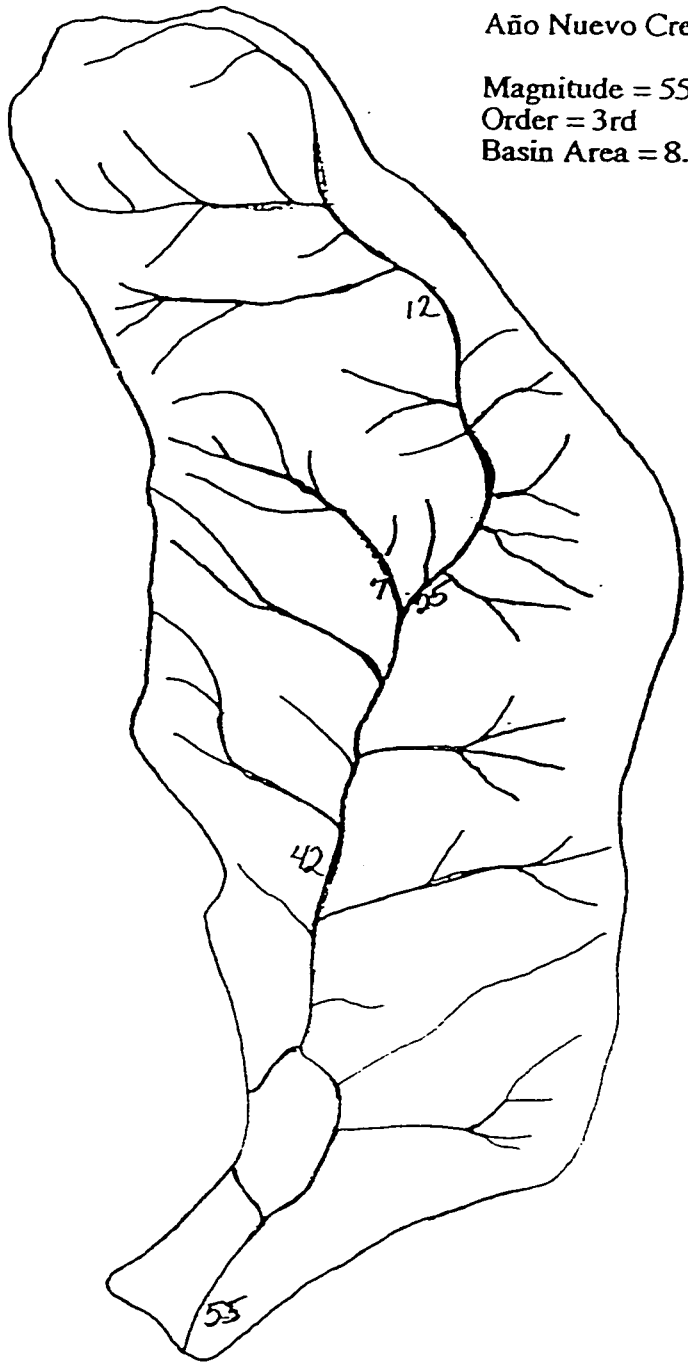
Año Nuevo Creek (AN)
Magnitude = 55
Order = 3rd
Basin Area = 8.03 km²
12
7
55
42
55

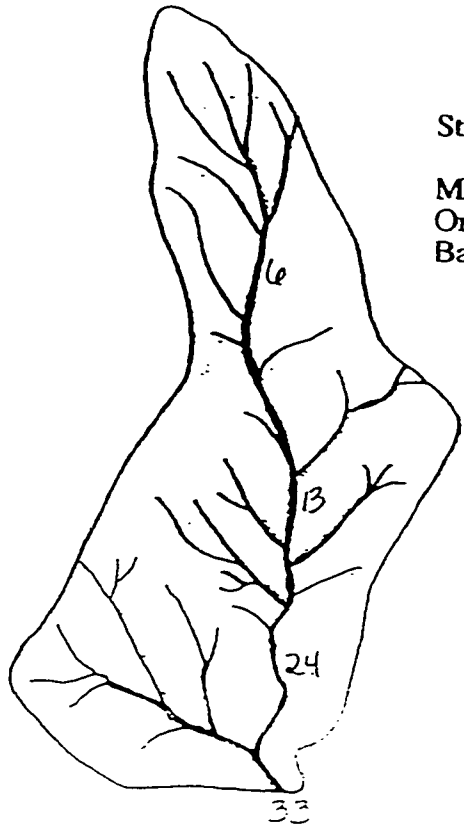

Stream B (B)

Magnitude = 33
Order = 4th
Basin Area = 1.71 km^2

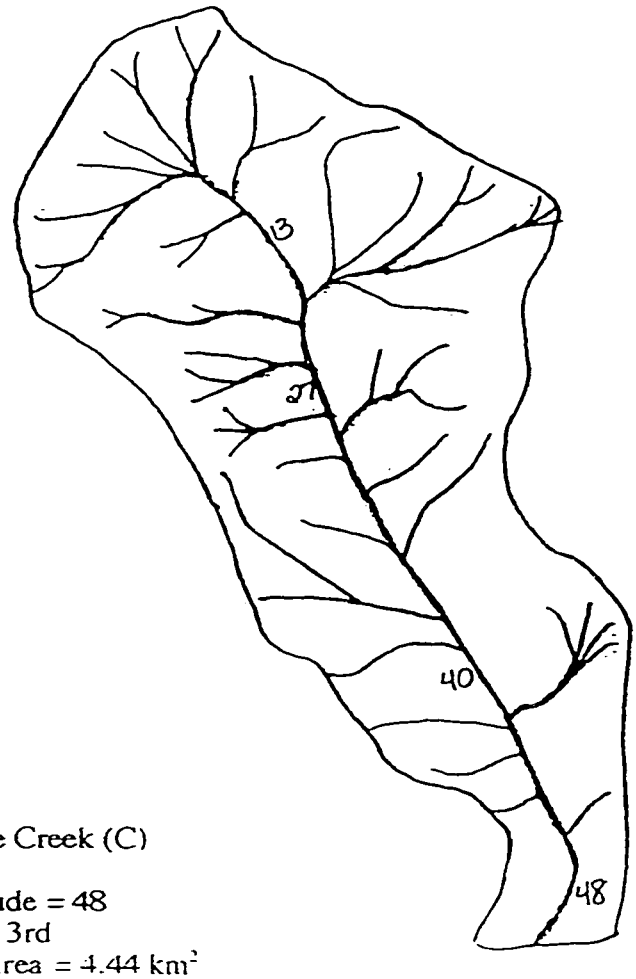

Cascade Creek (C)

Magnitude = 48
Order = 3rd
Basin Area = 4.44 km^2

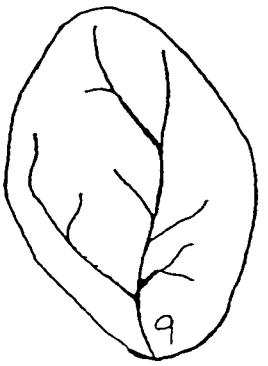

Cold Dip Creek (CD)

Magnitude = 9
Order = 3rd
Basin Area = 0.97 km^2

Elliot Creek (E)

Magnitude = 45
Order = 3rd
Basin Area = 3.96 km^2

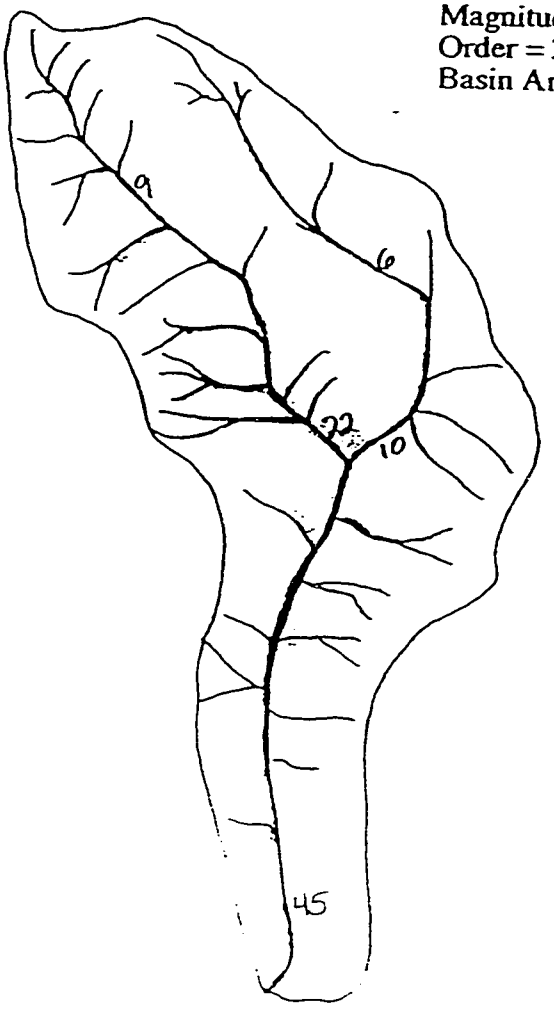

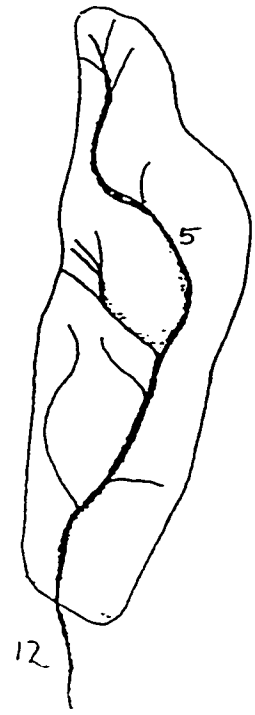

Finney Creek (F)

Magnitude = 12
Order = 3rd
Basin Area = 1.30 km^2

Gazos Creek

Magnitude = 237
Order = 5th
Basin Area = 33.03 km^2

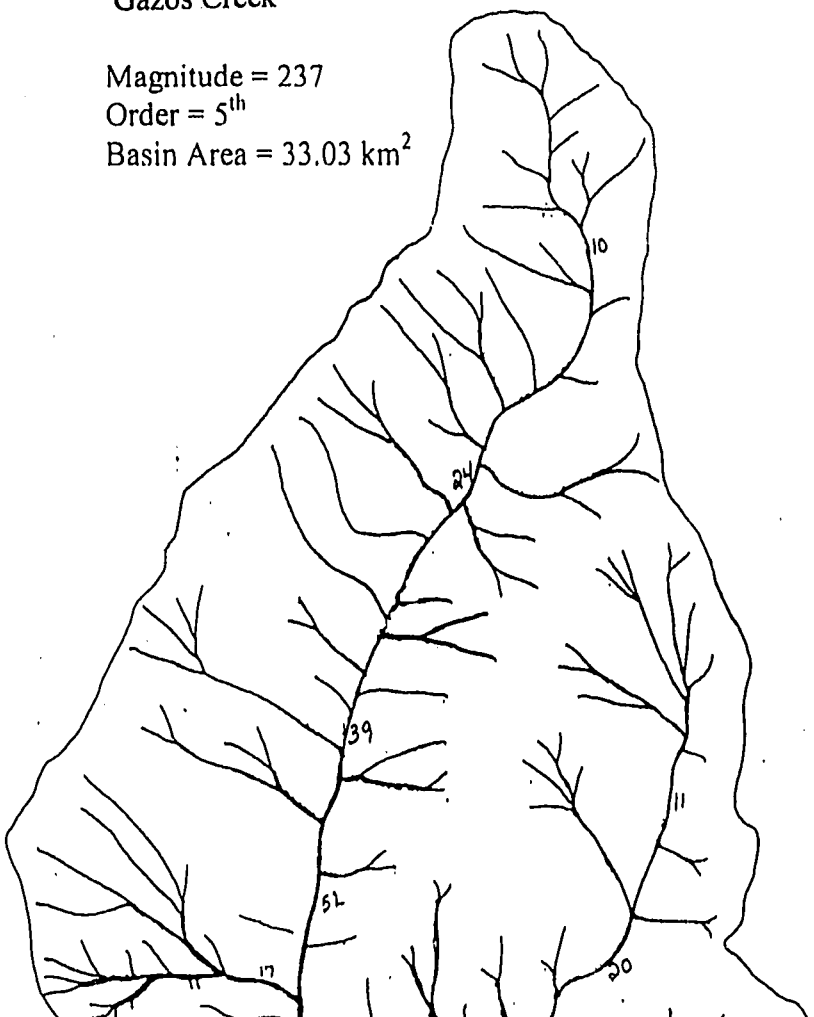

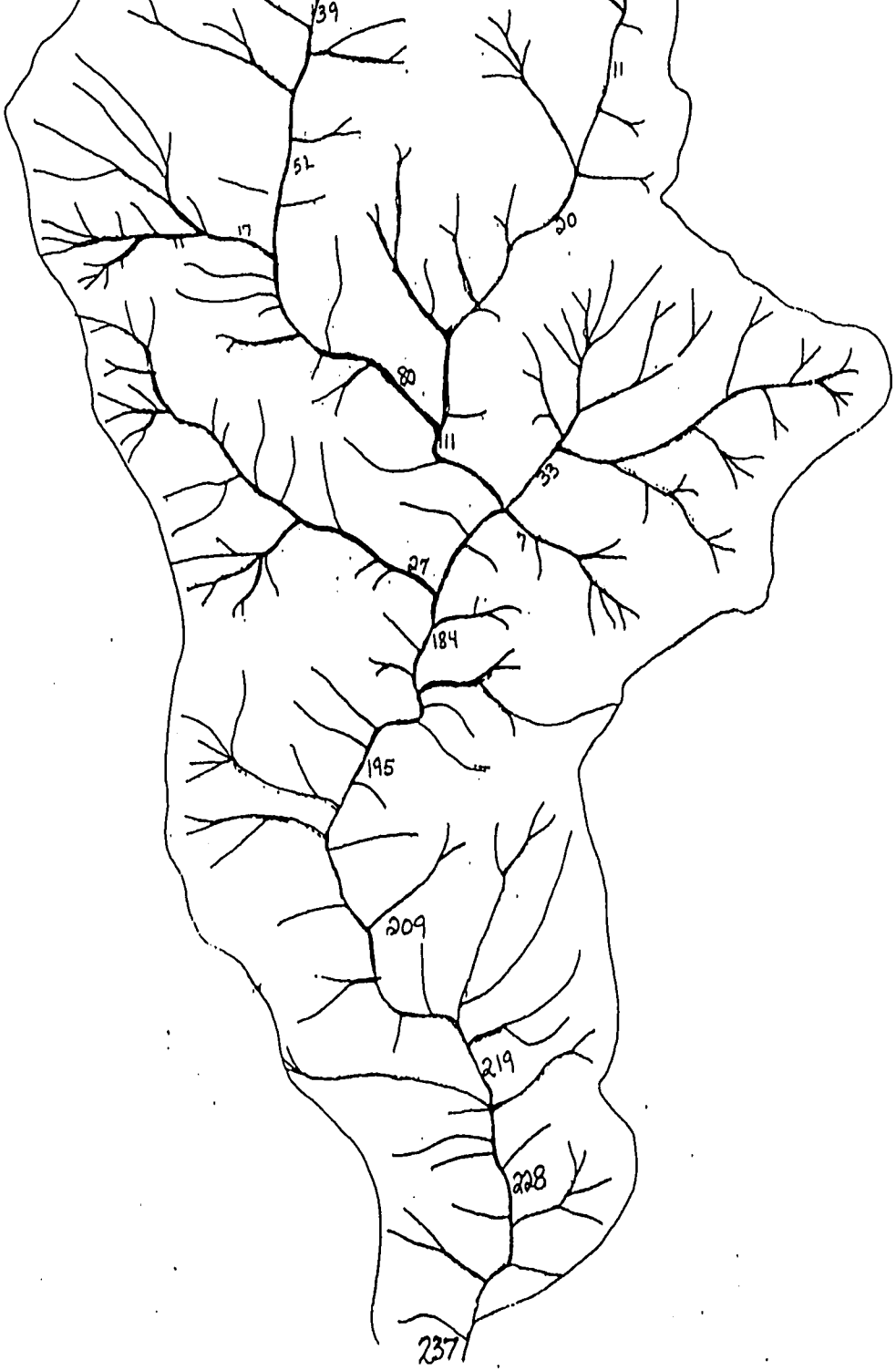
139
11
52
17
30
80
111
33
7
27
184
195
209
219
228
237

Green Oaks Creek (GO)

Magnitude = 14
Order = 3rd
Basin Area = 2.12 km^2

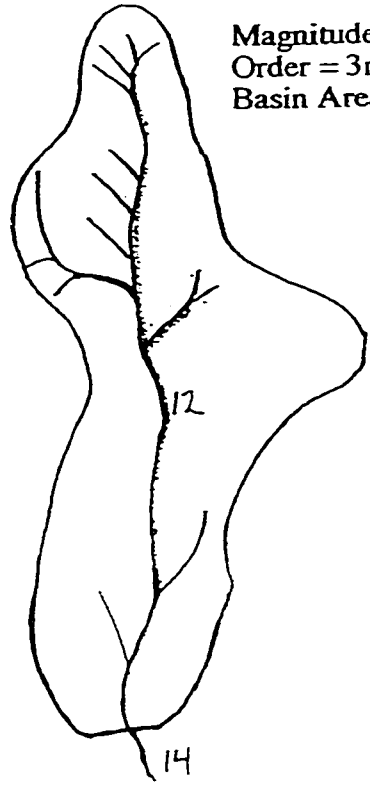

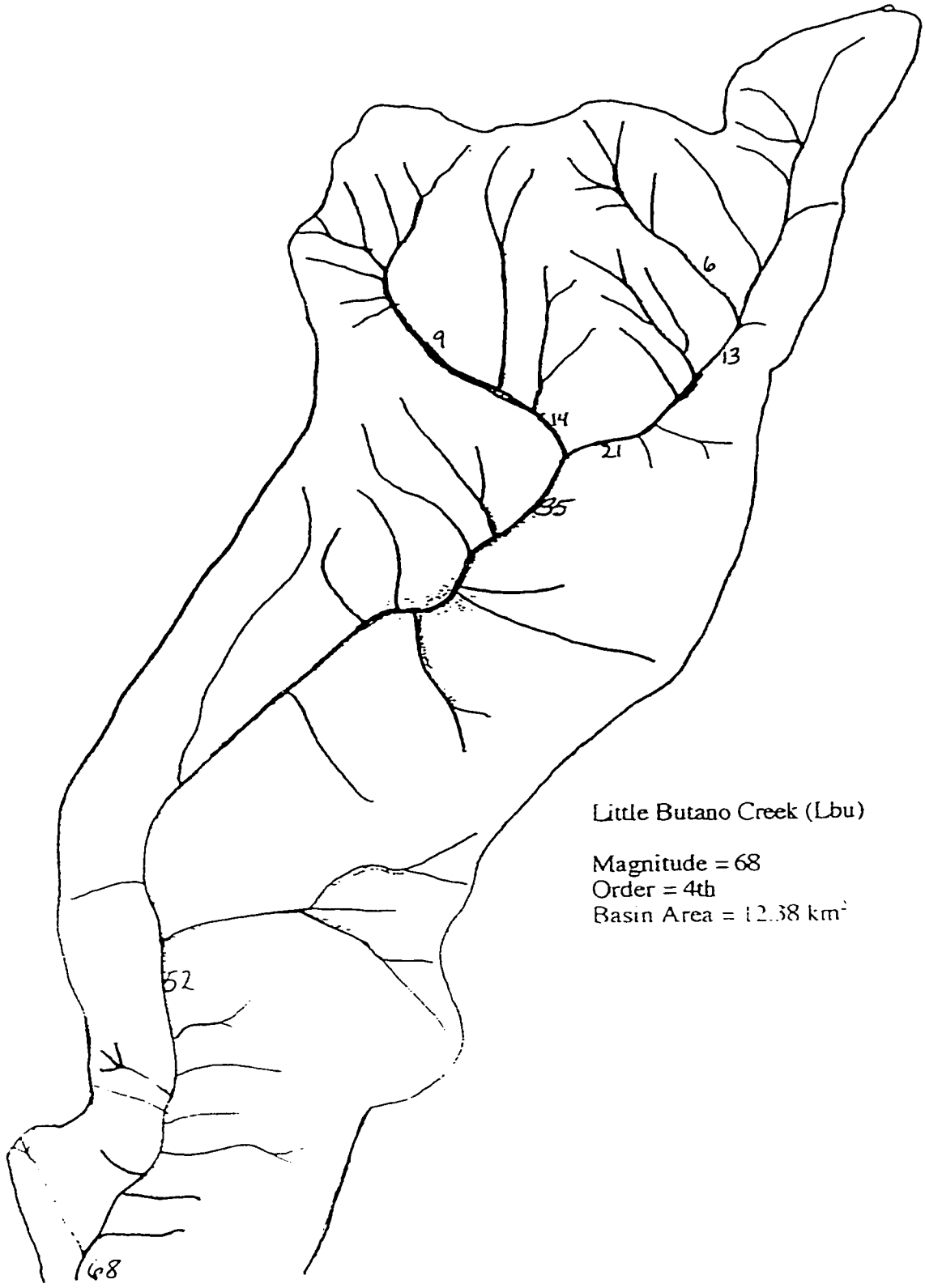

Little Butano Creek (Lbu)

Magnitude = 68
Order = 4th
Basin Area = 12.38 km^2

Old Womans Creek (OW)

Magnitude = 62
Order = 4th
Basin Area = 7.02 km^2

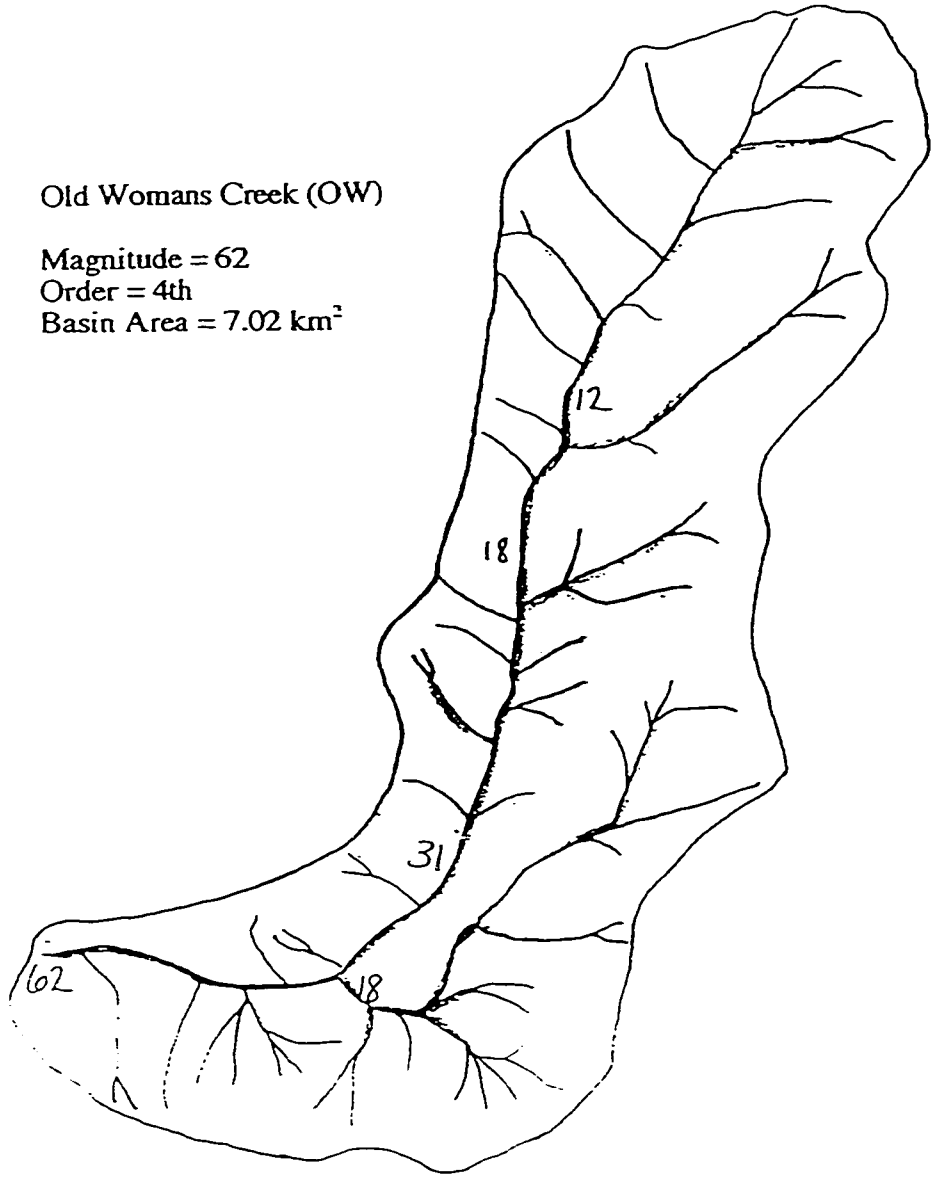

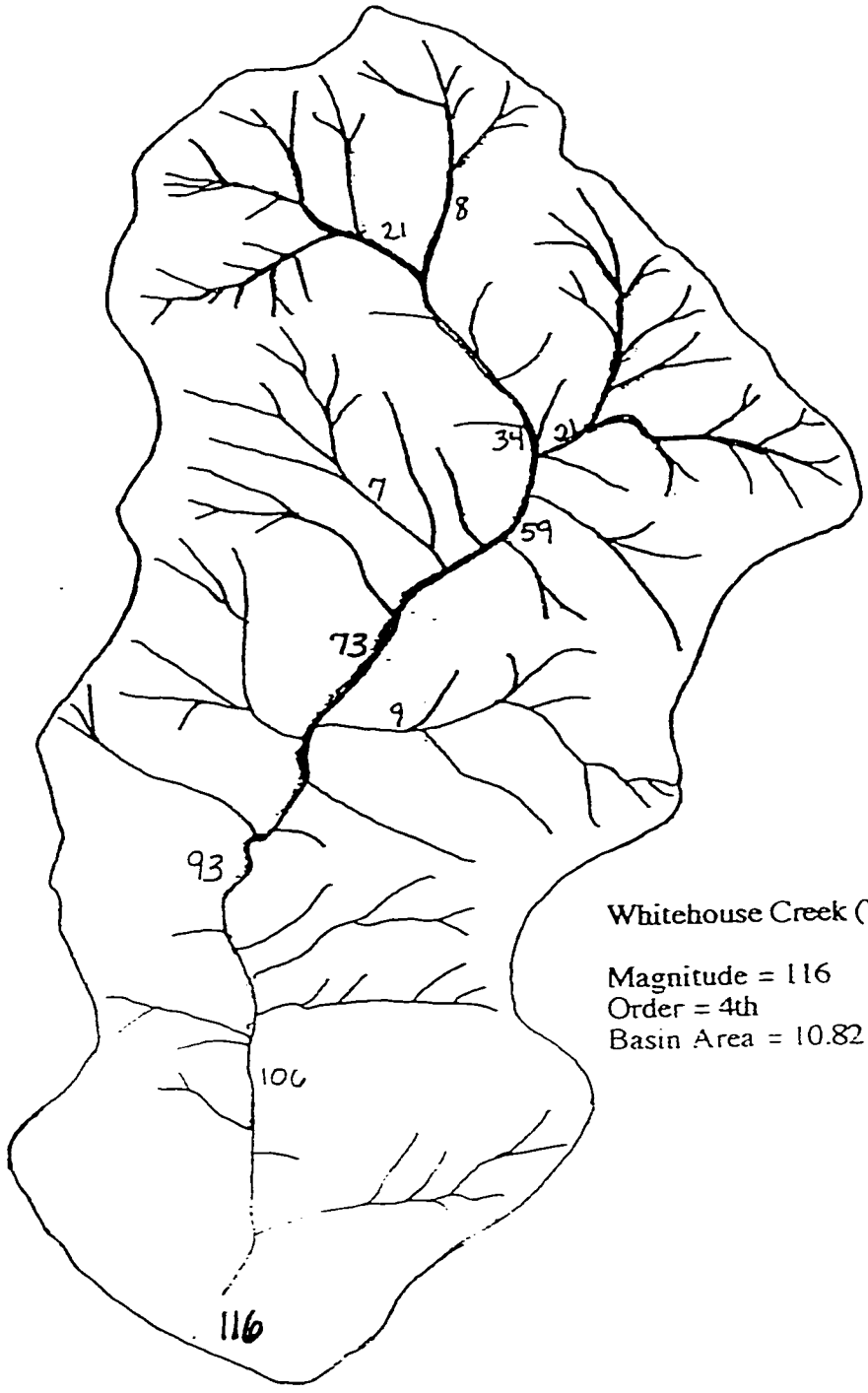

Whitehouse Creek (W)

Magnitude = 116
Order = 4th
Basin Area = 10.82 km^2

APPENDIX B

Stream cross-sections. All cross-sections were compiled from 1:24,000 USGS topographic maps with a 40-foot contour interval. All cross sections (except T-T') are drawn with a 6.5x vertical exaggeration (1:1300). The T-T' cross-section was reduced to a 5.5x (1:2500) vertical exaggeration. Streams are arranged in the order of Table 6. For cross-section locations, see Plate 1.

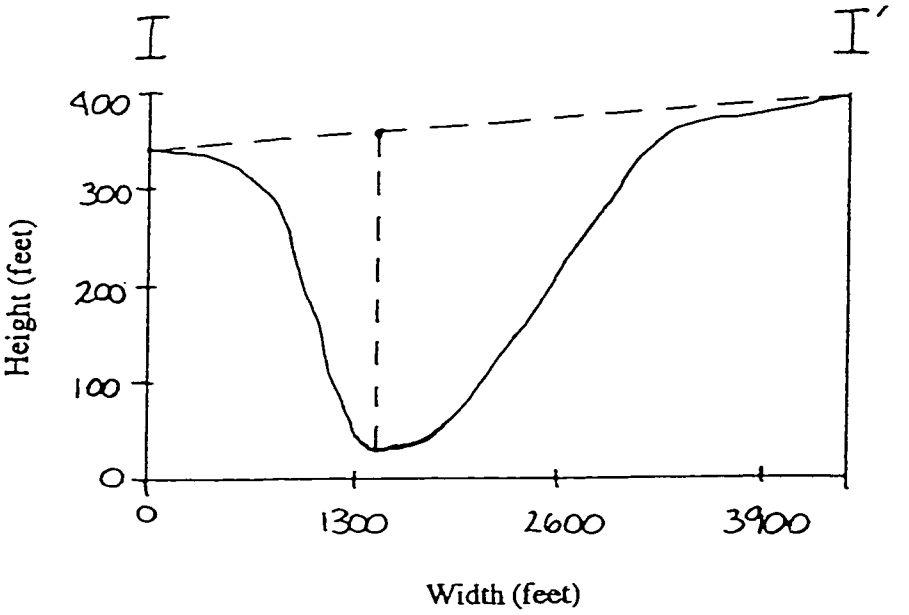

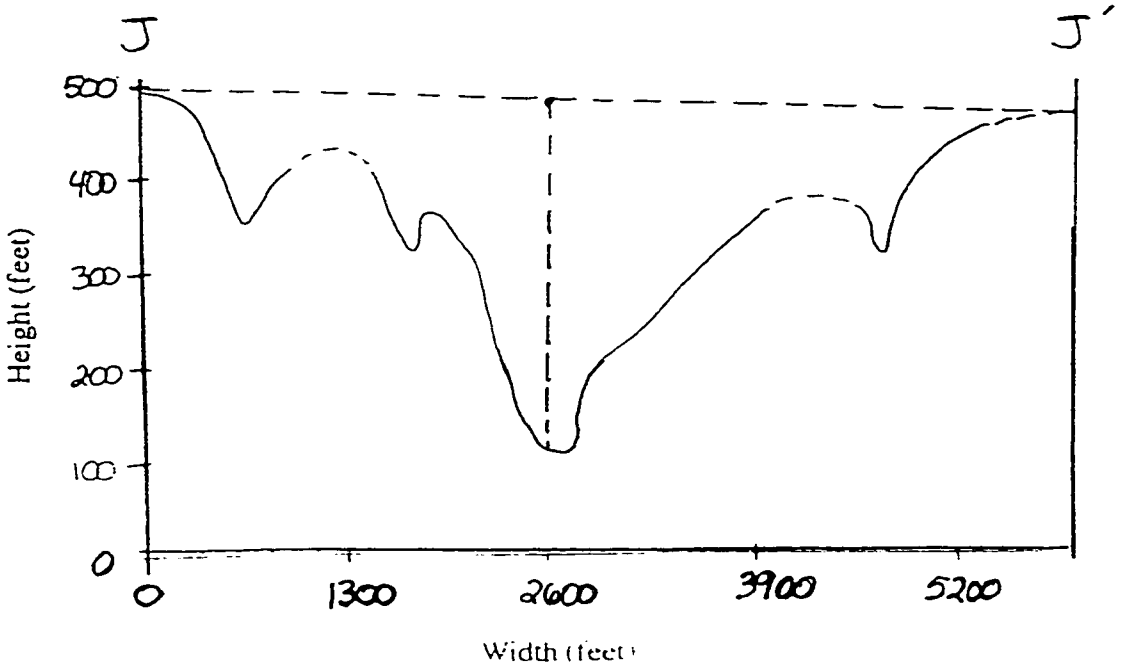

Arroyo de los Frijoles Creek

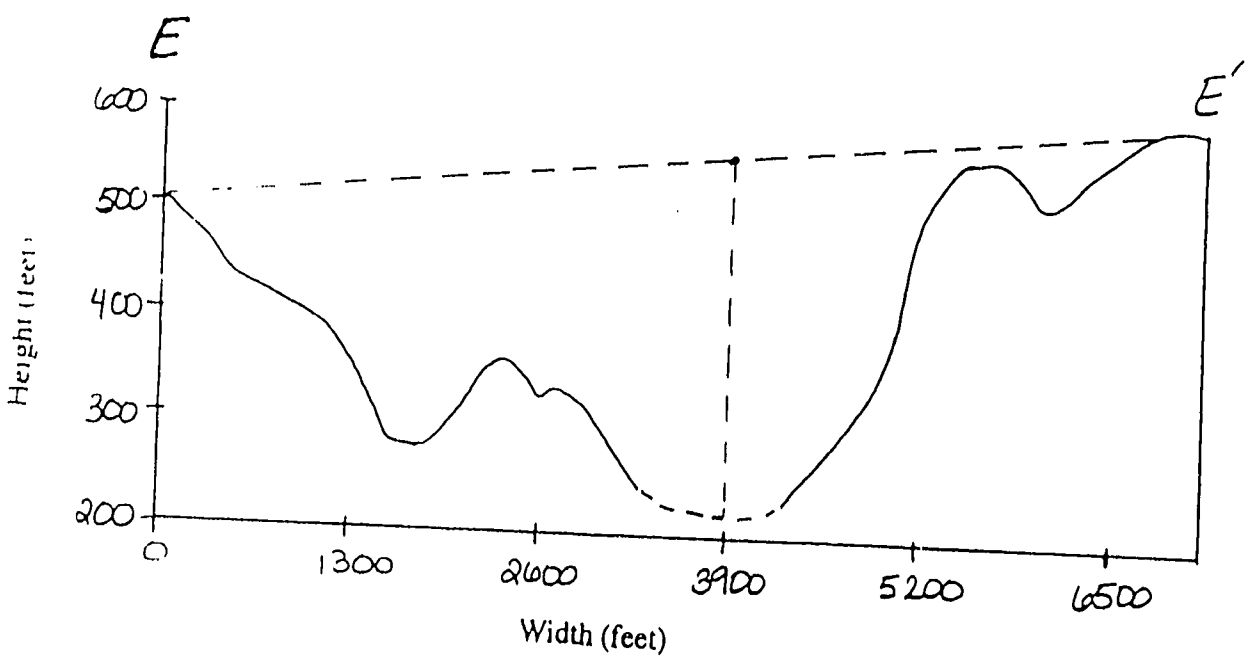

Arroyo de los Frijoles Creek

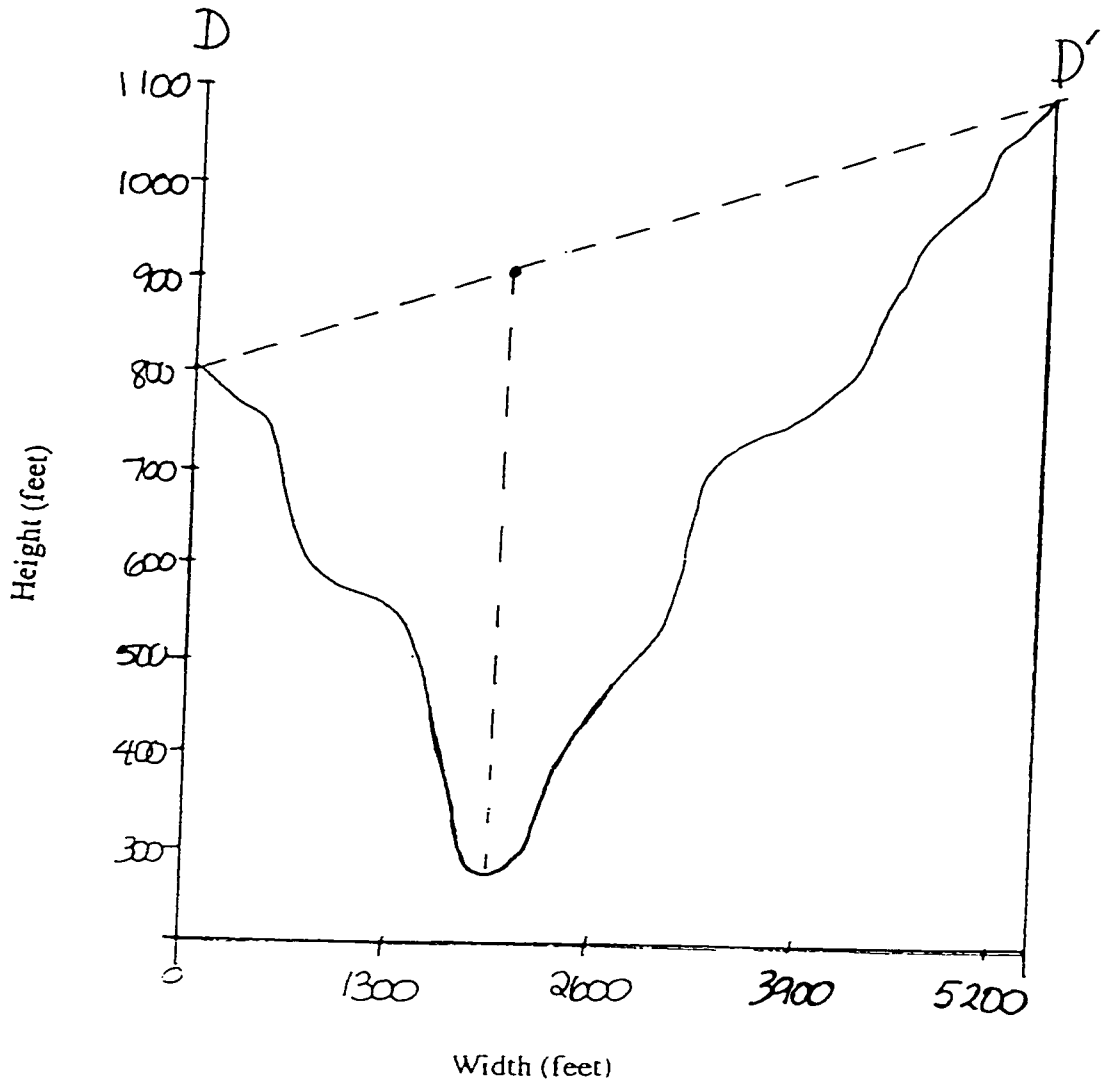

Arroyo de los Frijoles Creek

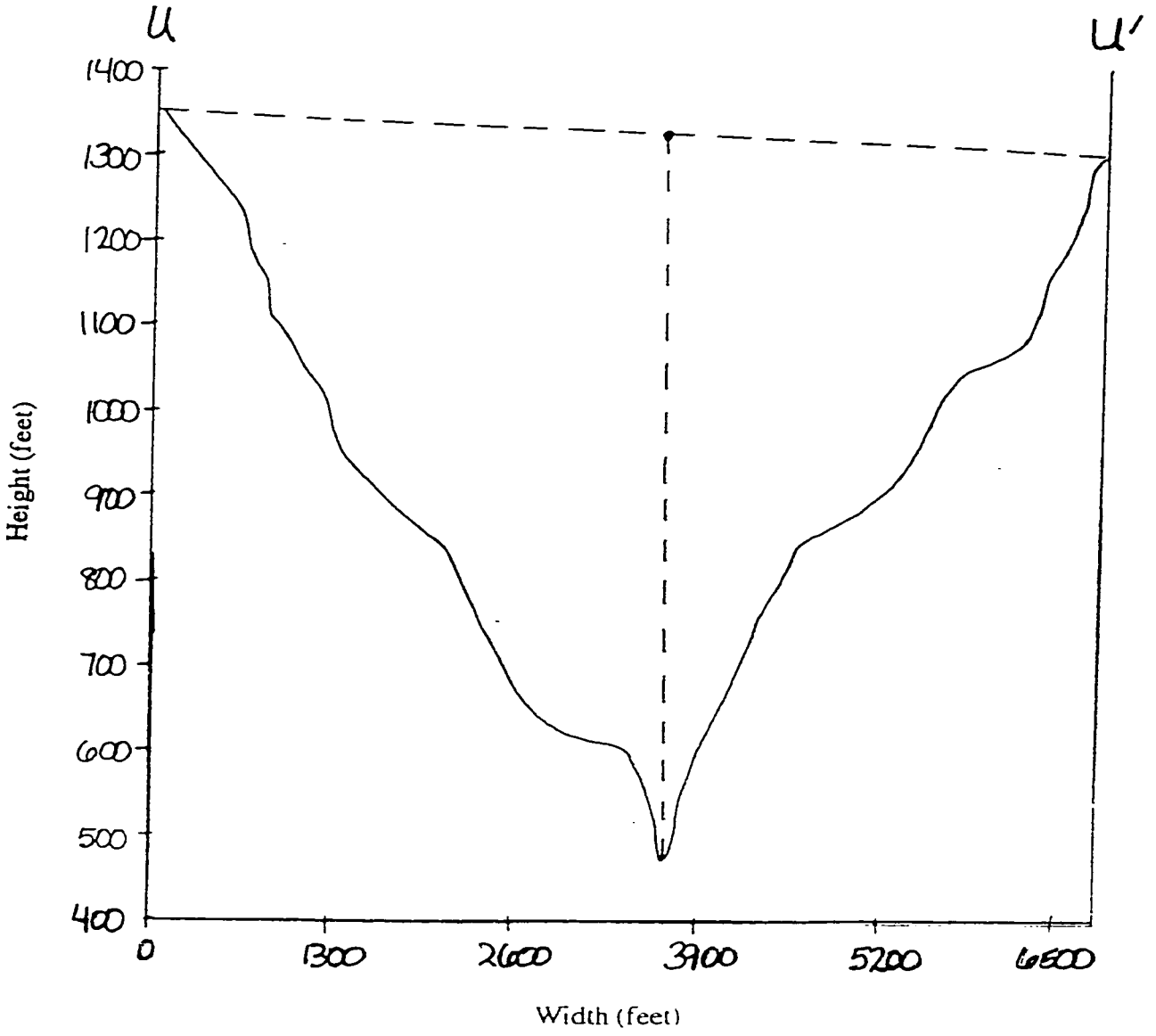

Arroyo de los Frijoles Creek

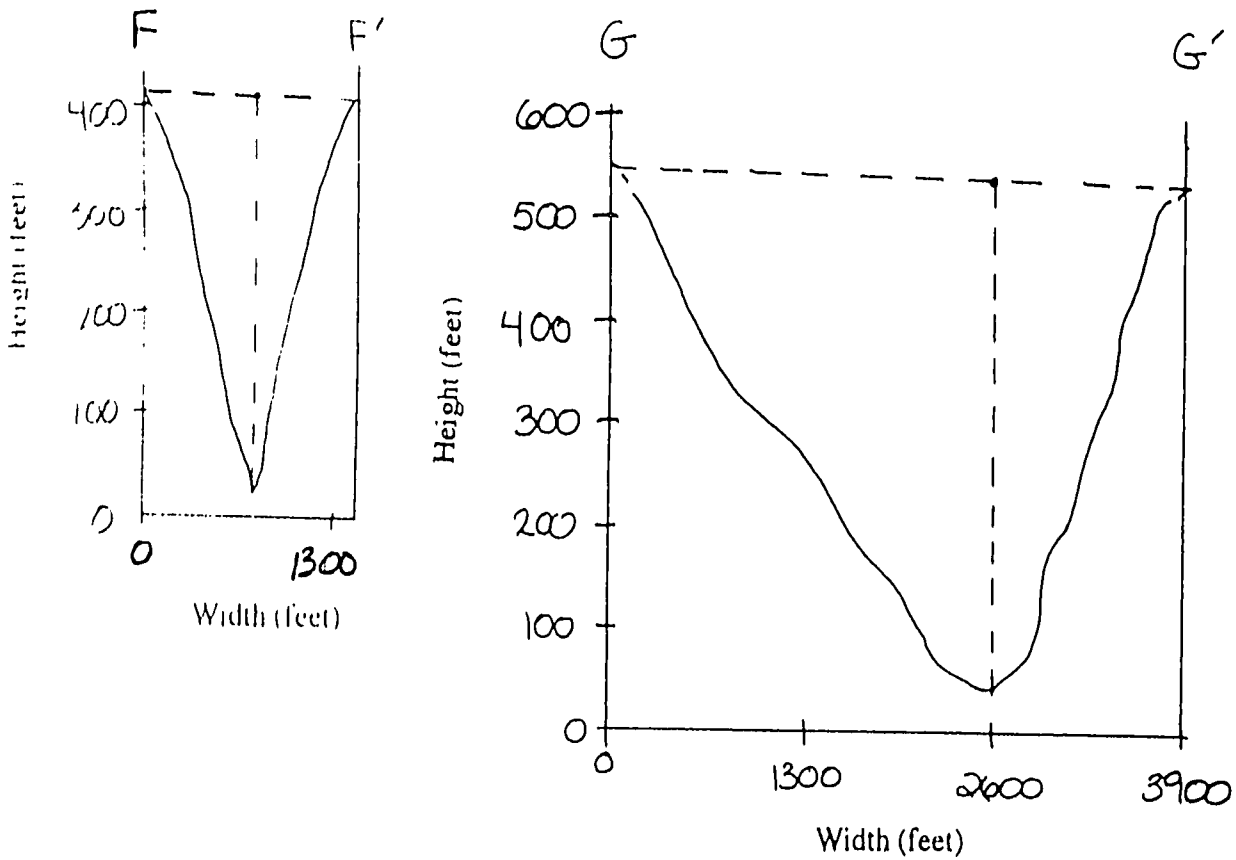

Gazos Creek/ Old Womans Creek

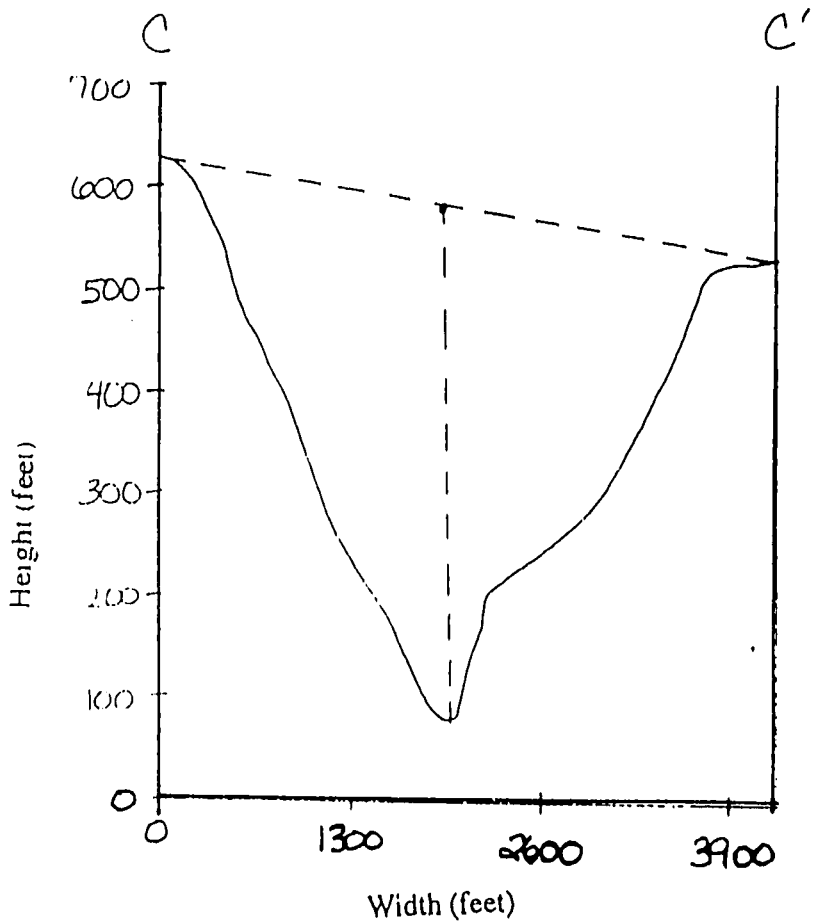

Gazos Creek/ Old Womans Creek

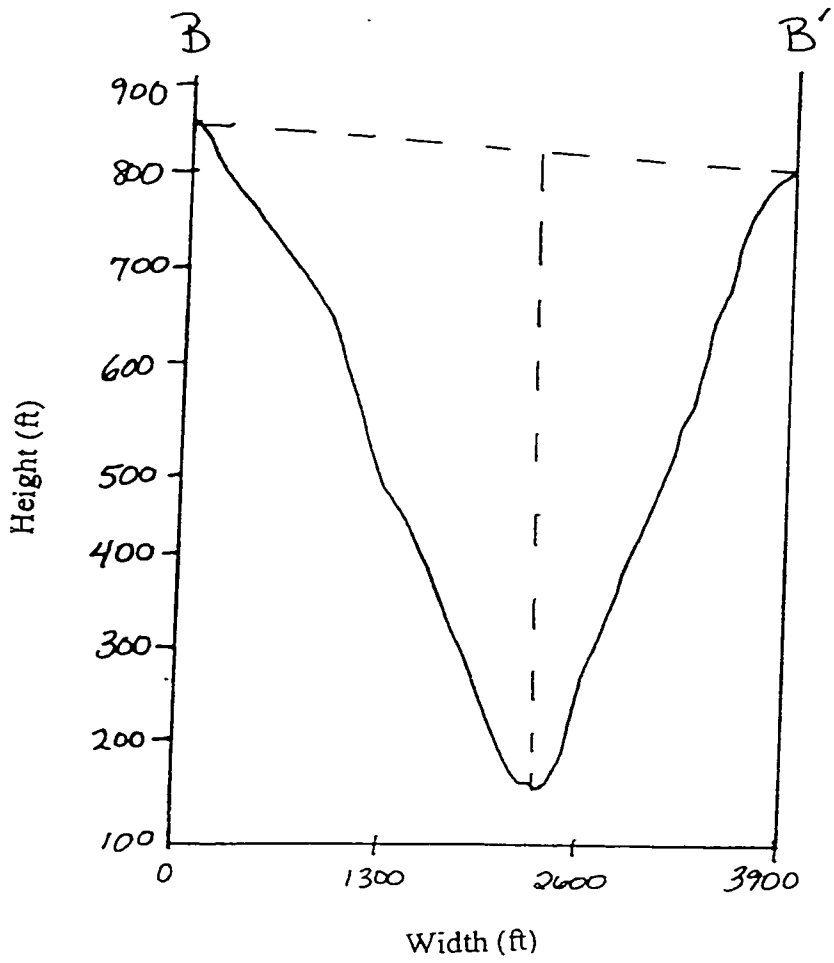
B
B'
900
800
700
600
500
400
300
200
100
Height (ft)
0
1300
2600
3900
Width (ft)

Gazos Creek

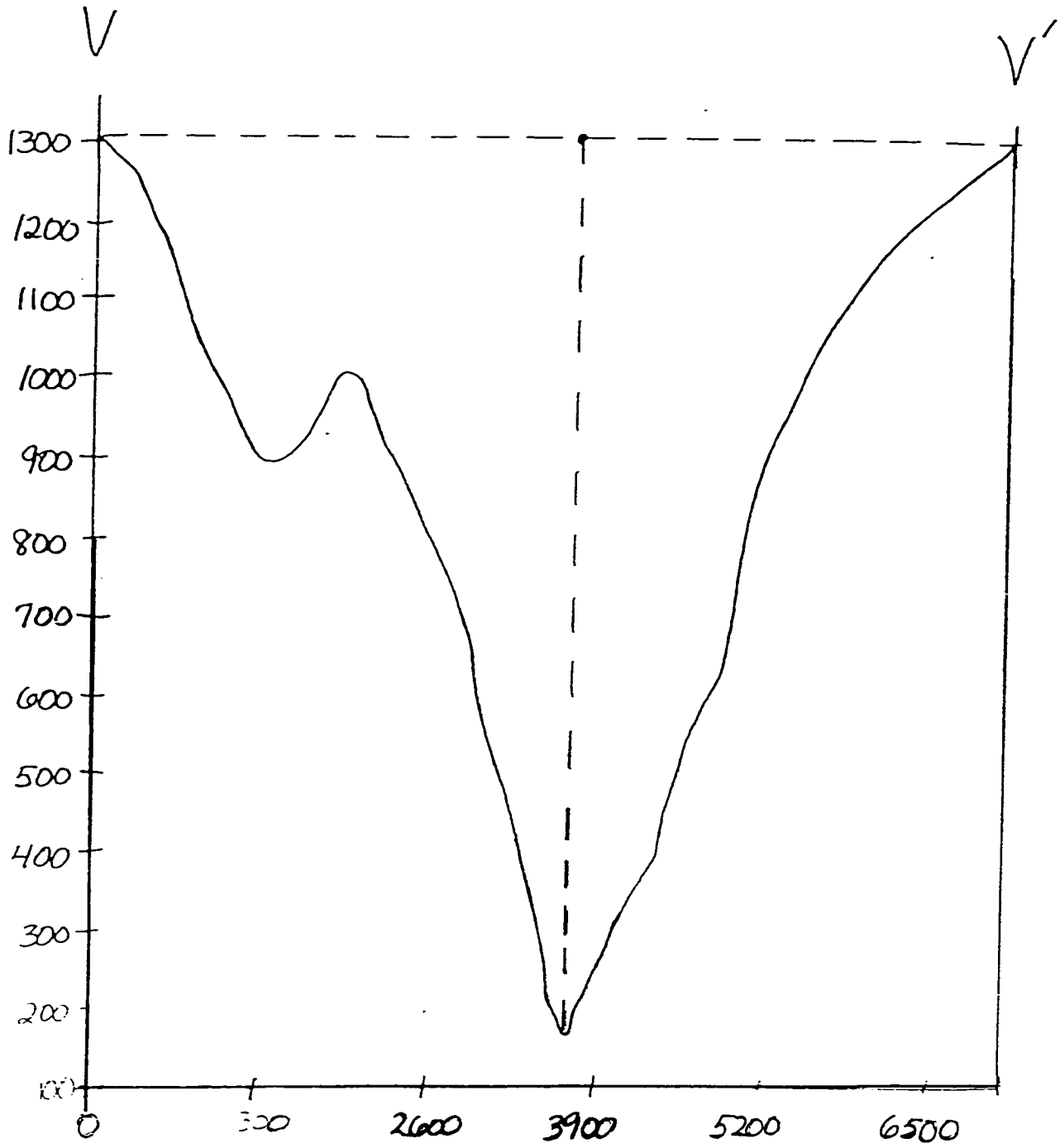
V
V'
1300
1200
1100
1000
900
800
700
600
500
400
300
200
100
0
2600
3900
5200
6500
Width (feet)
Height (feet)

Gazos Creek

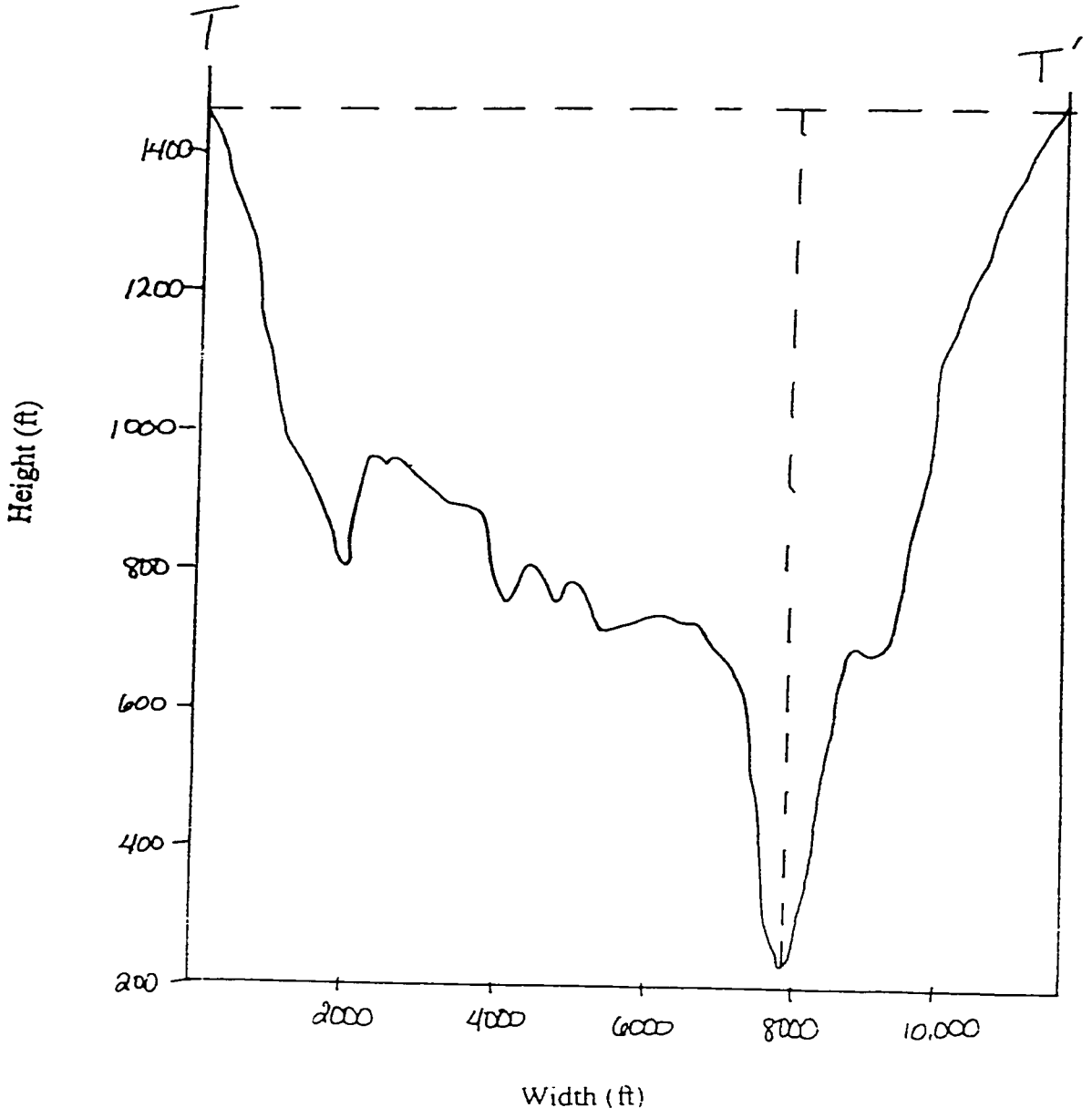
T
T'
1400
1200
1000
800
600
400
200
Height (ft)
2000
4000
6000
8000
10,000
Width (ft)

Gazos Creek

Old Womans Creek

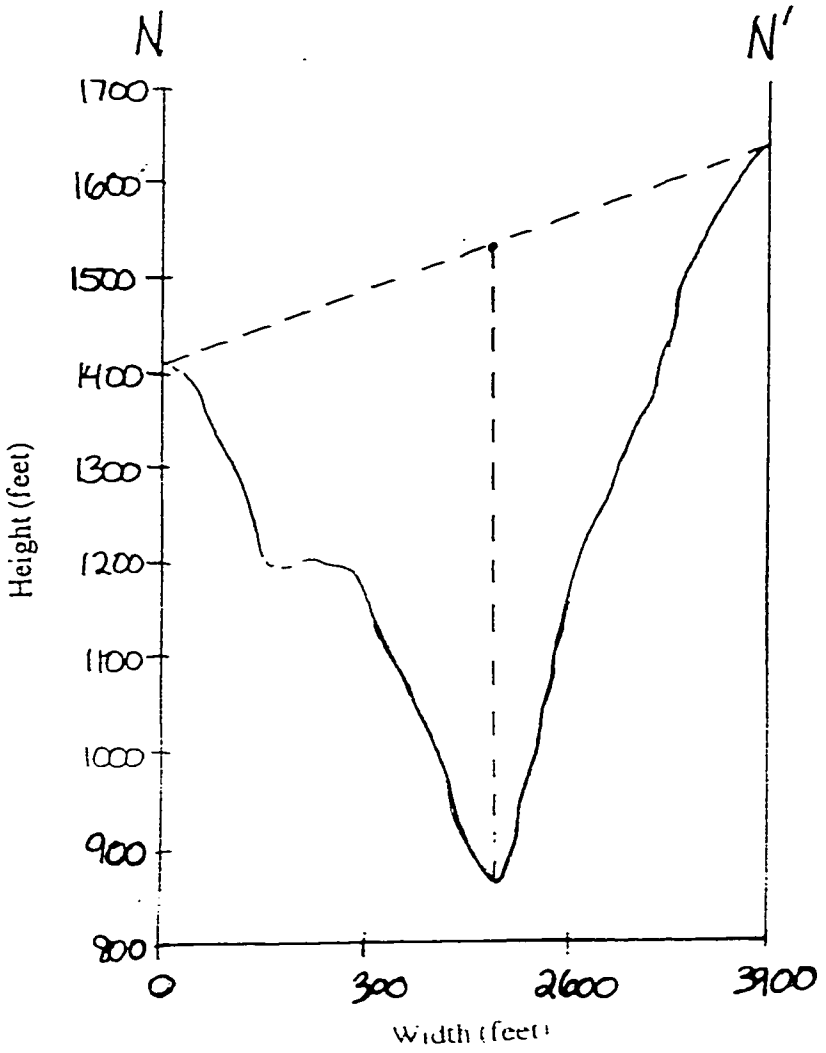

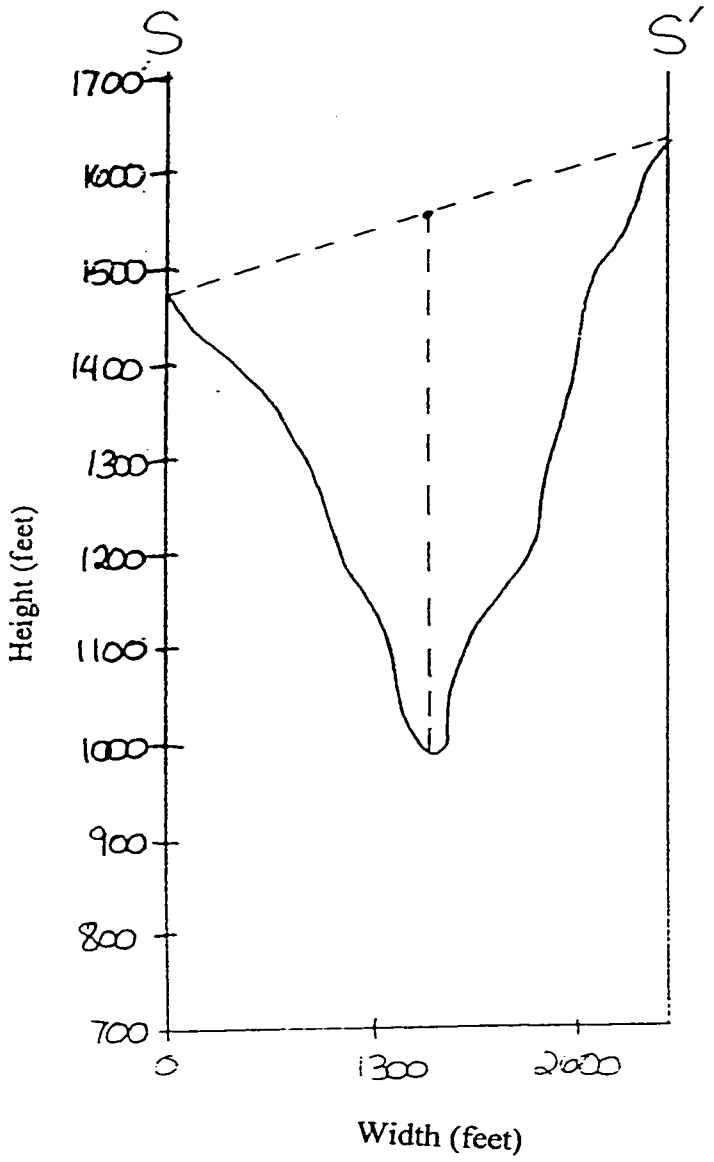

Old Womans Creek

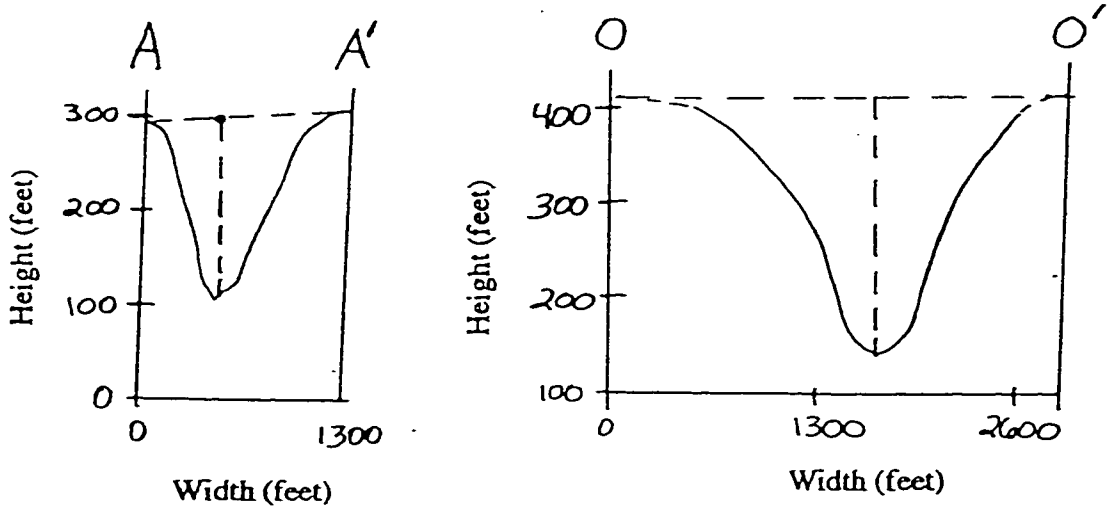

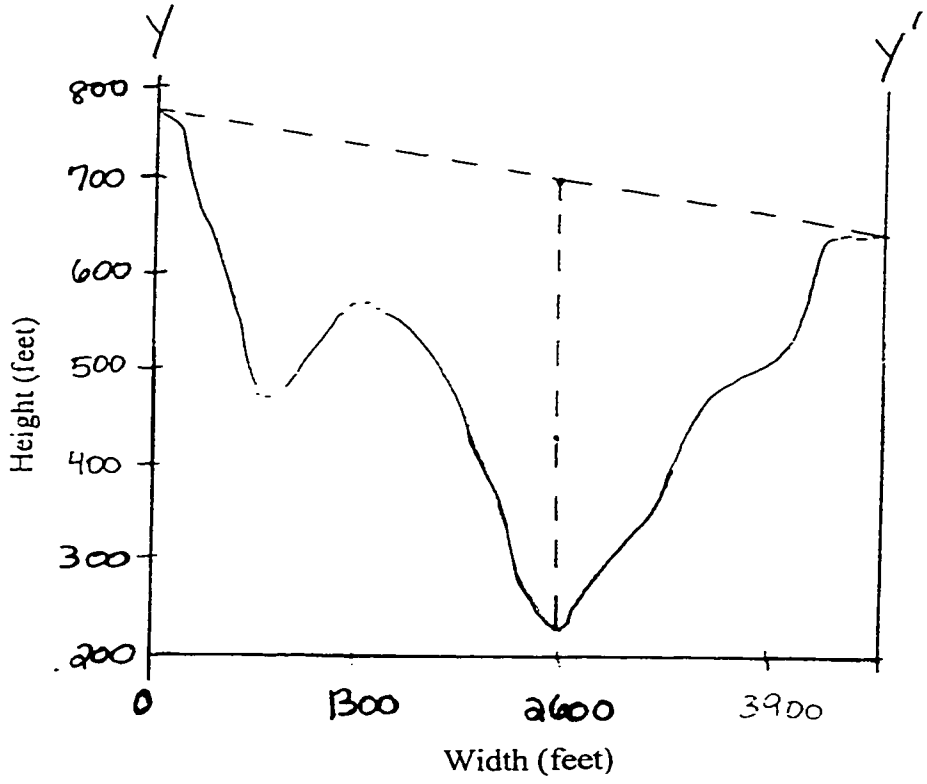

Whitehouse Creek

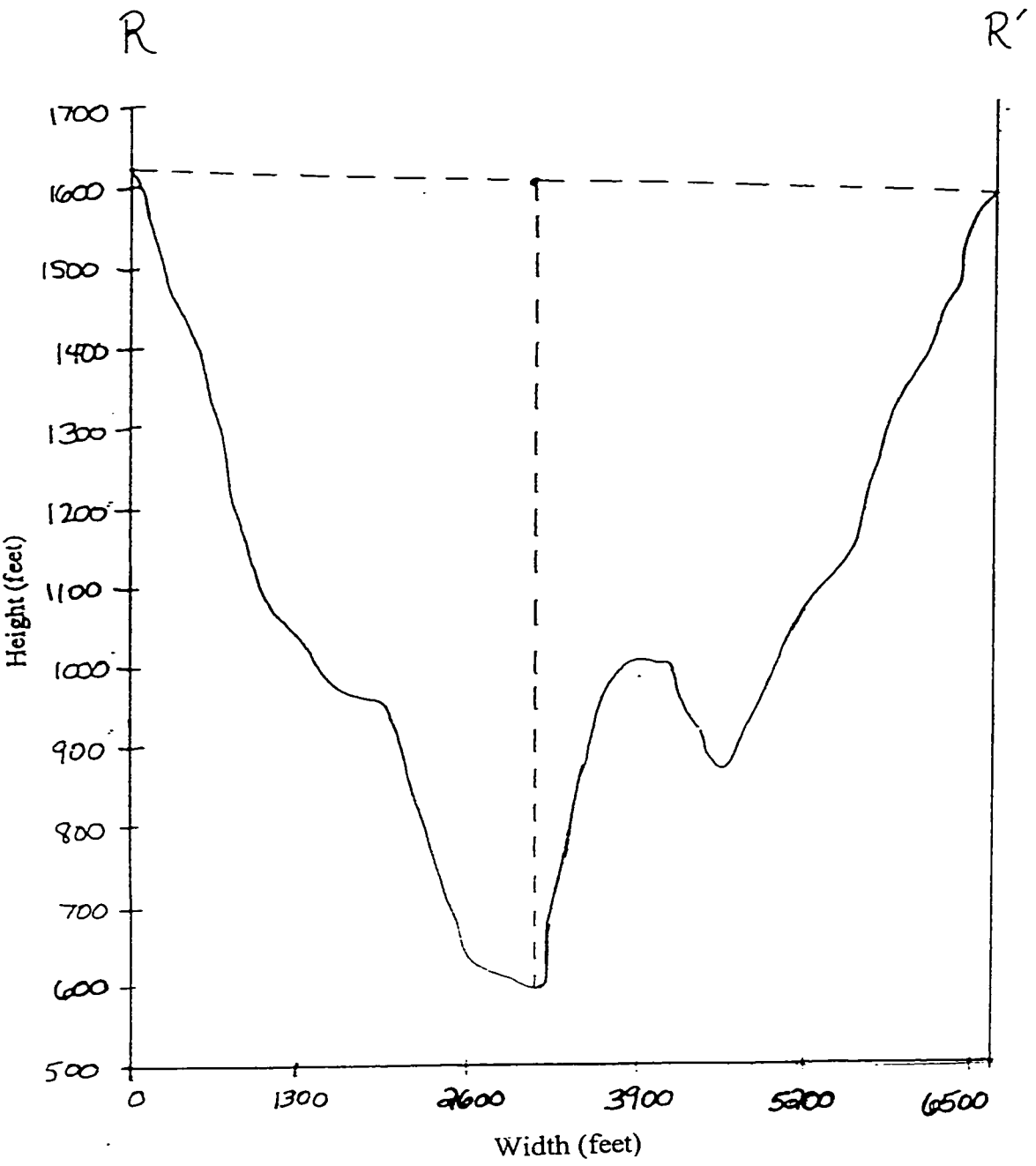

Whitehouse Creek

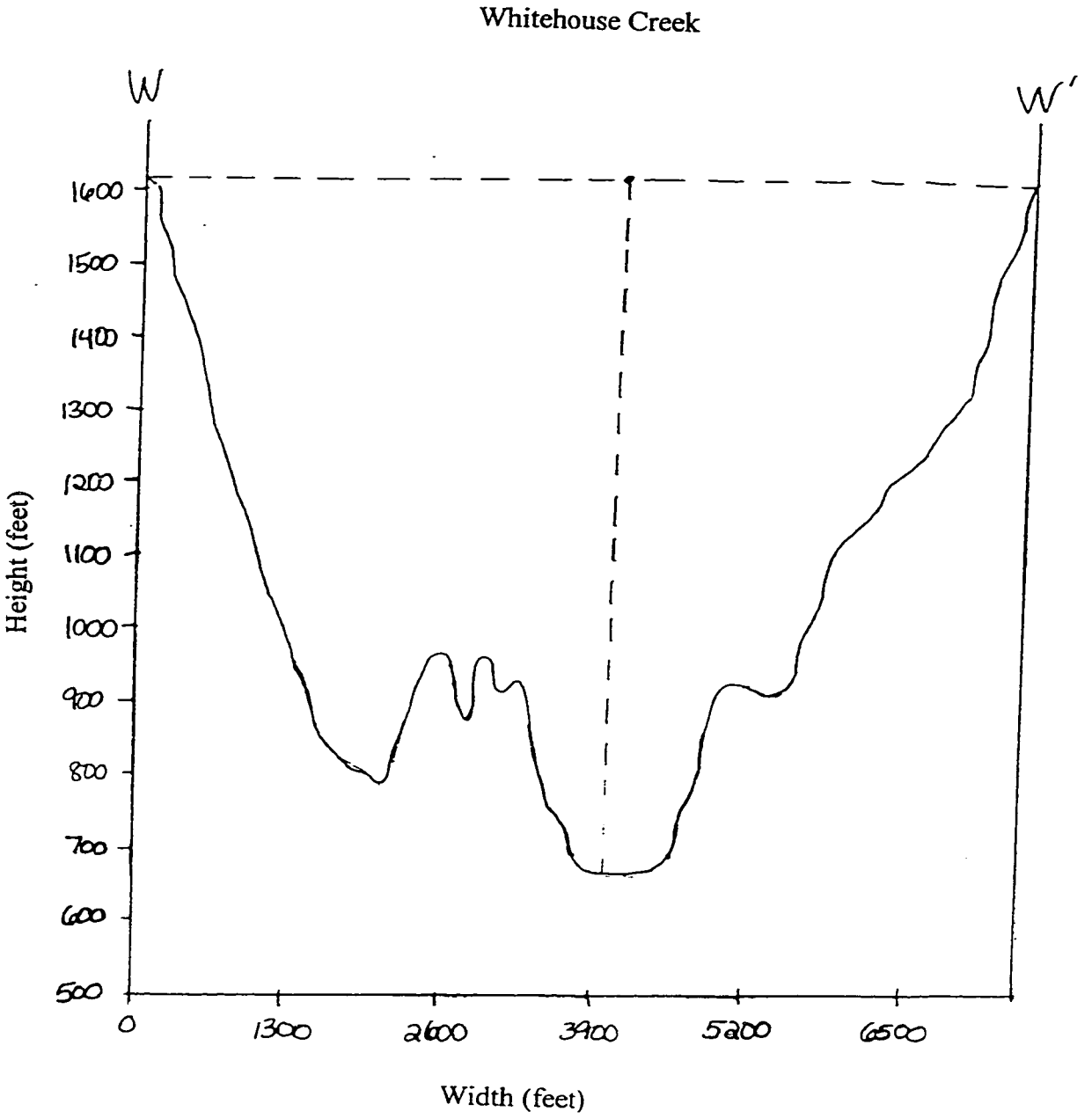
Whitehouse Creek
W
W'
1600
1500
1400
1300
1200
1100
1000
900
800
700
600
500
Height (feet)
0
1300
2600
3900
5200
6500
Width (feet)

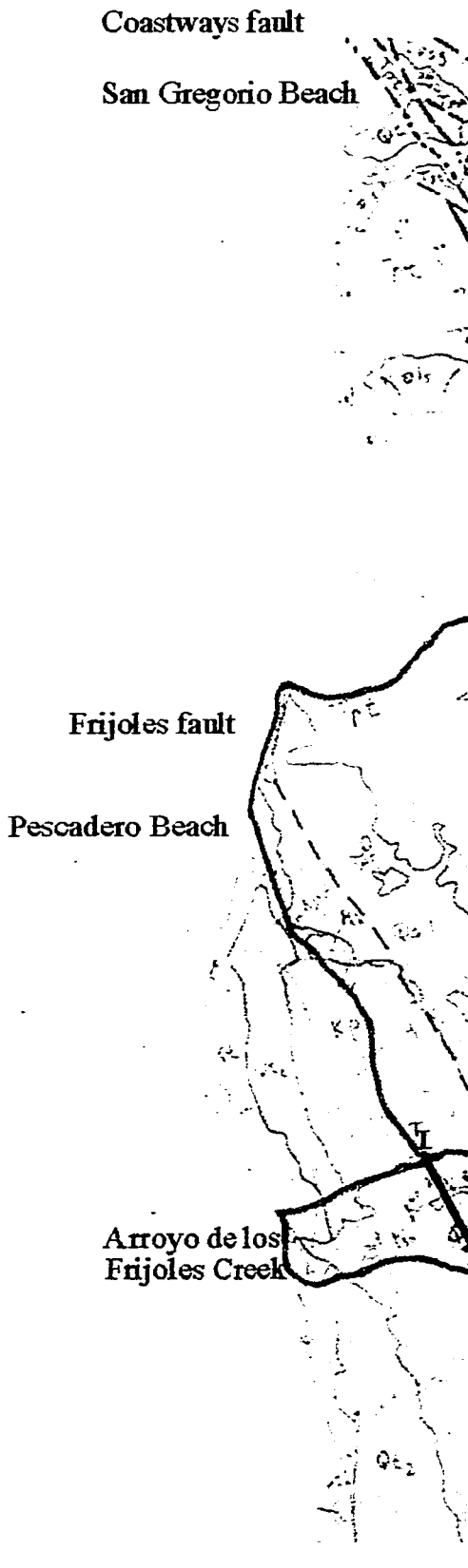
Coastways fault
San Gregorio Beach
Frijoles fault
Pescadero Beach
Arroyo de los
Frijoles Creek

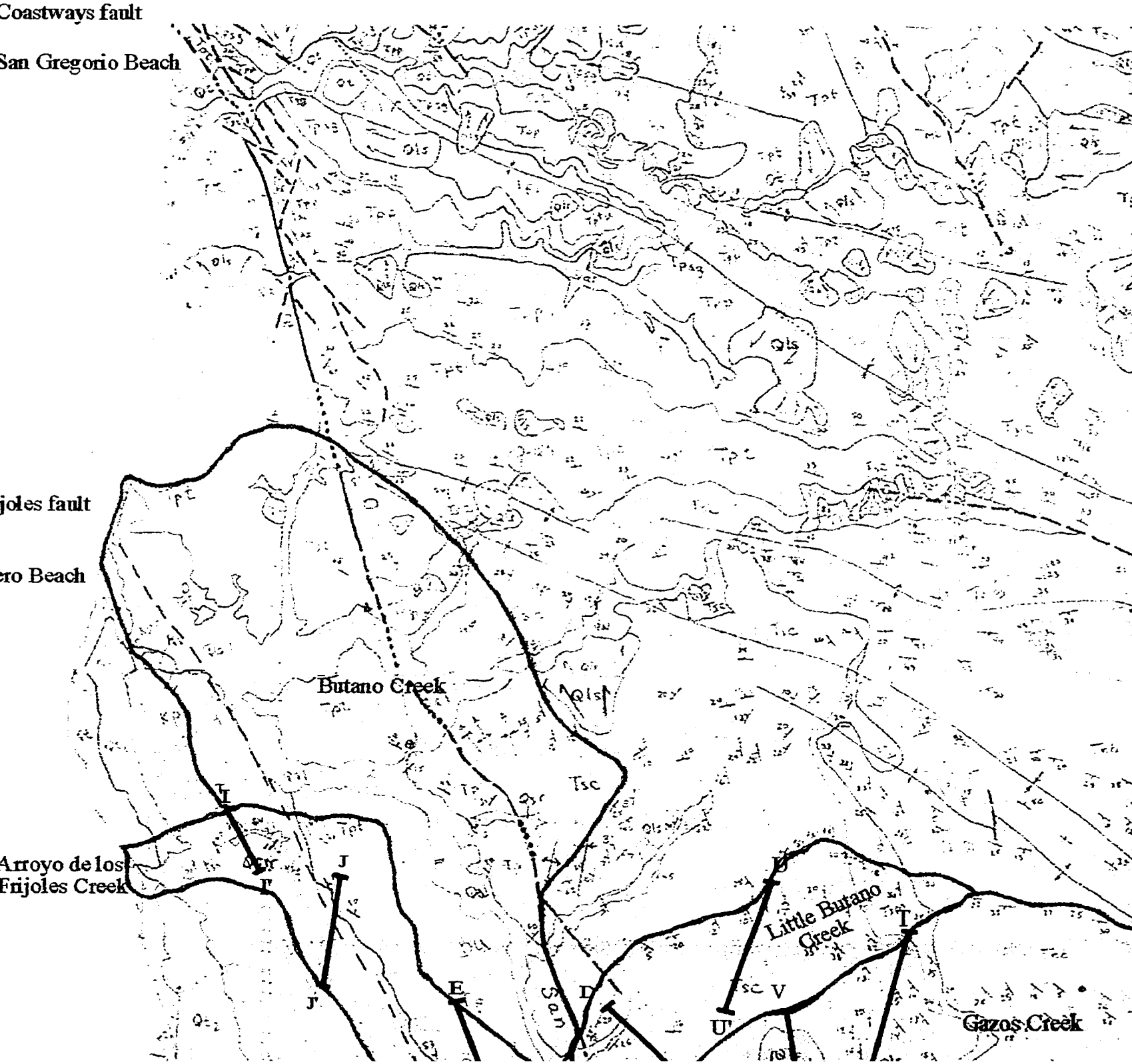
Coastways fault
San Gregorio Beach
joles fault
ero Beach
Butano Creek
Arroyo de los
Frijoles Creek
Little Butano
Creek
Gazos Creek
San
T
J
J'
E
D
U
U'
V
Tsc
Qls

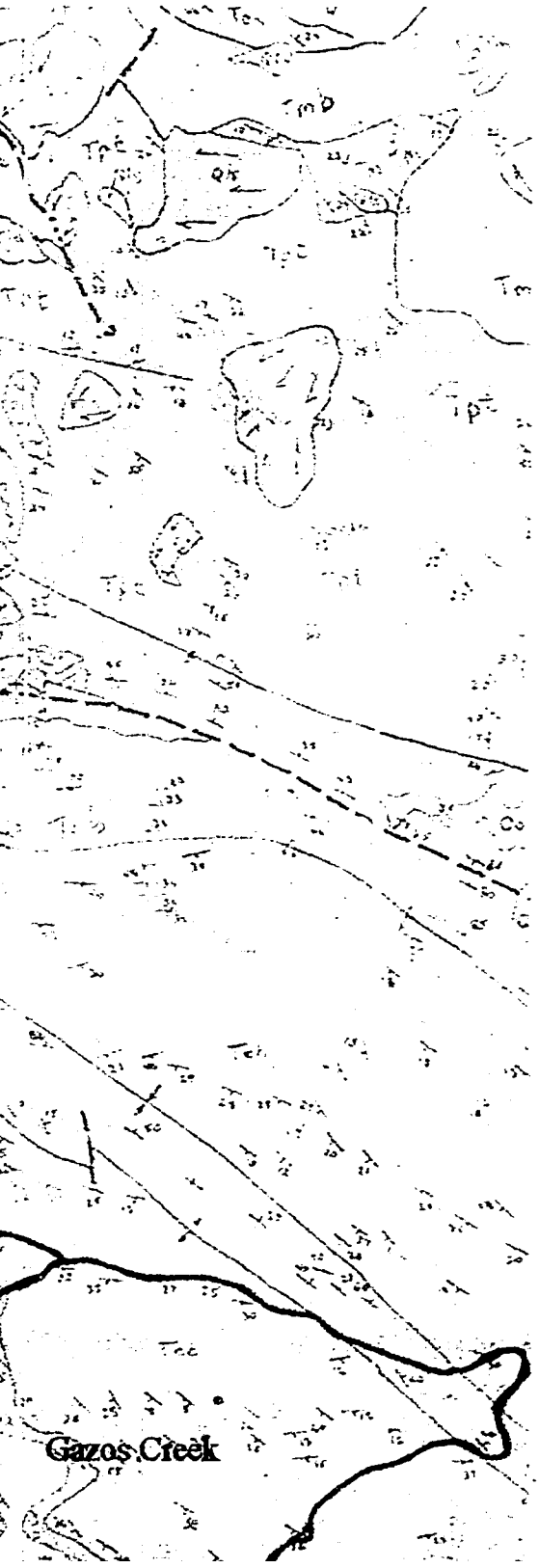

EXPLANATION

Quaternary

Qxx = Quaternary deposits including dunes, alluvium, landslides, and marine terrace deposits

Tertiary

Tp = Purisima Formation
Tpt = Tahana member of the Purisima Formation
Tsc = Santa Cruz Mudstone
Tsm = Santa Margarita Sandstone
Tm = Monterey Formation
Teb = Butano Sandstone

Cretaceous

Kpp = Pigeon Point Formation

Cross-section line

Lower basin outline

Upper basin outline

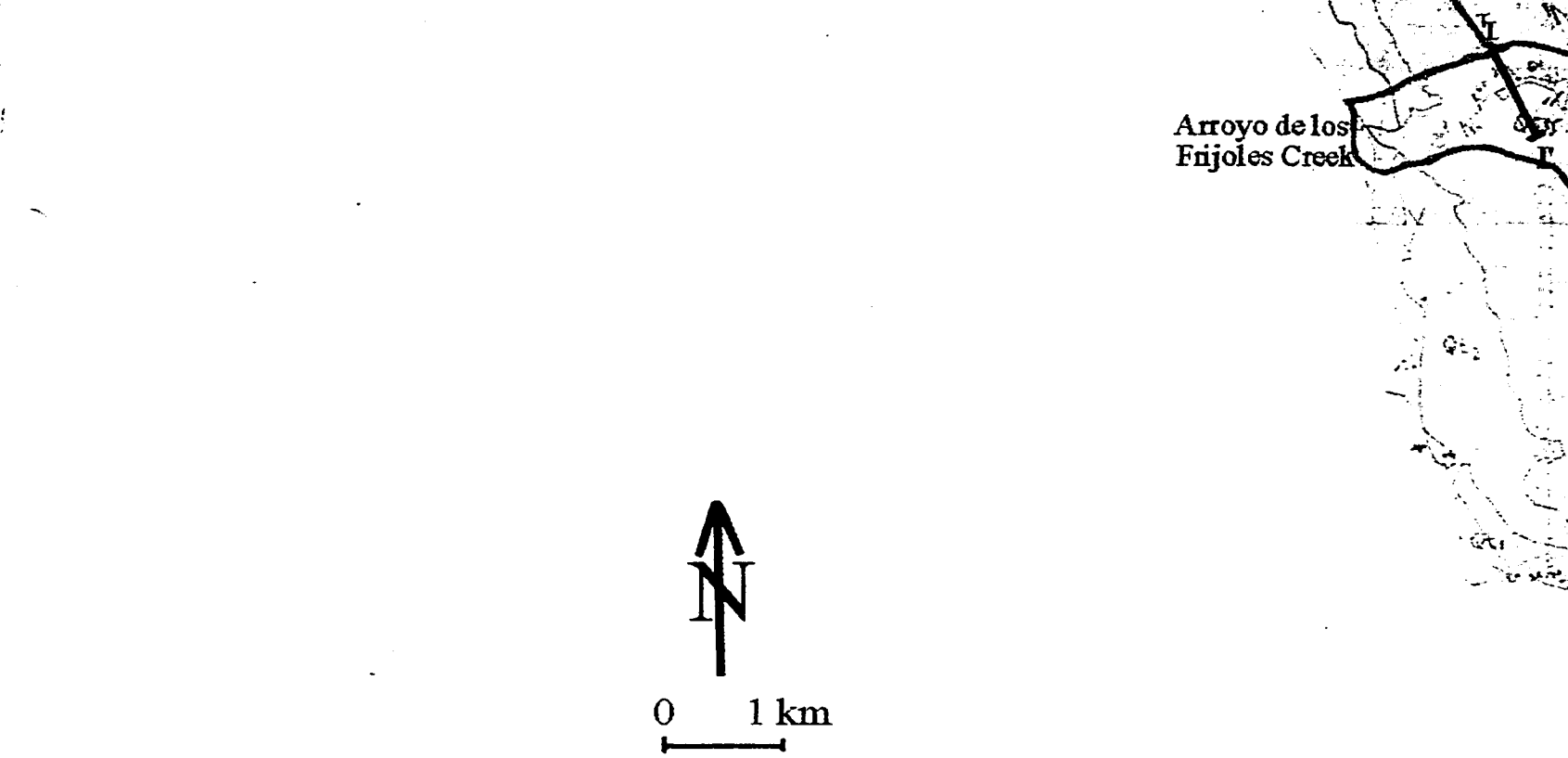

Plate 1. Upper (blue) and lower (red) basin boundaries and cr

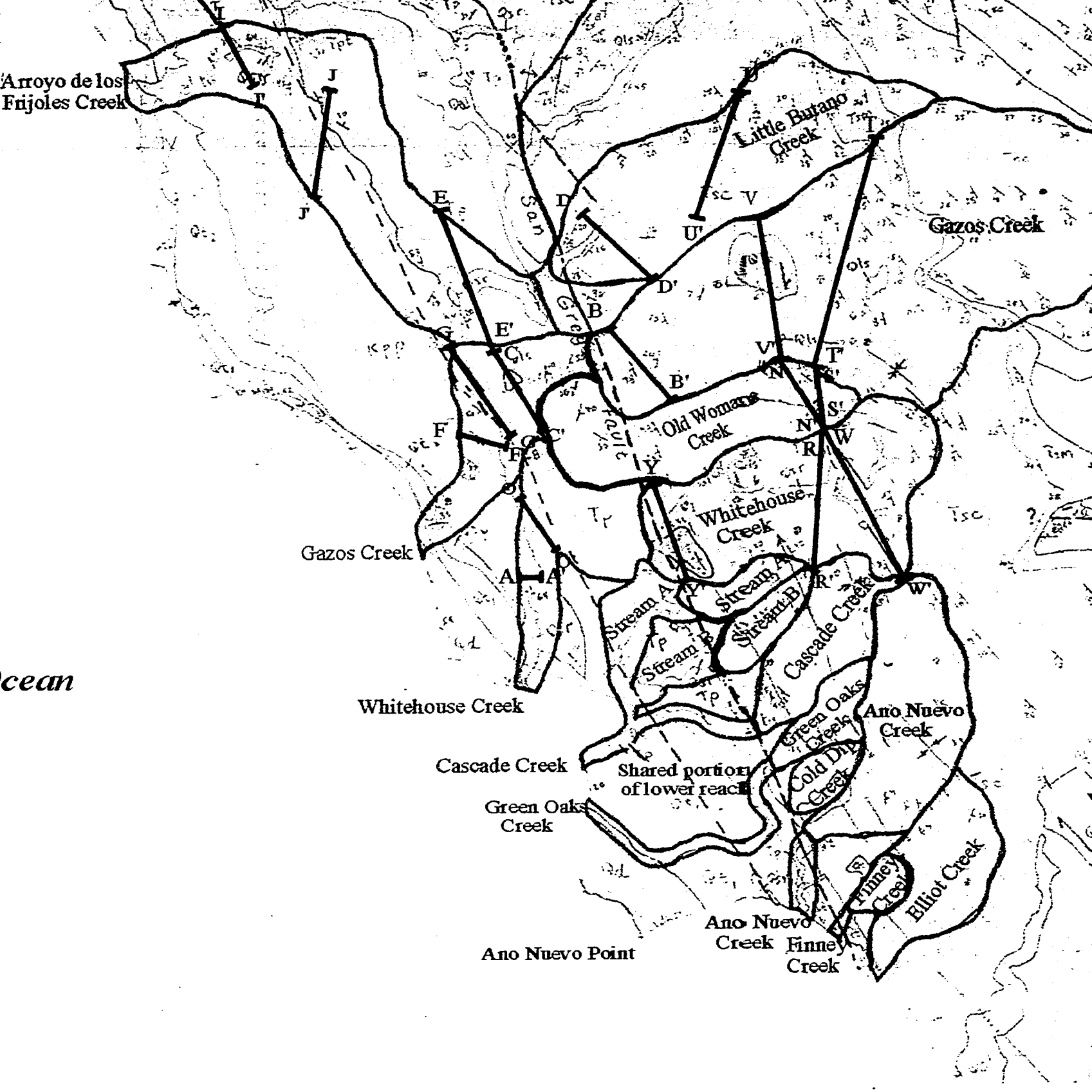

) basin boundaries and cross-section locations. Geologic map of San Mateo and Santa Cruz C

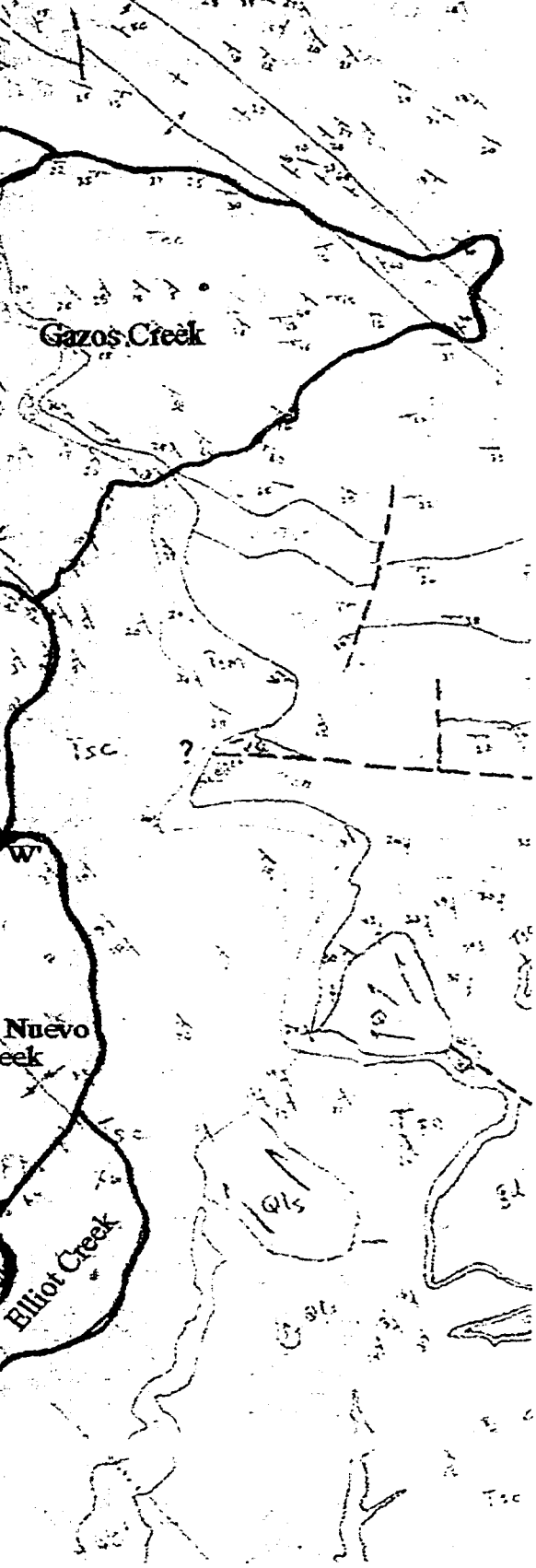

nd Santa Cruz Counties compiled by Brabb (1970).